1990-03

Transpolar sea ice drift in the vicinity of the Yermak Plateau as observed by ARCTEMIZ 86 buoys

Hoffman, Paul J.

Monterey, California. Naval Postgraduate School

(2)

NAVAL POSTGRADUATE SCHOOL

Monterey, California

THESIS

TRANSPOLAR SEA ICE DRIFT
IN THE VICINITY OF THE YERMAK PLATEAU
AS OBSERVED BY ARCTEMIZ 86 BUOYS

by

Paul J. Hoffman

March 1990

Thesis Advisor: Jean-Claude Gascard

REPORT DOCUMENTATION PAGE

Form Approved OMB No. 0704-0188

1a. REPORT SECURITY CLASSIFICATION: Unclassified	1b. RESTRICTIVE MARKINGS
2a. SECURITY CLASSIFICATION AUTHORITY	3. DISTRIBUTION / AVAILABILITY OF REPORT: Approved for public release; distribution is unlimited.
2b. DECLASSIFICATION / DOWNGRADING SCHEDULE	
4. PERFORMING ORGANIZATION REPORT NUMBER(S)	5. MONITORING ORGANIZATION REPORT NUMBER(S)
6a. NAME OF PERFORMING ORGANIZATION: Naval Postgraduate School; 6b. OFFICE SYMBOL (If applicable): 35	7a. NAME OF MONITORING ORGANIZATION: Naval Postgraduate School
6c. ADDRESS (City, State, and ZIP Code): Monterey, CA 93943-5000	7b. ADDRESS (City, State, and ZIP Code): Monterey, CA 93943-5000
8a. NAME OF FUNDING / SPONSORING ORGANIZATION; 8b. OFFICE SYMBOL (If applicable)	9. PROCUREMENT INSTRUMENT IDENTIFICATION NUMBER
8c. ADDRESS (City, State, and ZIP Code)	10. SOURCE OF FUNDING NUMBERS: PROGRAM ELEMENT NO. / PROJECT NO. / TASK NO. / WORK UNIT ACCESSION NO.

11. TITLE (Include Security Classification): TRANSPOLAR SEA ICE DRIFT IN THE VICINITY OF THE YERMAK PLATEAU AS OBSERVED BY ARCTEMIZ 86 BUOYS

12. PERSONAL AUTHOR(S): Hoffman, Paul Joseph

13a. TYPE OF REPORT	13b. TIME COVERED	14. DATE OF REPORT (Year, Month, Day)	15. PAGE COUNT
Master's Thesis	FROM _____ TO _____	March 1990	99

16. SUPPLEMENTARY NOTATION: The views expressed in this thesis are those of the author and do not reflect the official policy or position of the Department of Defense or the U.S. Government.

17. COSATI CODES			18. SUBJECT TERMS (Continue on reverse if necessary and identify by block number)
FIELD	GROUP	SUB-GROUP	Transpolar Drift, Sea Ice, ARCTEMIZ 86, Yermak Plateau, Diurnal Tidal Currents

19. ABSTRACT (Continue on reverse if necessary and identify by block number)

Strong diurnal tidal currents, in a region dominated by semidiurnal tidal surface displacements, were observed in the record of ARCTEMIZ 1986 buoys as they drifted over the Yermak Plateau, a submarine feature northwest of Svalbard. Similar diurnal currents in this area were first observed from observations taken during the FRAM III and FRAM IV ice station drift experiments. The selective enhancement of topographic vorticity waves by resonant forcing from the K_1 diurnal tide over the steeply sloping northern, northwestern and western flanks of the plateau is forwarded as an explanation for these anomalously strong diurnal currents.

Diurnal loops were observed in the trajectories of two buoys while they were over the northern flank of the Yermak Plateau. These loops

20. DISTRIBUTION / AVAILABILITY OF ABSTRACT: ☒ UNCLASSIFIED/UNLIMITED ☐ SAME AS RPT ☐ DTIC USERS	21. ABSTRACT SECURITY CLASSIFICATION: Unclassified
22a. NAME OF RESPONSIBLE INDIVIDUAL: Robert H. Bourke	22b. TELEPHONE (Include Area Code): 408-646-2270; 22c. OFFICE SYMBOL: OCBF

were similar to those observed during MIZEX 84. The loops occurred during diurnal clockwise velocity peaks which have the same periodicity as the fort nightly (spring-neap) beat of surface height inequality caused by the superposition of the two principal semi-diurnal tides.

Sea ice for ced by the added convergent grinding motion arising from these enhanced diurnal clockwise currents should have a surface morphology different from the ice which did not flow through this area, i.e., that which passes through Fram Strait to the west of the Yermak Plateau.

Approved for public release; distribution is unlimited.

Transpolar Sea Ice Drift
in the Vicinity of the Yermak Plateau
as Observed by ARCTEMIZ 86 Buoys

by

Paul J. Hoffman
Lieutenant, United States Navy
B.S., University of Washington

Submitted in partial fulfillment
of the requirements for the degree of

MASTER OF SCIENCE IN METEOROLOGY AND PHYSICAL OCEANOGRAPHY

from the

NAVAL POSTGRADUATE SCHOOL
March 1990

Author: [redacted]
Paul J. Hoffman

Approved by: [redacted]
Jean-Claude Gascard, Thesis Advisor

[redacted]
Robert H. Bourke, Second Reader

[redacted]
Curtis A. Collins, Chairman
Department of Oceanography

ABSTRACT

Strong diurnal tidal currents, in a region dominated by semidiurnal tidal surface displacements, were observed in the record of ARCTEMIZ 1986 buoys as they drifted over the Yermak Plateau, a submarine feature northwest of Svalbard. Similar diurnal currents in this area were first observed from observations taken during the FRAM III and FRAM IV ice station drift experiments. The selective enhancement of topographic vorticity waves by resonant forcing from the K_1 diurnal tide over the steeply sloping northern, northwestern and western flanks of the plateau is forwarded as an explanation for these anomalously strong diurnal currents.

Diurnal loops were observed in the trajectories of two buoys while they were over the northern flank of the Yermak Plateau. These loops were similar to those observed during MIZEX 84. The loops occurred during diurnal clockwise velocity peaks which have the same periodicity as the fortnightly (spring-neap) beat of surface height inequality caused by the superposition of the two principal semidiurnal tides.

Sea ice forced by the added convergent grinding motion arising from these enhanced diurnal clockwise currents should have a surface morphology observably different from ice which did not flow through this area, i.e., that which passes through Fram Strait to the west of the Yermak Plateau.

TABLE OF CONTENTS

I. INTRODUCTION

A. FRAM STRAIT AND THE ARCTIC SEA ICE TRANSPOLAR DRIFT

Fram Strait is the primary outflow region for sea ice from the central Arctic (Tucker et al., 1987). Through it passes approximately 90% of the heat exchange and 75% of the mass exchange between the Arctic and the World Ocean (Aagaard and Greisman, 1975). The oceanographic and meteorological processes active in the vicinity of Fram Strait therefore exert a profound effect on the climatology of the Arctic, and to a lesser extent the entire northern hemisphere. Along the western side of Fram Strait flows the cold polar waters of the East Greenland Current, a continuation of the southward flowing Transpolar Drift Stream. The eastern side of Fram Strait, to the west of Svalbard, is usually ice free year round due to the heat carried by the West Spitsbergen Current, a northern extension of the warm North Atlantic Current. This open area along the ice edge, known as Whaler's Bay or Svalbardbukta, is the northernmost year-round ice free sea area in the world (Wadhams, 1983).

The actual magnitude of the areal flux of ice is determined by atmospheric circulation, ocean currents, and the supply of ice at and upstream of Fram Strait. Englebretson and Walsh (1989) determined that the areal outflow of ice through Fram Strait, using geostrophic winds and ice concentration, was highly variable over both seasonal and interannual time scales. Their work also showed an apparent shift in the origin of the

majority of sea ice passing through the Fram Strait from the Alaskan to the Siberian coastal region around the 1972 time frame.

An anticyclonic gyre, with a mean central position of 75°N 155°W, and associated low pressure trough extending northeastward into the Barents Sea from near Iceland (Figure 1),

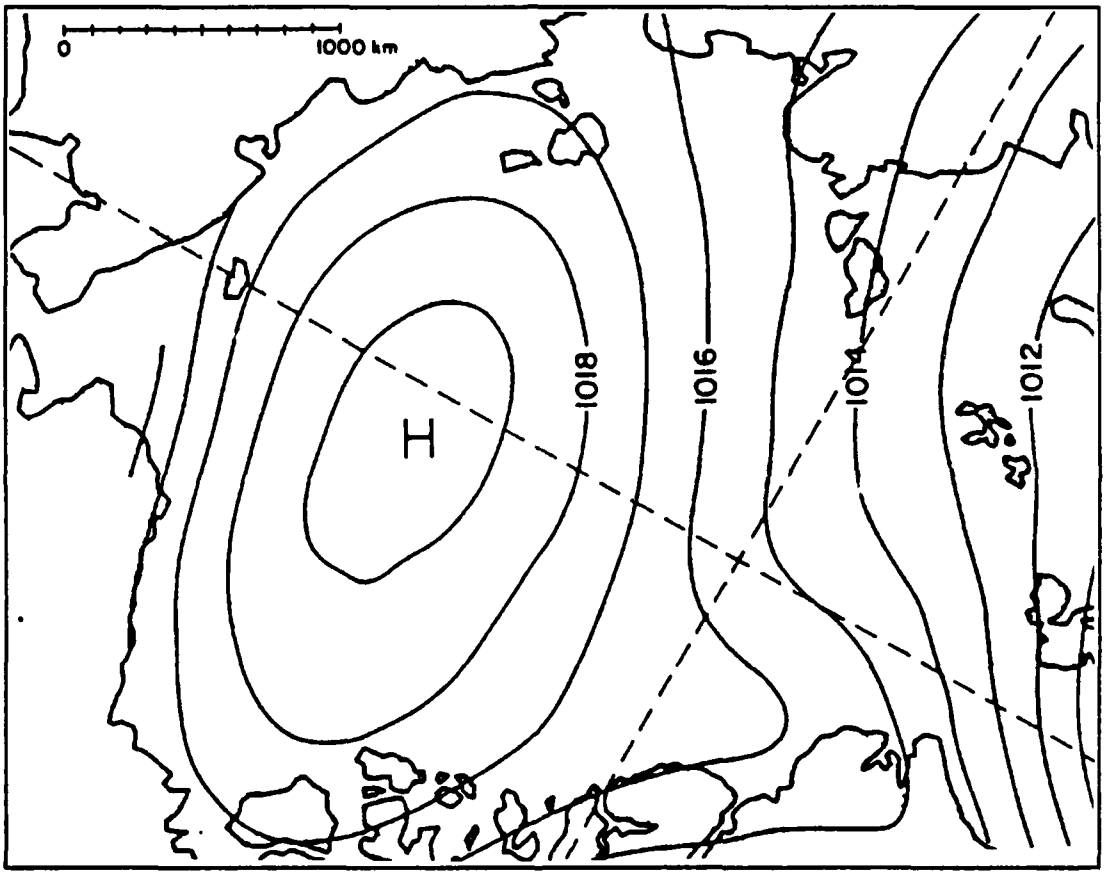

Figure 1 Climatological sea level pressure pattern over the Arctic Ocean (1979-1982). Isobars in mb (from Colony and Thorndike, 1984).

are the primary atmospheric mechanisms driving sea ice drift in the Arctic. Through the surface wind stress coupled to the ocean through the ice, this atmospheric forcing is transferred to the ocean currents creating the anticyclonic Beaufort gyre and the Transpolar

Drift. The drift of sea ice in the Transpolar Drift has been estimated at approximately 1-3 cm/s (Colony and Thorndike, 1984).

Buoy and sea ice drift observations made during MIZEX 84 (Gascard et al., 1988) and from the R/V Polarstern during July and August 1987 (Pfirman et al., 1989) led these researchers to conclude that the Transpolar Drift is actually composed of two branches, a Polar and a Siberian branch (Figure 2). The 1987 sea ice observations in the area of 84°N-86°N and 20°E-30°E showed large quantities of particulate material, often darkening half of the ice surface. The particulate matter was largely littoral in origin, suggestive of formation in a coastal regime. The actual constituents are representative of the northern coast of the Soviet Union. The drift patterns of buoys deployed north of 84°N showed that most of the ice in this region drifted out of the Eurasian Basin through Fram Strait and was incorporated into the East Greenland Current. Buoys deployed south of 84°N drifted to the east of the Yermak Plateau or into the Barents Sea.

Moritz and Colony (1988) estimated the spatial variations in sea ice velocity statistics using observations of ice drift and geostrophic wind in the area between the North Pole and Fram Strait. They concluded that daily sea ice motions are not predictable, in detail, beyond the range of deterministic surface wind forecasts, about 3 days. They calculated shear and divergence of the ice to be largest in the northern Greenland Sea and Fram Strait. They also concluded an average sea ice drift velocity of about 10 km per day through the southern reaches of Fram Strait and that the large scale opening of the ice pack typical of the region arises mainly from mean divergence acting on ice advected with the mean flow.

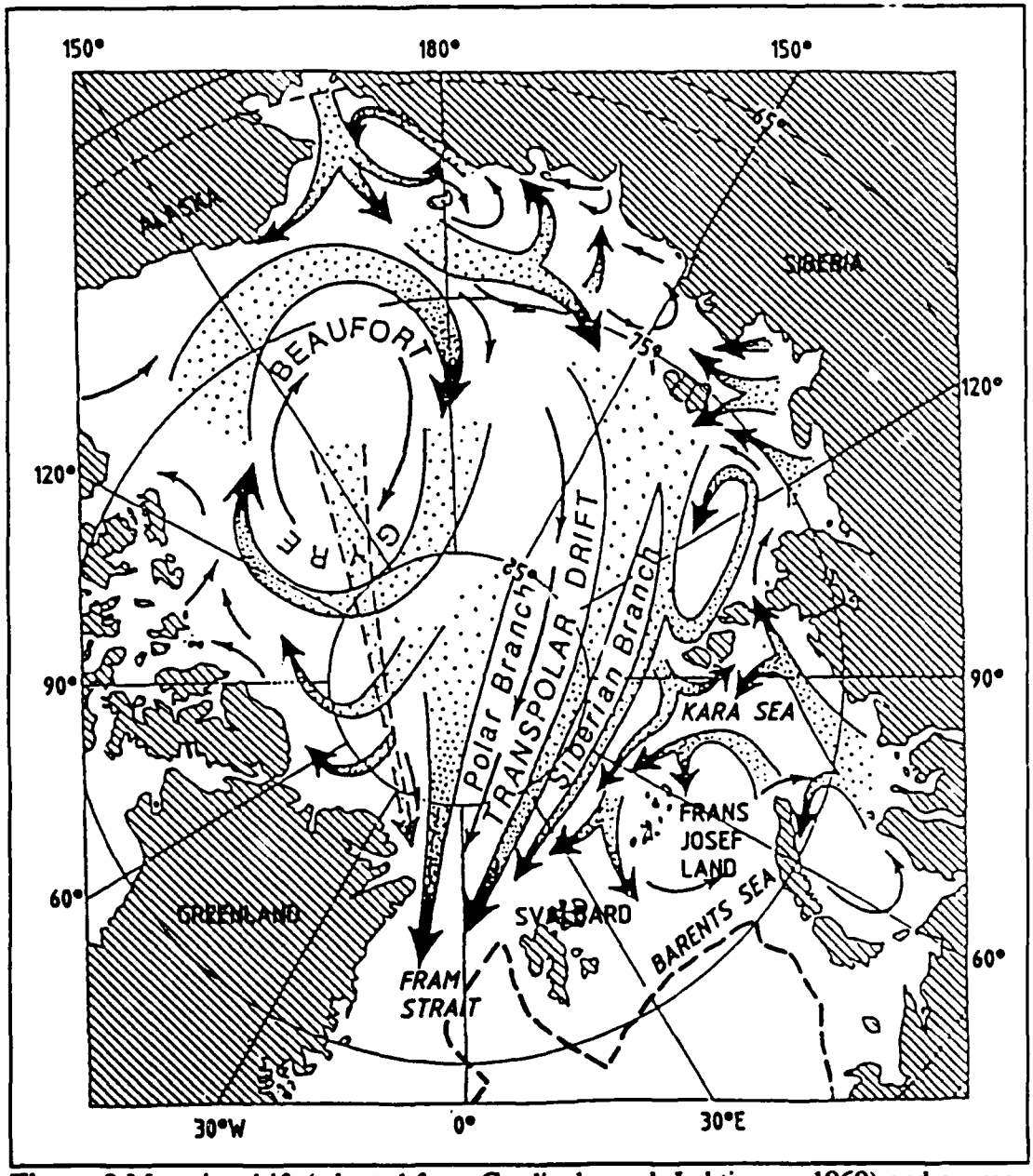

Figure 2 Mean ice drift (adapted from Gordienko and Laktionov, 1969) and average extent of sea ice (1973-1976, based on the 15% concentration level from Parkinson et al., 1987) (from Pfirman et al., 1989).

Of particular interest is their determination that in the Fram Strait, where wind variances are the smallest, the ice velocity variance is largest.

B. THE YERMAK PLATEAU

The Yermak Plateau (Figure 3) is a gnarled finger-like extension of the Barents Sea continental slope occupying roughly 20,000 km^2 off the northwestern coast of Svalbard. Jutting initially north-northwest and then to the northeast, the plateau extends roughly 400 km into the Arctic Ocean. Relatively flat, with depths ranging from 1,000 m to 600 m, the plateau's shallowest depths measured to date are 425 m at 81°18'N, 7°24'E and 485 m at 81°33.5'N, 6°57'E. To the north and northwest the plateau slopes to depths of approximately 3,500 m. The western slope levels out to a 3,000 m plain before plunging to depths greater than 4,000 m associated with the Lena Trough and the Molloy Deep. The eastern slope gradually levels off to an enclosed, broad ?,000 m deep basin. (Perry, 1986).

C. TIDES AND CURRENTS IN THE VICINITY OF THE YERMAK PLATEAU

1. Tides

The Arctic Ocean's tidal surface signature is dominated by semidiurnal displacements. Schwiderski's (1986) method of tidal prediction combines the Newtonian tide-generating potential and hydrodynamical features of the ocean into the Navier-Stokes equations of motion to produce a global tidal prediction system with accuracy of better than ±10 cm. Through the use of tidal decomposition he has produced corange and cotidal maps for eleven tidal constituents covering the entire globe. The leading semidiurnal (M_2, principal

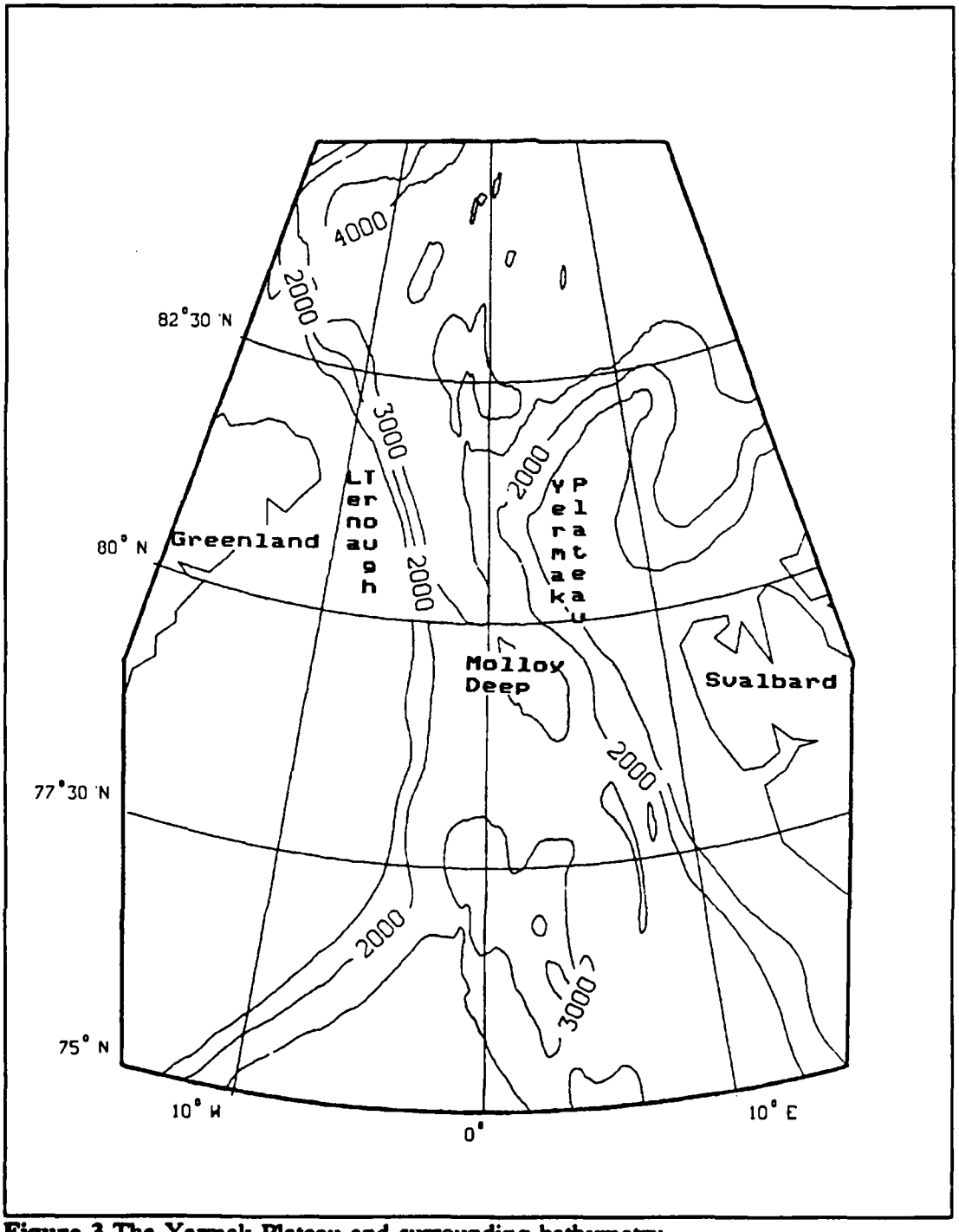

Figure 3 The Yermak Plateau and surrounding bathymetry.

lunar) and diurnal (K_1, declination luni-solar) tidal components respectfully, show the dominance of semidiurnal tidal surface displacement in the Nordic Seas (Figures 4 and 5). Although the diurnal K_1 tide has a power input of about 58% of the dominant semidiurnal M_2 tide, its surface height amplitude in the open Nordic Seas reaches only about 10 cm while the M_2 surface height amplitude extends to about 80 cm. The superposition of the two principal semidiurnal lunar (M_2) and solar (S_2) tides creates a beat which is evident as a fortnightly (14.77 day) spring-neap inequality of surface heights. In the vicinity of the Yermak Plateau, Schwiderski's (1986) data show semidiurnal amplitudes on the order of 20 cm and diurnal amplitudes of only 2 to 3 cm.

2. Tidal currents

Morison et al. (1987) examined data collected as part of MIZEX 84 and noted the difficulty in analyzing the current data because the measurements were made from a platform drifting with the ice in a region with intense spatial variability and also because the semidiurnal-inertial currents were in part due to inertial motions that arose as a result of wind transients and were therefore of random phase. They concluded that standard tidal analysis was not suitable to this area and overcame the problem by using the complex demodulation technique developed by McPhee (1986) and discussed later in this paper.

The water velocity structure in the Greenland Sea marginal ice zone was observed with current meters deployed beneath the ice from floes occupied by the R/V Polar Queen during June and July of 1984. The drift track of the Polar Queen is shown in Figure 6. Morison et al. (1987) and McPhee (1987) presented results which showed both strong semidiurnal and diurnal motions during this period. During the period of drift over the

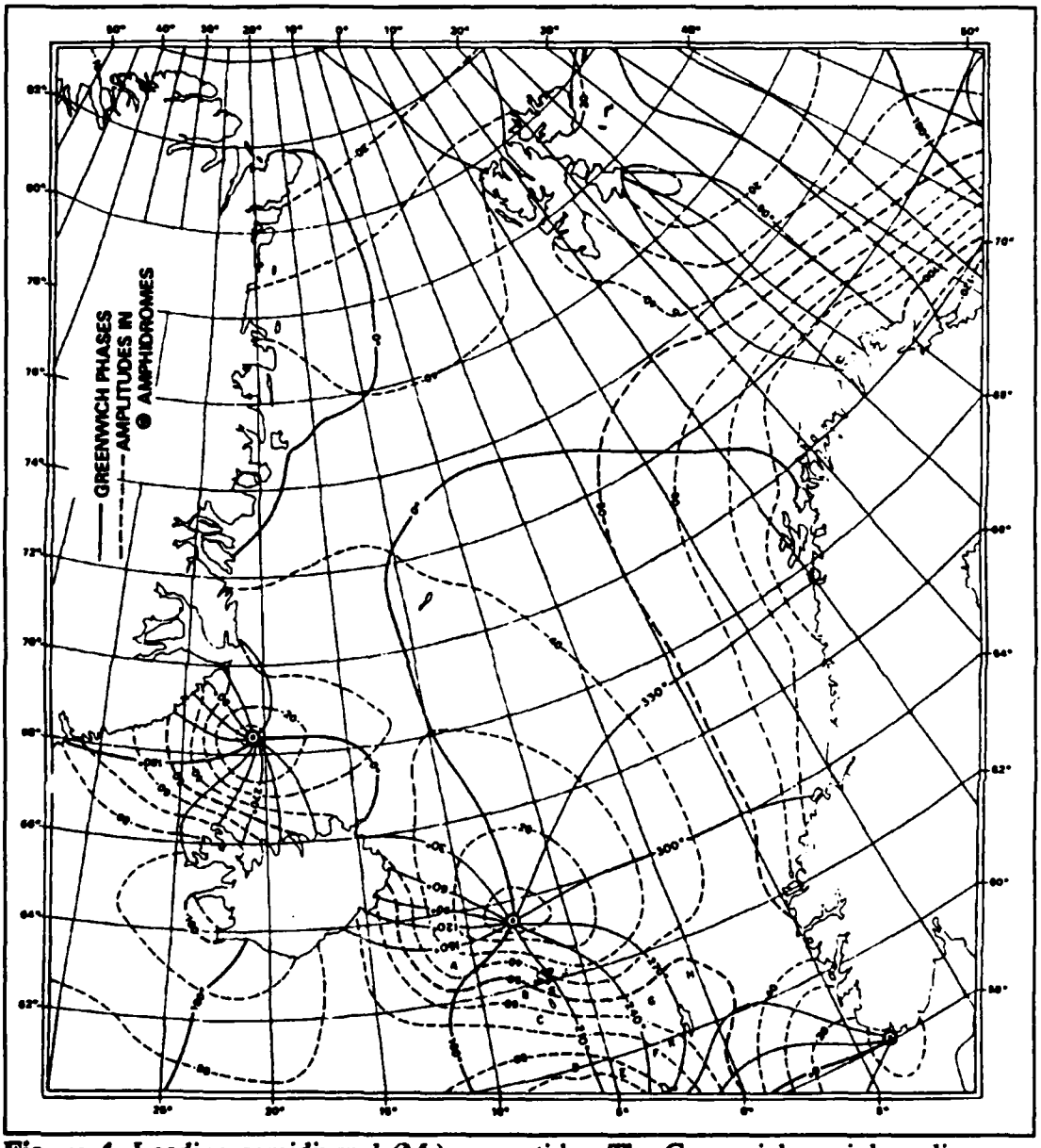

Figure 4 Leading semidiurnal (M_2) ocean tide. The Greenwich equiphase lines are spaced every 30° ≈ 1 hour, and the equiamplitude lines are spaced every 10 cm (from Schwiderski, 1986).

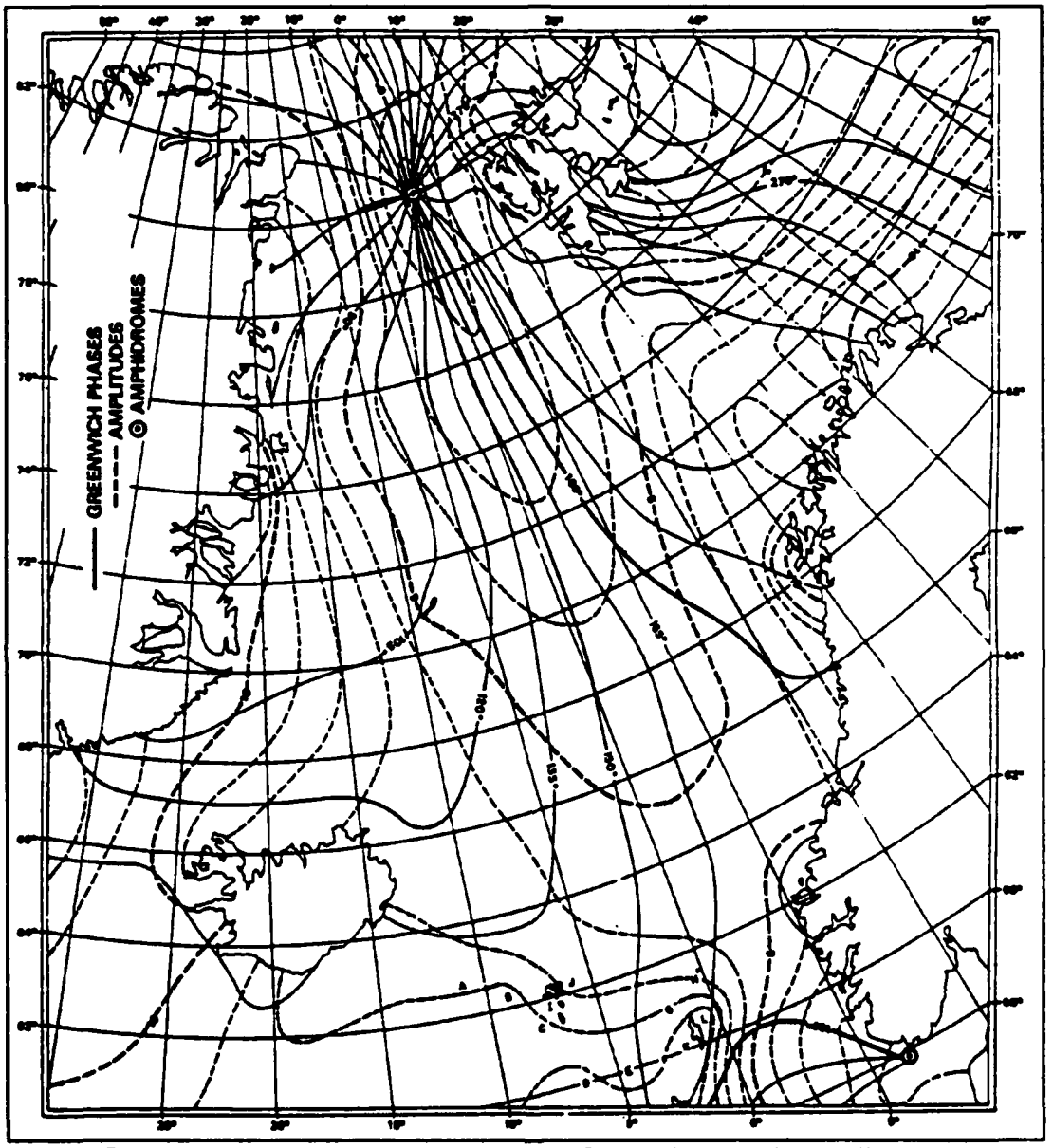

Figure 5 Leading diurnal (K_1) ocean tide. The Greenwich equiphase lines are spaced every 15° ≈ 1 hour, and the equiamplitude lines are spaced every 1 cm (from Schwiderski, 1986).

southwest slope of the Yermak Plateau the diurnal component of motion was especially apparent. The remainder of the record showed little energy at the diurnal period. Morison reasoned the observed diurnal motion which occurred while over the plateau may have been a combination of forced internal tidal motion with a barotropic motion. McPhee cited the topographic vorticity wave theory presented by Hunkins (1986) as a possible explanation.

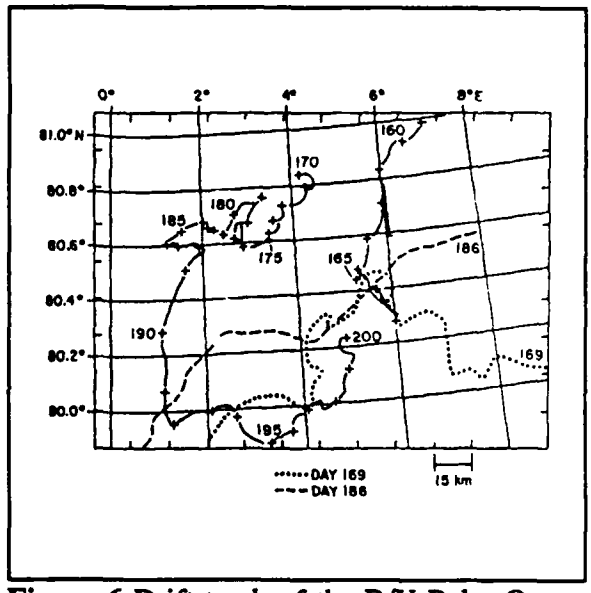

Figure 6 Drift track of the R/V Polar Queen during MIZEX 84 (numbered solid line). Broken lines indicate the ice edge (modified from Morison et al., 1987)

Tidal currents in the northern reaches of Fram Strait were examined by Hunkins (1986) using current meter data from the FRAM III (1981) and FRAM IV (1982) drifting ice stations. The stations were occupied during the April/May time frame of their respective years and followed similar, but not identical, tracks. Both ice stations initially were over the abyssal depths, approximately 4,000 m, north of 84°N and later drifted over the shallower depths associated with the flank of the Yermak Plateau (Figure 7).

FRAM III had current meters suspended below it at two levels, 25 and 104 m. FRAM IV had current meters at five levels: 29, 55, 104, 153 and 303 m. Absolute, relative to the bottom, current velocities were determined by vectorial subtraction of the ice motion, obtained via Transit satellite navigation, from the observed currents. These absolute currents were then resolved into orthogonal components with the *y*-axis parallel to the

bathymetric contours of the northwestern slope of the plateau (060° T), and the *x*-axis directed across the slope (150°T).

Hunkins' analysis of the current record for FRAM III revealed a noisy character during the early portion of the drift, while over deep water, showing some evidence of semidiurnal tides. Over the steep northwestern slope of the plateau, a gradient of 1,200 m over approximately 45 km, diurnal tidal currents dominated. In the later part of the drift, while the ice station was over the top of the plateau, semidiurnal motion again dominated.

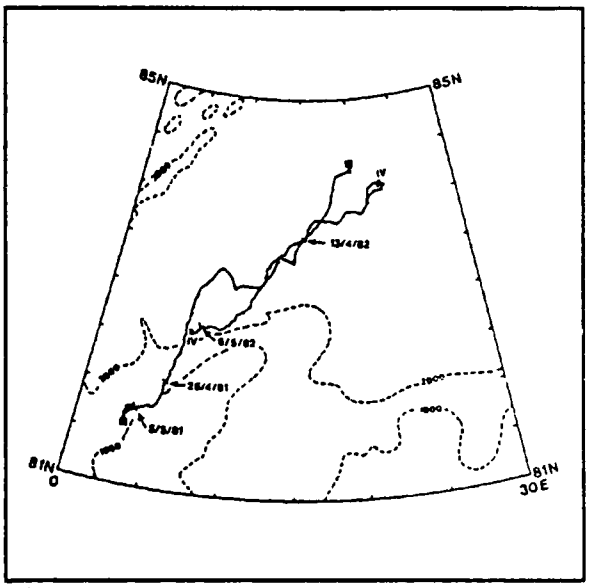

Figure 7 Drift tracks of the ice stations FRAM III and FRAM IV (solid lines). Dates indicate beginning and ending of current meter recordings (from Hunkins, 1986).

FRAM IV's record showed strong diurnal tidal currents while over depths between 1,800 to 3,500 m. Again the early section of the record was noisy with a weak semidiurnal signal. Ice drift, i.e. FRAM IV's position, also showed evidence of tidal motion, but with amplitudes less than that of the current meters suspended below it.

The diurnal current vector over the upper portions of the slope, as observed from the record of FRAM III, described a clockwise, nearly circular rotation. Over the deeper and middle portion of the slope, as observed from the record of FRAM IV, the diurnal motion was nearly rectilinear and aligned in the cross-slope direction.

Hunkins pointed out that the dominance of diurnal tidal currents over the slopes of the Yermak Plateau is in contrast with the overall tidal regime of the area which, as noted above, is a semidiurnal regime. He also noted that the amplitude and phase of the tidal currents changed little with depth, even though there was strong stratification. This lack of shear suggests that the tidal currents are predominantly barotropic in nature.

Hunkins performed time series analysis on the current records and found that while in contact with the plateau the kinetic energy spectra confirmed that the diurnal current amplitude exceeded the semidiurnal amplitude. FRAM IV's along-slope spectrum at 303 m (Figure 8) showed a diurnal peak which is slightly greater than the semidiurnal peak. The across-slope (Figure 9) spectrum, on the other hand, showed the diurnal peak significantly exceeding the semidiurnal. The diurnal tidal ellipse is aligned in the cross-slope direction, while the semidiurnal is aligned along-slope. Hunkins points out that the along-slope alignment of the semidiurnal currents is consistent with an interpretation in terms of Kelvin waves (Kowalik, 1979), while the cross-slope diurnal currents are suggestive of topographic vorticity waves.

It should be noted that surface current velocities, as measured by ice drift, were less than the subsurface current velocities measured by the current meters in all of the above mentioned studies.

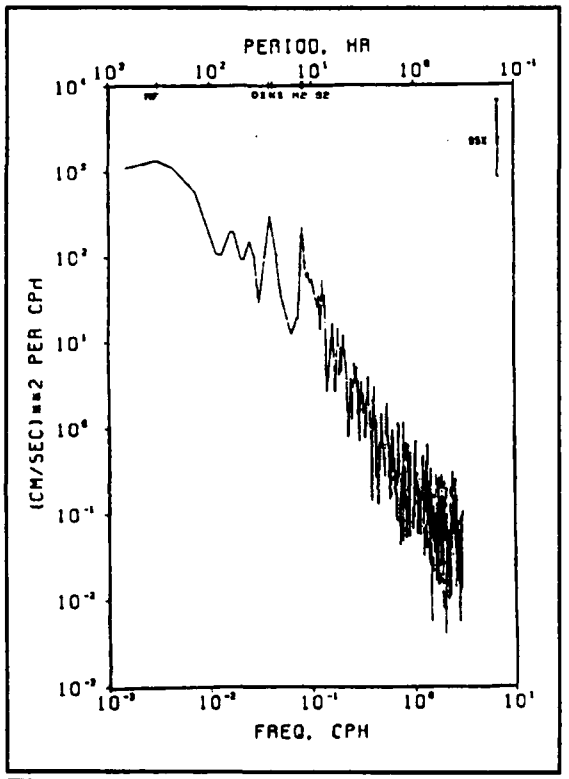

Figure 8 Kinetic energy spectrum for along-slope velocity components, Fram IV, 303 m (from Hunkins, 1986).

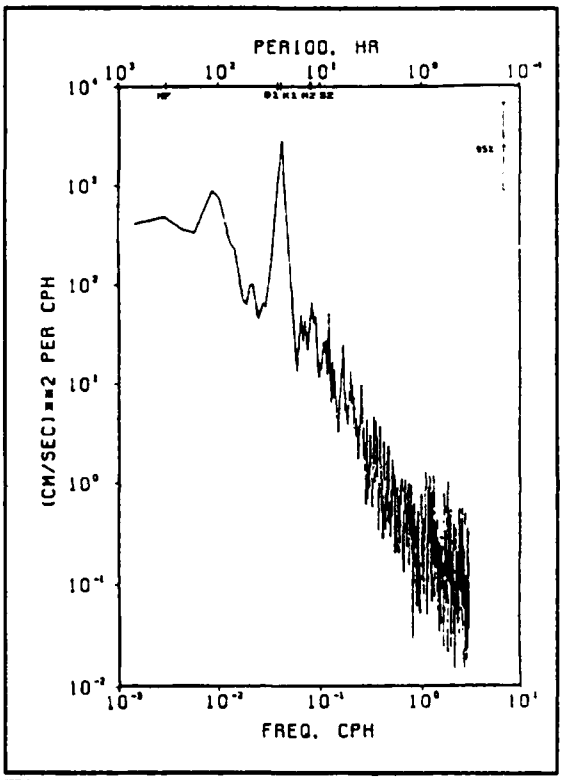

Figure 9 Kinetic energy spectrum for across-slope velocity components, Fram IV, 303 m (from Hunkins, 1986).

D. TOPOGRAPHIC VORTICITY WAVES

Topographic vorticity waves can exit over continental slopes or deep mid-ocean slopes. The restoring force for these waves is the vorticity gradient provided by the sloping bottom. The waves propagate with shallow water to the right in the northern hemisphere. Particle motion conserves potential vorticity Q

$$Q=(f+\zeta)/h$$

where f is the local Coriolis parameter, ζ is the relative vorticity and h is the depth. If h_{und} is the depth of water when the particle is in its undisturbed state ($\zeta=0$), then $Q=f/h_{und}$, and

$$\zeta/f=(h-h_{und})/h_{und}$$

Particles displaced into deeper water will acquire positive, cyclonic vorticity and particles displaced into shallower water will acquire negative, anticyclonic vorticity. Figure 10 shows the motion of particles as they conserve vorticity after being displaced. The solid line represents a line of particles that, in their undisturbed state, lie along a depth contour parallel to the shore. Arrows show the motion induced by vorticity conservation for particles near their undisturbed state. The result is that the particles move to the positions marked by the dashed line.

A theory for vorticity waves around circular islands with sides sloping according to a power law was developed by Longuet-Higgins (1970). Hunkins (1986), following the mathematical development of Longuet-Higgins, made modifications to the boundary conditions and developed a modified theory for a submarine plateau. He used a three-

dimensional circular truncated paraboloid with a flat-top and convexly sloping sides surrounded by a flat bottom to represent the Yermak Plateau. A cross-section through this plateau model is shown in Figure 11.

The relationship between dimensionless frequency, ω/f (where ω is the waves's angular frequency), and the ratio, b, of outer, r, to inner, a, slope boundaries is shown in Figure 12 for the lower modes of oscillation. Hunkins found through inspection of the Yermak Plateau's bathymetry that application of his model required a value of b in the range of 2 and 3. The only diurnal modes which exist in this range are (1,1) with $b = 2.0$ and (1,2) with $b = 2.47$. Profiles for these two values of b are shown in Figure 11. Values of a = 70 km and h_1 = 800 m (depth of the plateau) were chosen as appropriate for application of this model to the Yermak Plateau.

Hunkins concluded that his model, using the above physical representation of the Yermak Plateau and appropriate latitude has free vorticity wave solutions at the diurnal frequency. He also concluded that in a forced wave model these free wave solutions would be associated with resonance conditions and that the model is capable of explaining the anomalously large diurnal currents observed in terms of resonant amplification of weak basin-wide diurnal tides over the plateau's steep slopes. His model has free wave solutions at the diurnal frequency only for the fundamental cross-slope mode. Higher modes occur at lower frequencies well outside of the diurnal range.

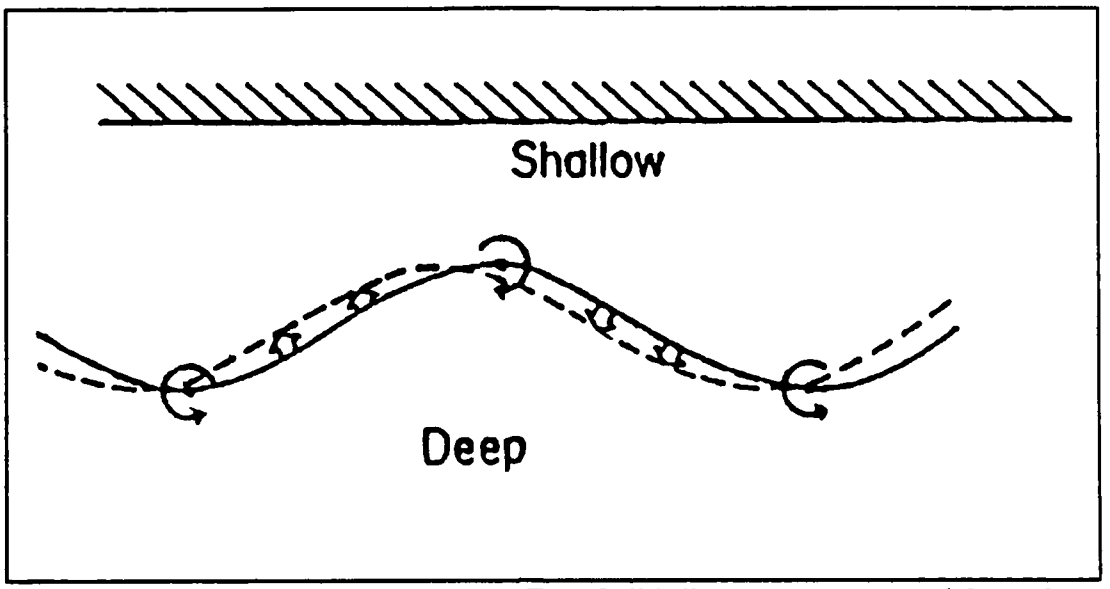

Figure 10 Shelf wave propagation. The Solid line represents particles whose undisturbed position lie along a depth contour. Arrows indicate motion induced by vorticity conservation. The dashed line indicates final position (from Gill, 1982).

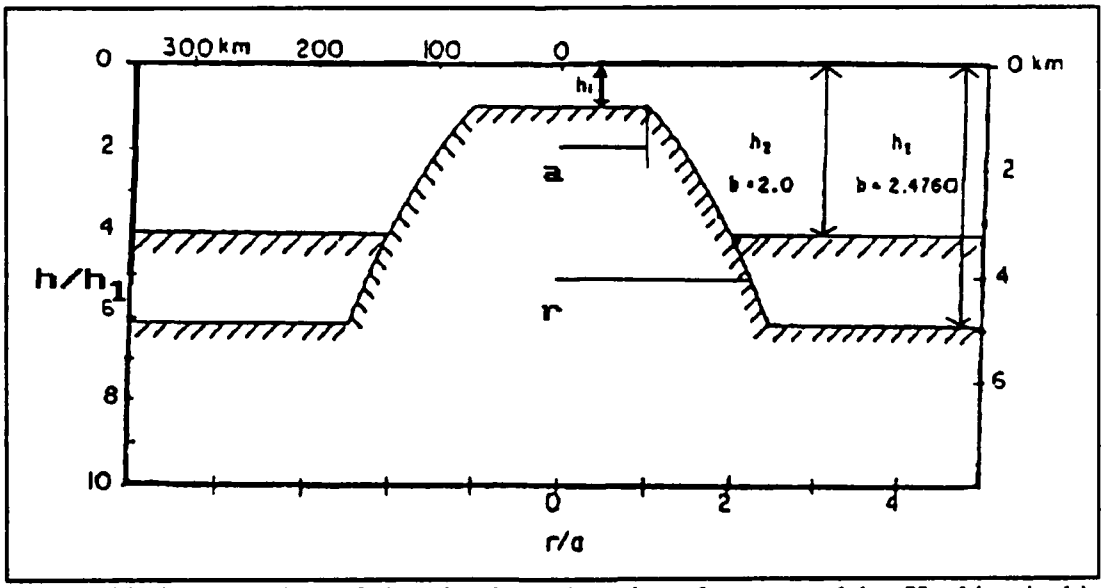

Figure 11 Cross-section of the circular submarine plateau used by Hunkins in his development of a model for trapped topographic vorticity waves (modified from Hunkins, 1986).

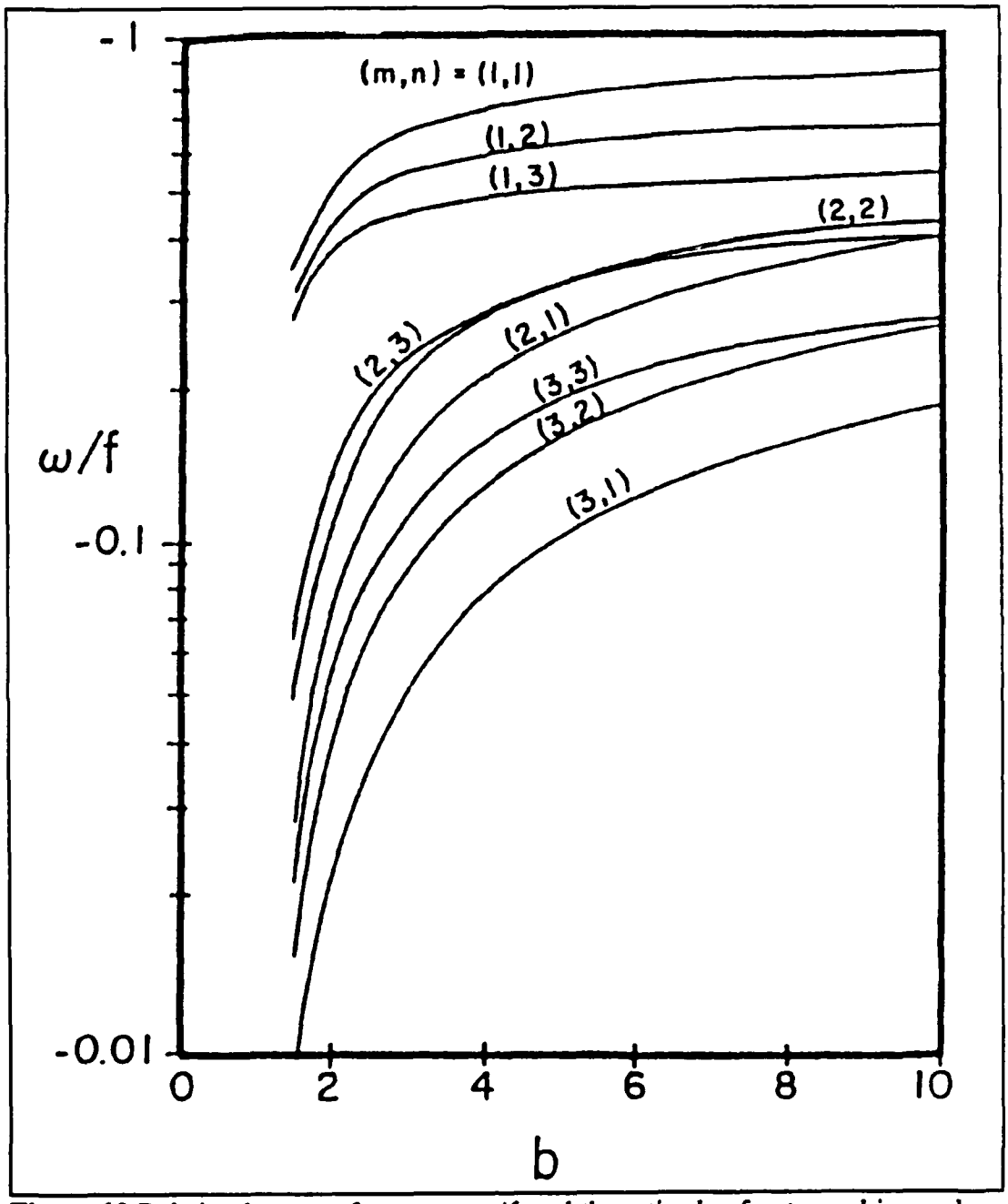

Figure 12 Relation between frequency, ω/f, and the ratio, b, of outer and inner slope boundaries for low modes, m is radial mode number and n is azimuthal mode number (from Hunkins, 1986).

For a given mode the ratio of radii, b, or ratio of depths, b^2, must be tuned to the diurnal frequency. For the (1,1) mode $b = 2$ and $b^2 = 4$. Assuming an average depth of 800 m for the plateau this would put the ocean floor at 3,200 m, a good approximation for the north, northwestern and western approaches to the plateau. For the (1,2) mode $b = 2.47$ and $b^2 = 6.10$. This wave would require a surrounding ocean depth of 4,800 m which is deeper than any of the ocean basins near the plateau.

The flat, eastern approach to the plateau has a basin depth of 2,000 m. For the (1,1) mode wave to exist the plateau would have to be only 500 m deep. For the (1,2) mode the plateau would have to be only 328 m deep. Depths such as these are not found on the plateau.

The idealized topography of Hunkins' model does not lend itself to the determination of which modes will actually dominate on the slopes of the plateau. The existence of resonant modes at the diurnal period in the model are the important result.

II. ARCTEMIZ 86 DATA ANALYSIS

A. ARCTEMIZ 86

ARCTEMIZ 86 was the University of Paris' first attempt in deploying an observational network both for meteorology and marine glaciology in the European Sector of the Arctic Ocean between Svalbard, Greenland and the North Pole. The main objective of the program was to understand, both from a dynamical and thermodynamical point of view, the seasonal and interannual cycle of transpolar sea ice drift in the Nansen Basin while approaching the Fram Strait and the fate and consequences of this drift in the Greenland and Barents Seas (Gascard, 1987). Sea ice motions were obtained by Lagrangian techniques such as ARGOS tracked buoys (examined in this paper). In conjunction with the French/Canadian expedition "Women to the Pole" 15 satellite tracked buoys were deployed during the period of 24 March through 22 May. Their deployment positions and sensors are given in Table 1.

B. RAW DATA

The buoys were tracked by the ARGOS satellite system with position accuracies of approximately 0.5 km. Figure 13 shows the trajectories of all the buoys. The irregularly spaced position data were smoothed using a cubic spline which produced latitude and longitude values at three hour intervals. Figure 14 shows a comparison of the ARGOS fixes (every other fix is plotted) and the resultant smoothed latitude and longitude during a portion of buoy 4985's record. Total (V), east-west (u), and north-south (v) velocities were

TABLE 1 ARCTEMIZ 86 ARGOS BUOYS (from Gascard, 1987)

Buoy Num.	Buoy Type	Deployment Latitude	Deployment Longitude	Deployment Date(julian)
4986	L	83°511 N	24°823 E	24 March(83)
4987	L	83°515 N	23°841 E	30 March(89)
4988	L	83°119 N	23°138 E	11 April(101)
4989	L	83°249 N	21°808 E	18 April(108)
4990	L	83°478 N	23°087 E	25 April(115)
4991	L	83°379 N	22°738 E	1 May(121)
4985	L Ta	83°655 N	20°583 E	6 May(126)
4982	L Ta	84°174 N	17°983 E	13 May(133)
4984	L Ta	85°943 N	4°316 E	18 May(138)
4980	L Ta	87°383 N	9°112 E	19 May(139)
5097	L Met Ice	87°383 N	9°112 E	19 May(139)
5088	L Ti	86°403 N	25°430 W	21 May(141)
5078	L Met	86°429 N	25°243 W	17 May(137)
5098	L Met Ice	84°048 N	22°073 W	21 May(141)
5079	L Met	81°601 N	16°664 W	22 May(142)

L = Localization buoy
Ta = Air temperature
Ti = Ice temperature
Met = Atmospheric pressure
Ice = Ice temperature profile

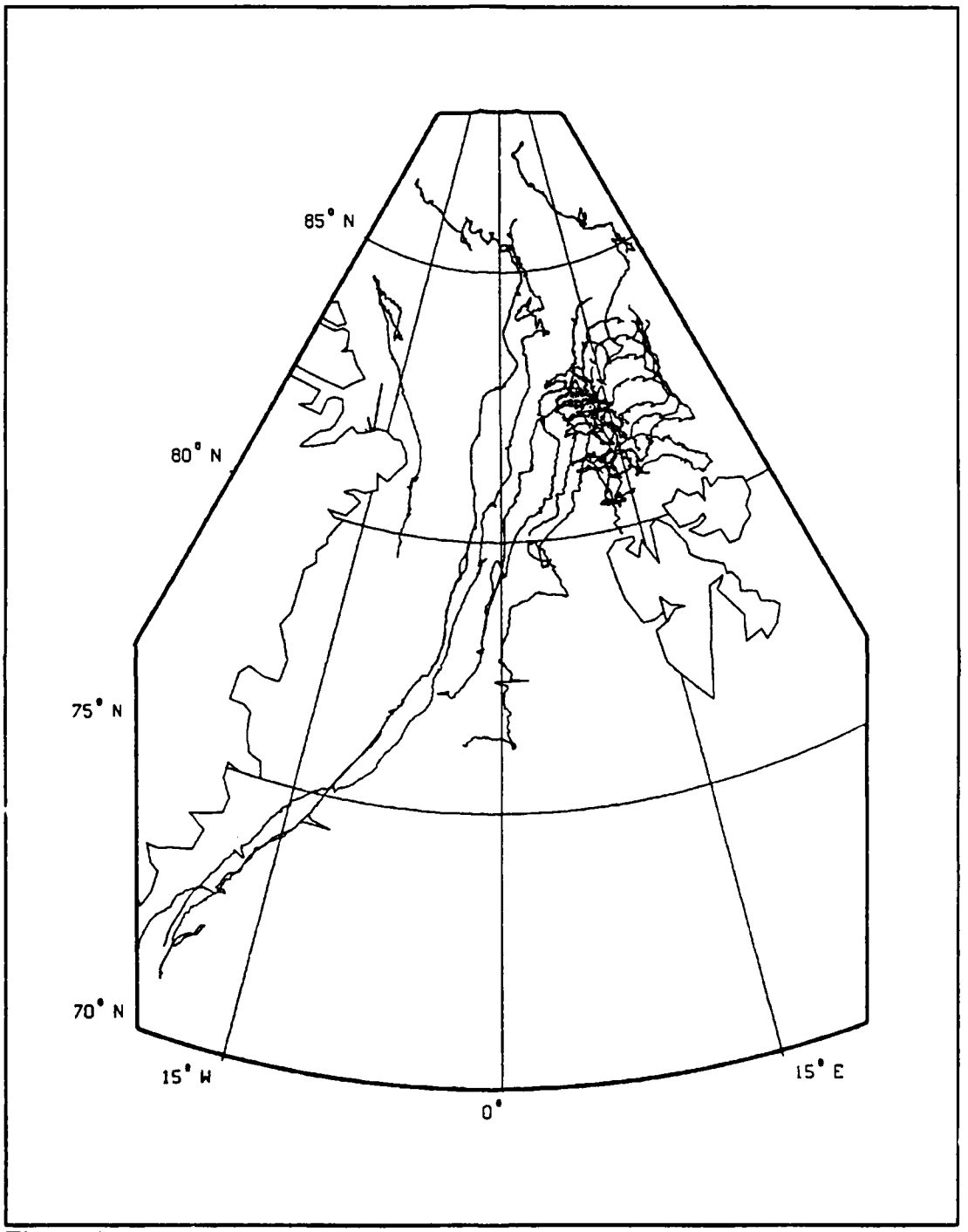

Figure 13 Trajectories of ARCTEMIZ 86 sea ice drift buoys.

computed from these smoothed positions based on the distance covered by the buoys since their previous position, three hours earlier.

All of the buoy's trajectories are illustrated in Appendix A. Of the fifteen buoys deployed during ARCTEMIZ 86, nine drifted through the region of the Yermak Plateau. Enhanced views of their tracks while in the vicinity of the plateau are found in Appendix B. Buoy 5079 remained trapped north of Greenland between Perry Land and Cape Nordostrundingen and because its motion is not really indicative of the Transpolar Drift, unlike the other buoys, it will not be considered in any further computations.

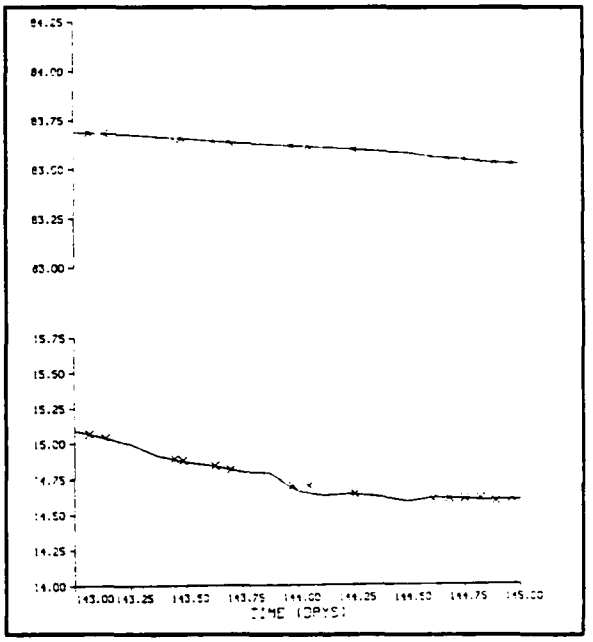

Figure 14 Comparison of the smoothed (solid line) latitude (top) and longitude (bottom) calculated by cubic spline method and ARGOS fixes (X) for buoy 4985. Every other ARGOS fix is plotted.

C. TIME SERIES ANALYSIS

Time series analysis was performed using a fast fourier analysis of velocity data to produce kinematic energy spectra (data were assumed to be ergodic). Initially the effort was directed towards discerning differences in long period motions (on the order of one month) between buoys deployed in the western entrances to Fram Strait (buoys 4980, 4984, 5078, 5079, 5088 and 5098 corresponding to the Polar Branch of the Transpolar Drift) and eastern entrances to Fram Strait (buoys 4982, 4985, 4986, 4987, 4988, 4989, 4990, 4991 and 5097 corresponding to the Siberian Branch).

The rational was to observe dynamical differences between the two regions indicating the two tongued Transpolar Drift as theorized by Gascard et al. (1988) and Pfirman et al. (1989).

Dividing the sampling periods into months and seasons brought out only subtle differences between the two regions for long period motions. By far the most striking difference was in shorter, chiefly the diurnal and semidiurnal, period motions. Whereas the western buoys showed little diurnal energy, the eastern buoys showed diurnal energies exceeding that of even the semidiurnal frequency (Figures 15 and 16). Upon examining the bathymetry along the buoy trajectories the hypothesis was made that the anomalously high diurnal energy levels observed for the eastern buoys during periods when they were in the vicinity of the Yermak Plateau were a surface signature of the topographically trapped vorticity wave described by Hunkins (1986). Fourier analysis was performed for periods before and after the eastern buoys passed over the 3,000 m contour associated with the plateau. While the buoys were in the deep waters of the Arctic basin there is no significant peak in the energy spectrum at the semidiurnal or diurnal periods is discernable (Figures 17 and 18). After crossing the 3,000 m contour, the energy spectrum shows a diurnal peak significantly exceeding the semidiurnal peak (Figures 19 and 20).

D. DEMODULATION

Complex u and v velocity demodulation was performed using the technique developed by McPhee (1986) for each of the buoys to determine the temporal and spatial extent of the enhanced diurnal currents. The method assumes the ice drift trajectory to be a superposition of the mean motion, the circular or elliptical oscillations at the semidiurnal tidal (or inertial)

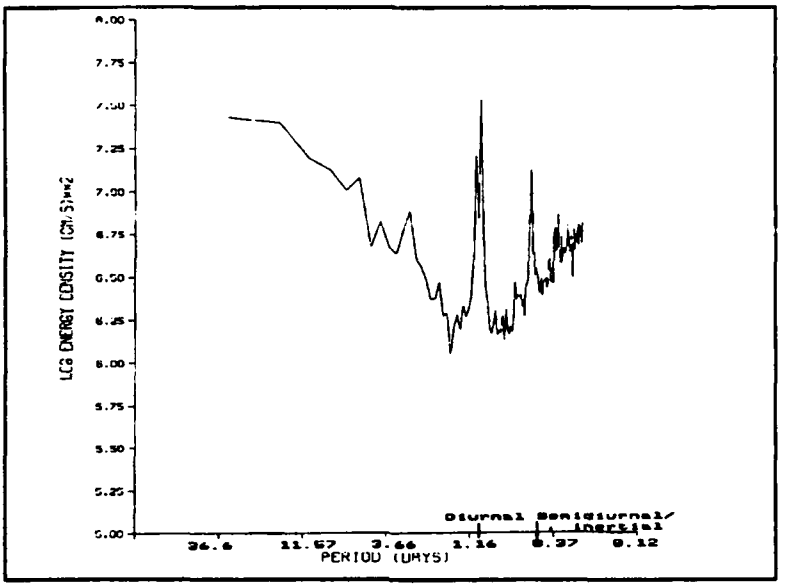

Figure 15 Kinetic energy spectrum for *u* component of velocity for the eastern buoys. 47 samples, each sample is 32 days long.

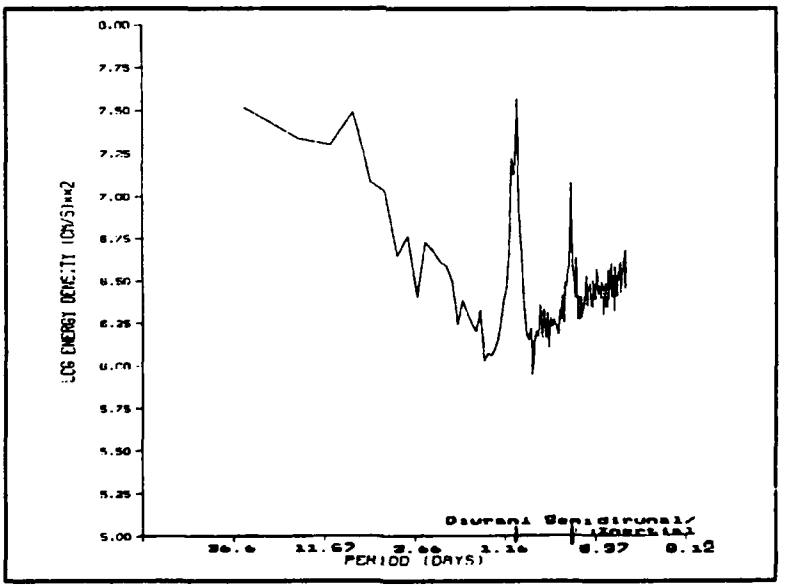

Figure 16 Kinetic energy spectrum for *v* component of velocity for the eastern buoys. 47 samples, each sample is 32 days long.

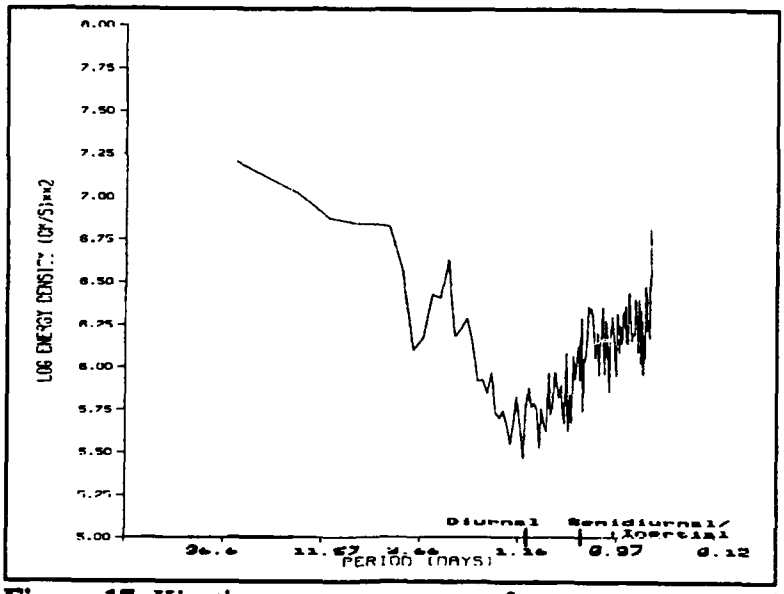

Figure 17 Kinetic energy spectrum for *u* component of velocity for the eastern buoys while in deep (depth greater than 3,000 m). 15 samples, each sample is 32 days long.

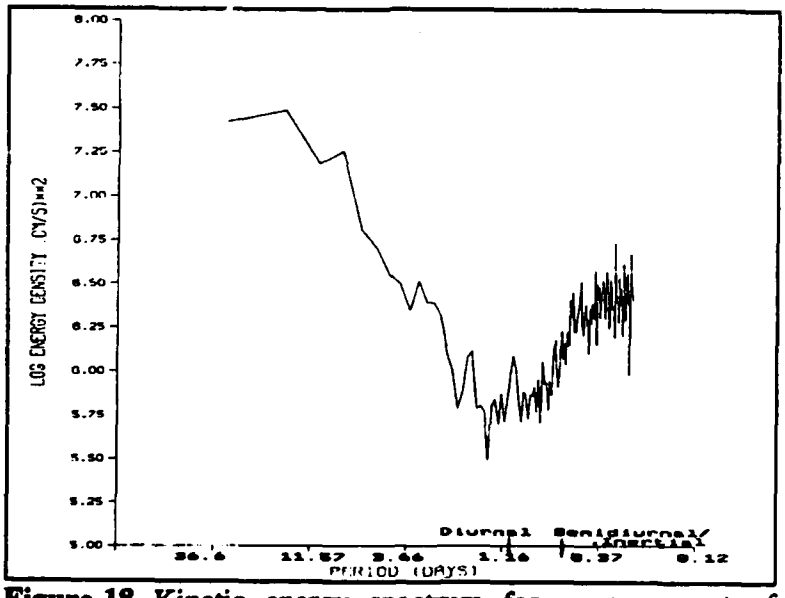

Figure 18 Kinetic energy spectrum for *v* component of velocity for the eastern buoys while in deep (depth greater than 3,000 m). 15 samples, each sample is 32 days long.

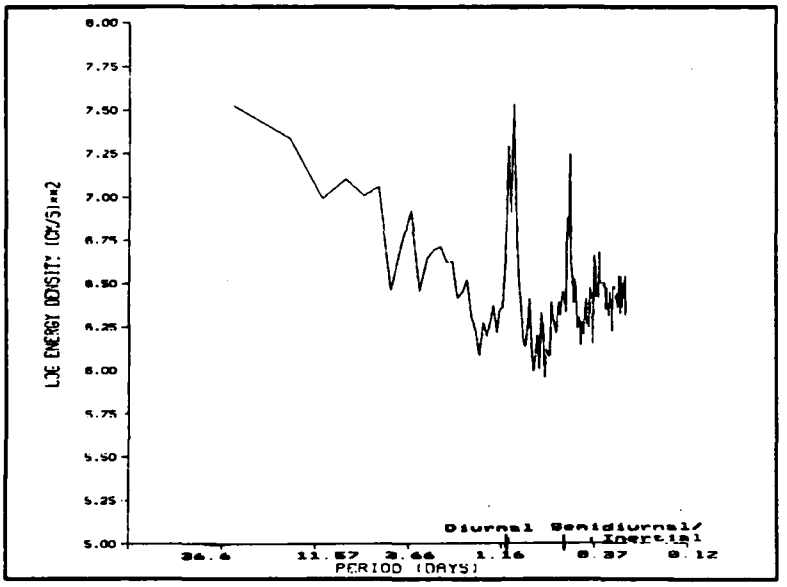

Figure 19 Kinetic energy spectrum for u component of velocity while the eastern buoys were in contact with the Yermak Plateau (depth less than 3000 m). 28 samples, each sample is 32 days long.

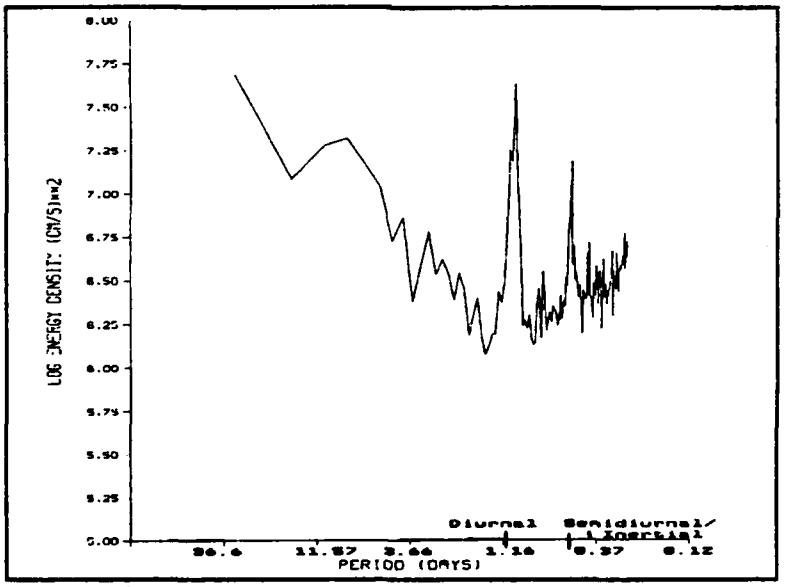

Figure 20 Kinetic energy spectrum for v component of velocity while the eastern buoys were in contact with the Yermak Plateau (depth less than 3000 m). 28 samples, each sample is 32 days long.

and the diurnal tidal frequency. The complex demodulation algorithm separates the diurnal and semidiurnal tidal components from the lower frequency 'synoptic' drift.

$$V = V_m + S_{cw}e^{-ft} + S_{ccw}e^{ft} + D_{cw}e^{-\omega t} + D_{ccw}e^{\omega t}$$

where V is the total complex velocity, V_m is mean complex velocity and S_{cw}, S_{ccw}, D_{cw} and D_{ccw} are the semidiurnal clockwise, counterclockwise and diurnal clockwise, counterclockwise complex coefficients, respectively. The complex coefficients are chosen to produce a least squares error fit to the total velocity. f is the semidiurnal frequency and ω is the diurnal frequency. In the latitudes of interest, 80°N-84°N, the leading, M_2, semidiurnal period (12.2 hours) is nearly identical to the inertial period (an average of 12.1 hours) and the two will be treated as one and the same. In fact, the two can be discriminated by examining their phase and/or polarization.

Appendix C is a collection of plots showing the u and v velocity components of the complex tidal coefficients for all the buoys. Figures 21a and b show the total diurnal clockwise velocity, $D_{cw}e^{-\omega t}$, for all the buoys. The western buoys do not show any periods of significant amplification of the diurnal signal. The eastern buoys can be divided into two groups, one with significant, and one with only minor, if any, amplification of the diurnal signal. The distinction between the two latter groups is associated with the slope of the plateau where the buoys cross the 3,000 m contour (Figures 21a and b and Appendix B).

The record for buoys 4985 and 4991 are good examples of the amplification of the diurnal signal. A comparison of Figures 21a and b with Figure 22, a portion of the drift tracks of buoys 4985 and 4991 while they were over the Yermak Plateau, reveals that prior to day 175 (24 June), while the buoys were over deep water, they had very little energy in

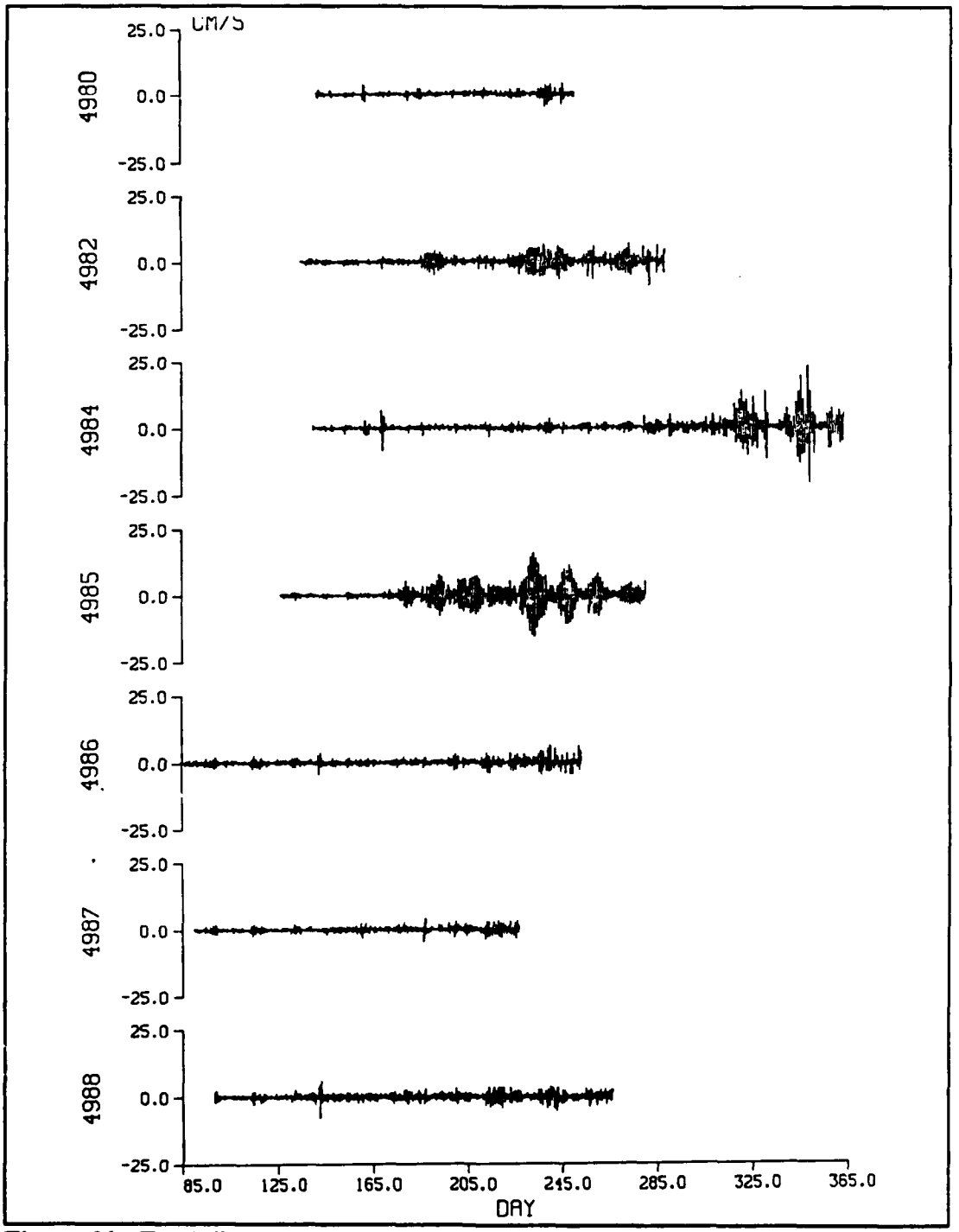

Figure 21a Total diurnal clockwise velocity, $D_{cw}e^{-\alpha t}$, for ARCTEMIZ 86 sea ice drift buoys computed using McPhee's (1986) demodulation technique.

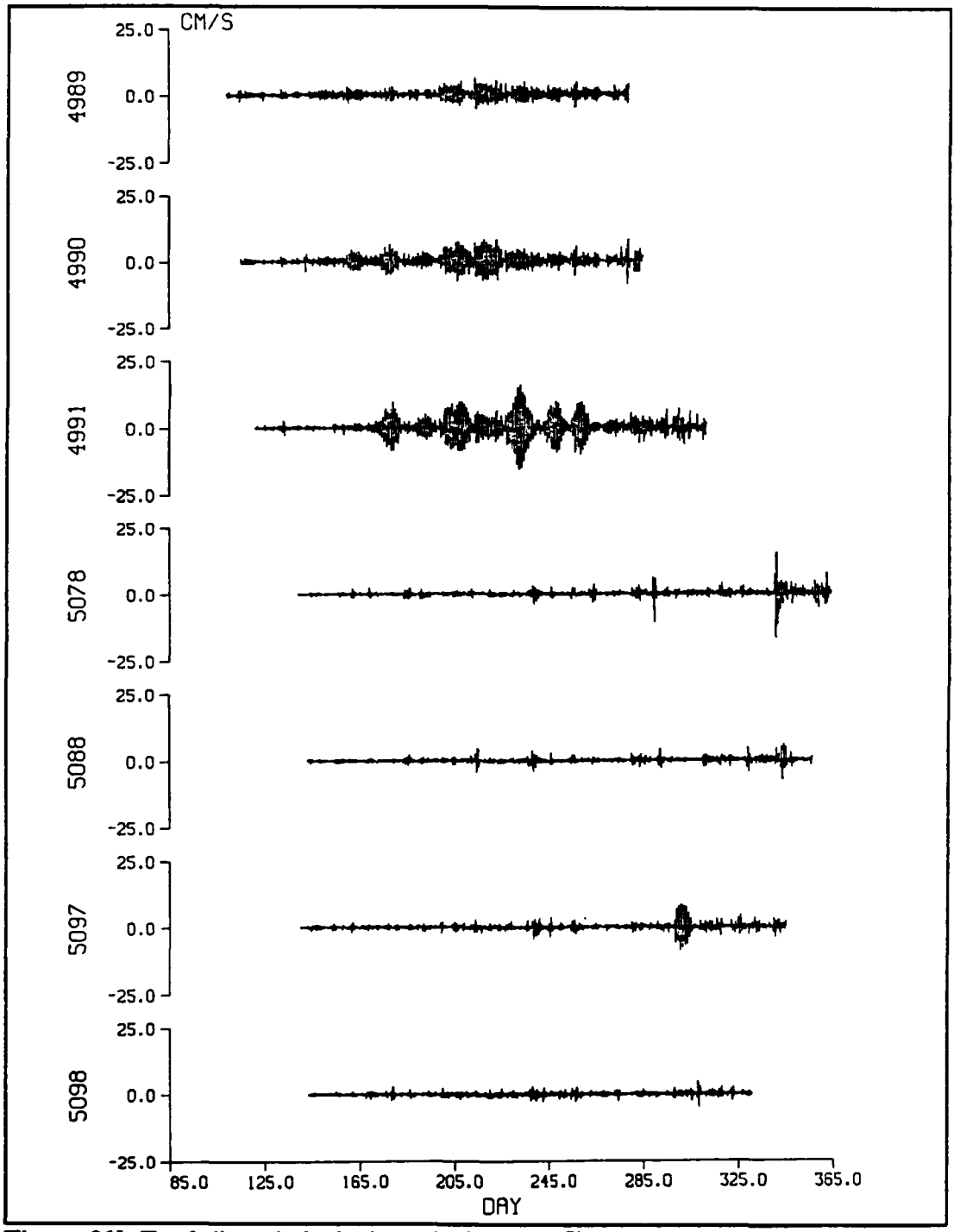

Figure 21b Total diurnal clockwise velocity, $D_{cw}e^{-\alpha t}$, for ARCTEMIZ 86 sea ice drift buoys computed using McPhee's (1986) demodulation technique.

the diurnal components of velocity. Upon crossing the 3,000 m contour these same diurnal components began to increase.

E. DIURNAL LOOPS

Buoys 4985 and 4991 displayed significant along and across-slope oscillations during the period of late June through early September (Figure 22). These oscillations occurred while the buoys were over the northern slope of the Yermak Plateau, between the 1,000 m and 3,000 m contours. Buoy 4985 was slightly down slope of buoy 4991 during the majority of the period. Averaged depth for buoy 4985 is 2,200 m, and 1,400 m for buoy 4991. Evident in these figures is a looping motion during the middle and end of August. Figure 23 shows three of these loops for those two buoys during the period of 18-21 August (day 230-233). Figure 24 shows the diurnal clockwise peak in velocity for buoys 4985 and 4991 during this looping period.

Current vector recomposition (Figures 25 and 26) was performed on the 20 August loop of both buoys using the u and v velocity components of the demodulated tidal coefficients. Both buoys demonstrated approximately an order of magnitude difference between their diurnal clockwise velocity and the other three rotational velocities. The mean flow for buoys 4985 and 4991 (Figure 27) is an order of magnitude less than the dominant diurnal clockwise current during this period. The diurnal clockwise signal also shows a strong across-slope orientation. This motion agrees well with Hunkins' (1986) description of the rectilinear across-slope diurnal motion from the FRAM IV record.

Within the positioning accuracy of the ARGOS system (± 0.5 km) some qualitative and semi-quantitative comments can be made about these loops. The first loop, day 230,

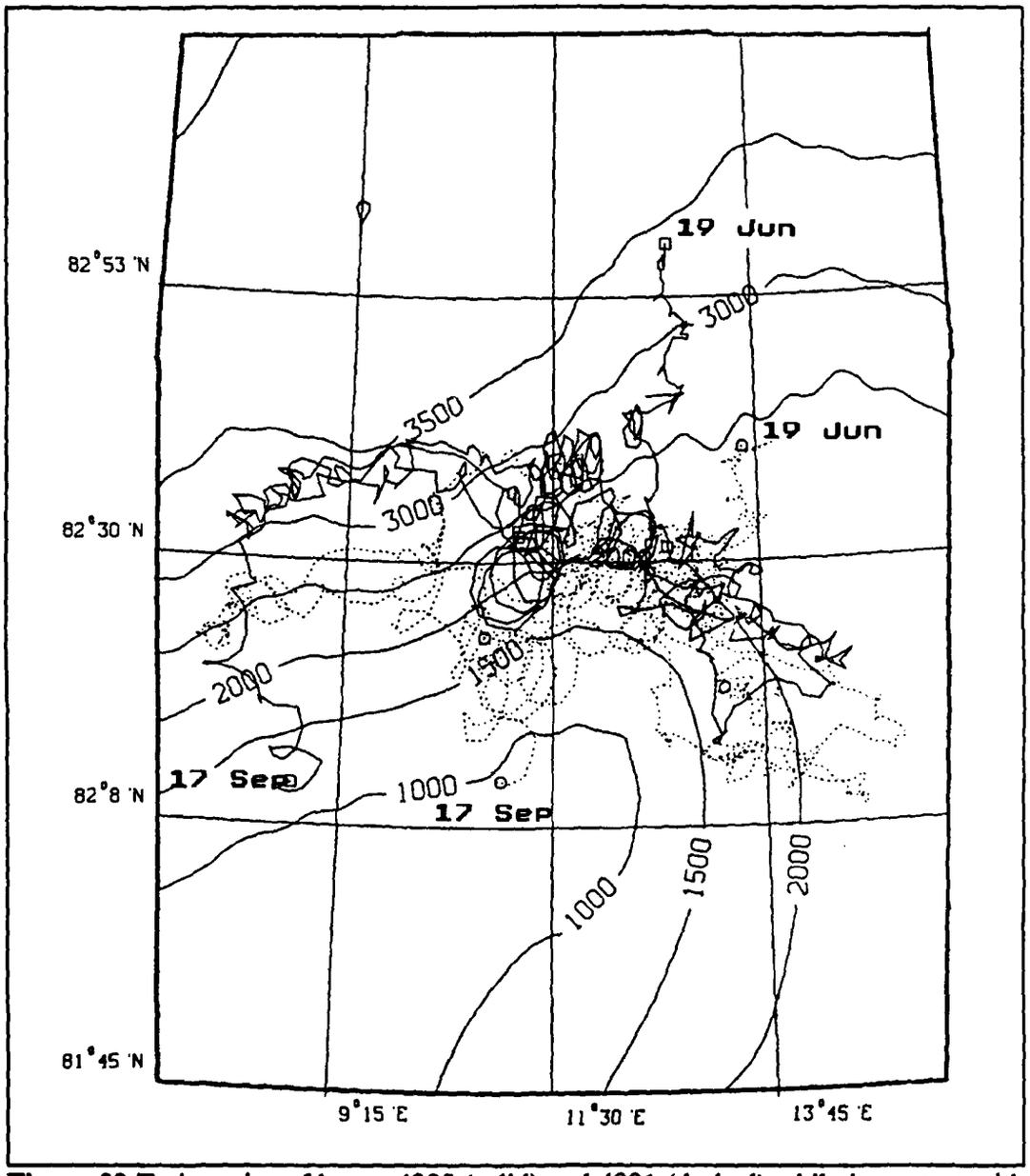

Figure 22 Trajectories of buoys 4985 (solid) and 4991 (dashed) while in contact with the Yermak Plateau.

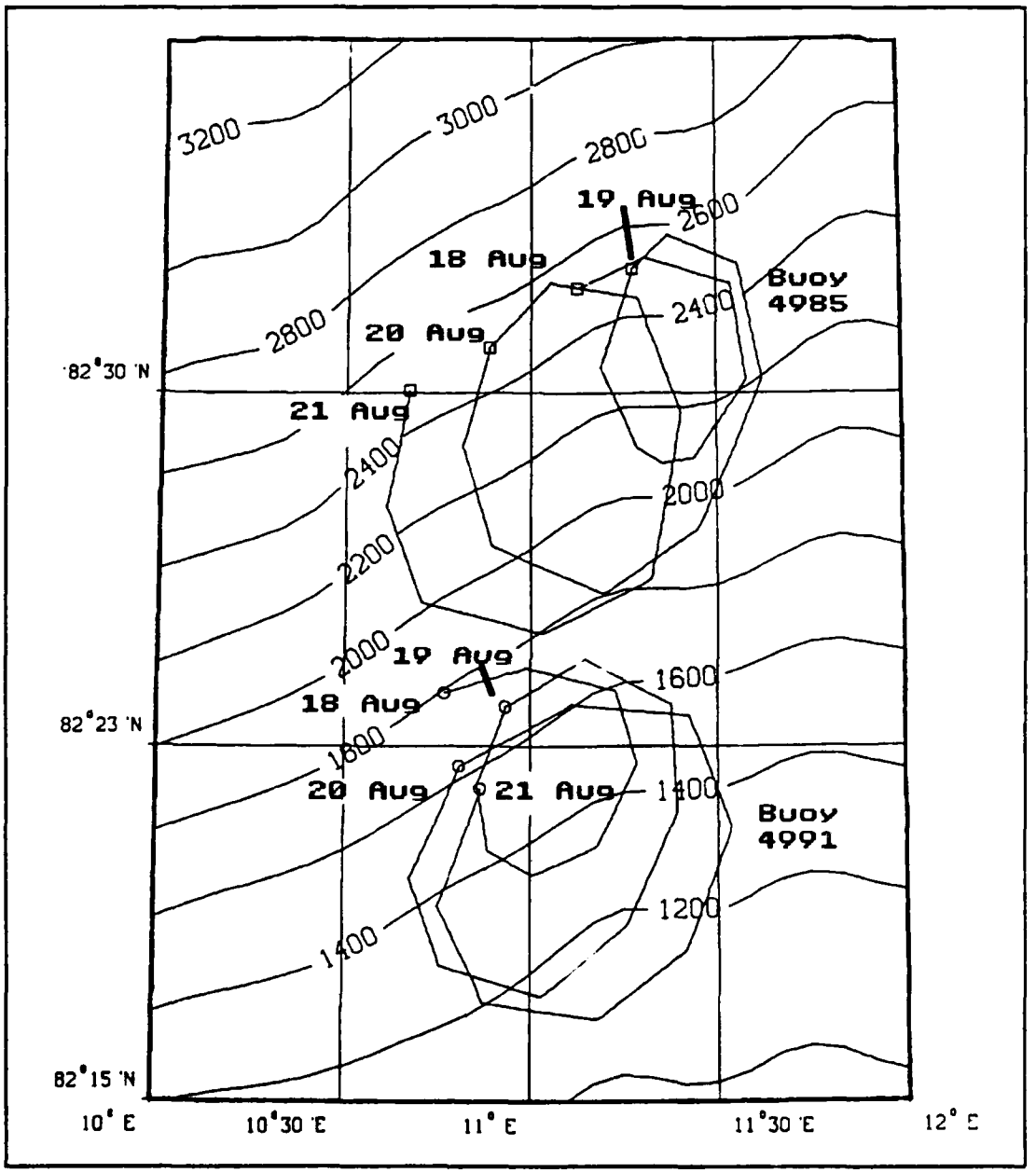

Figure 23 Diurnal looping of buoys 4985 and 4991 during the period of 18-21 August (day 230-233).

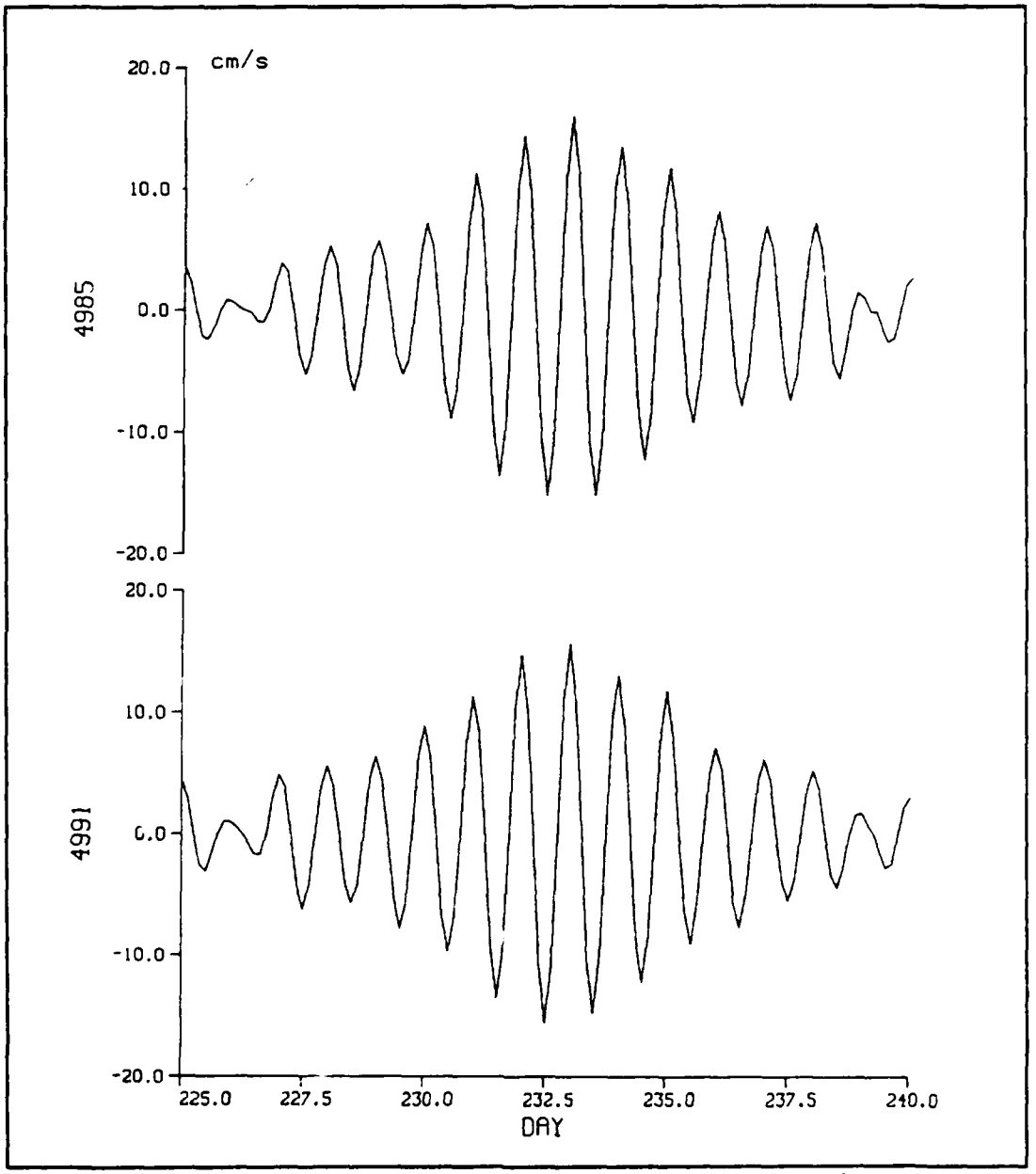

Figure 24 Diurnal clockwise velocity peak associated with the three loop period.

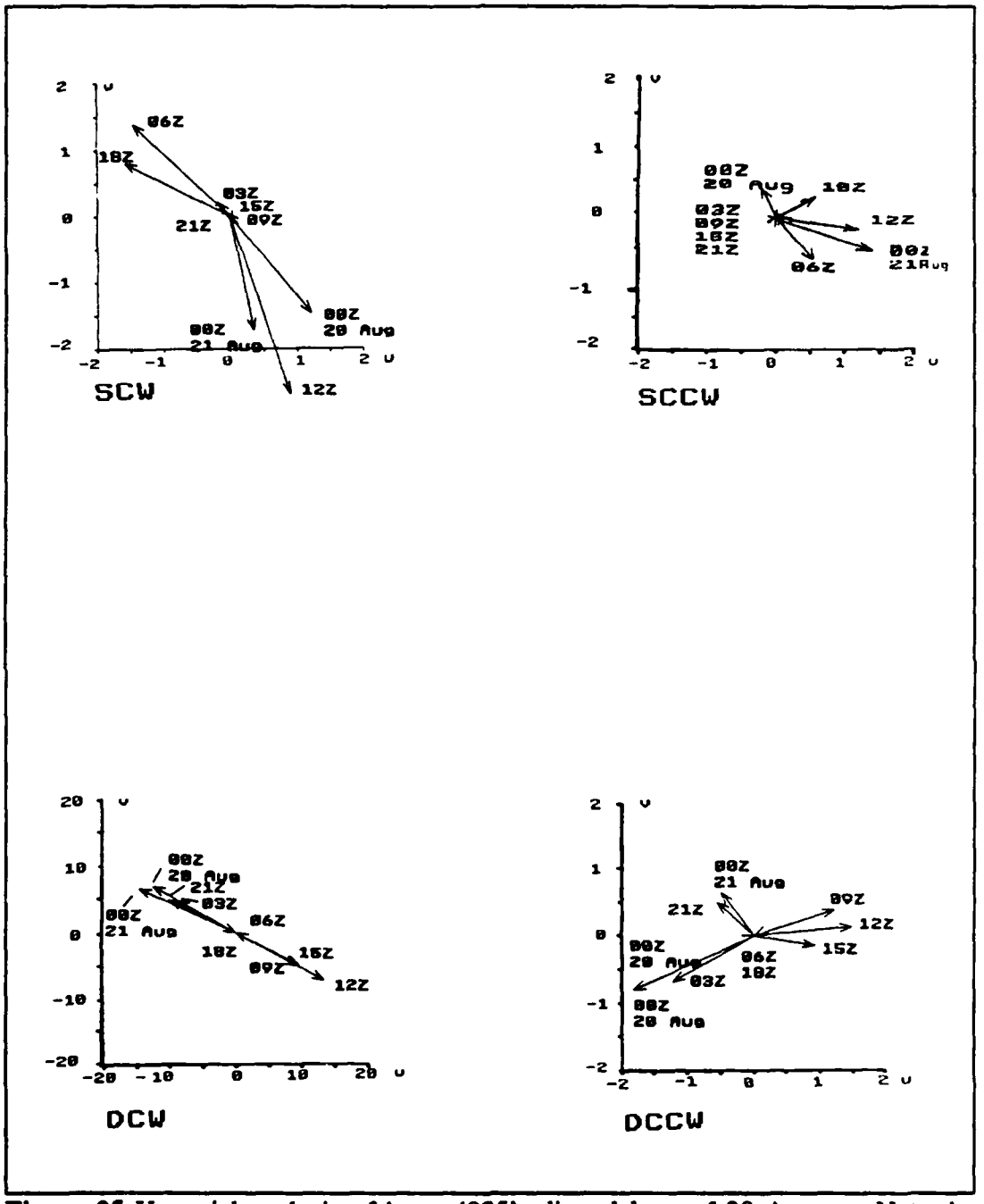

Figure 25 Vectorial analysis of buoy 4985's diurnal loop of 20 August. Note the order of magnitude scale difference for the diurnal clockwise component of motion.

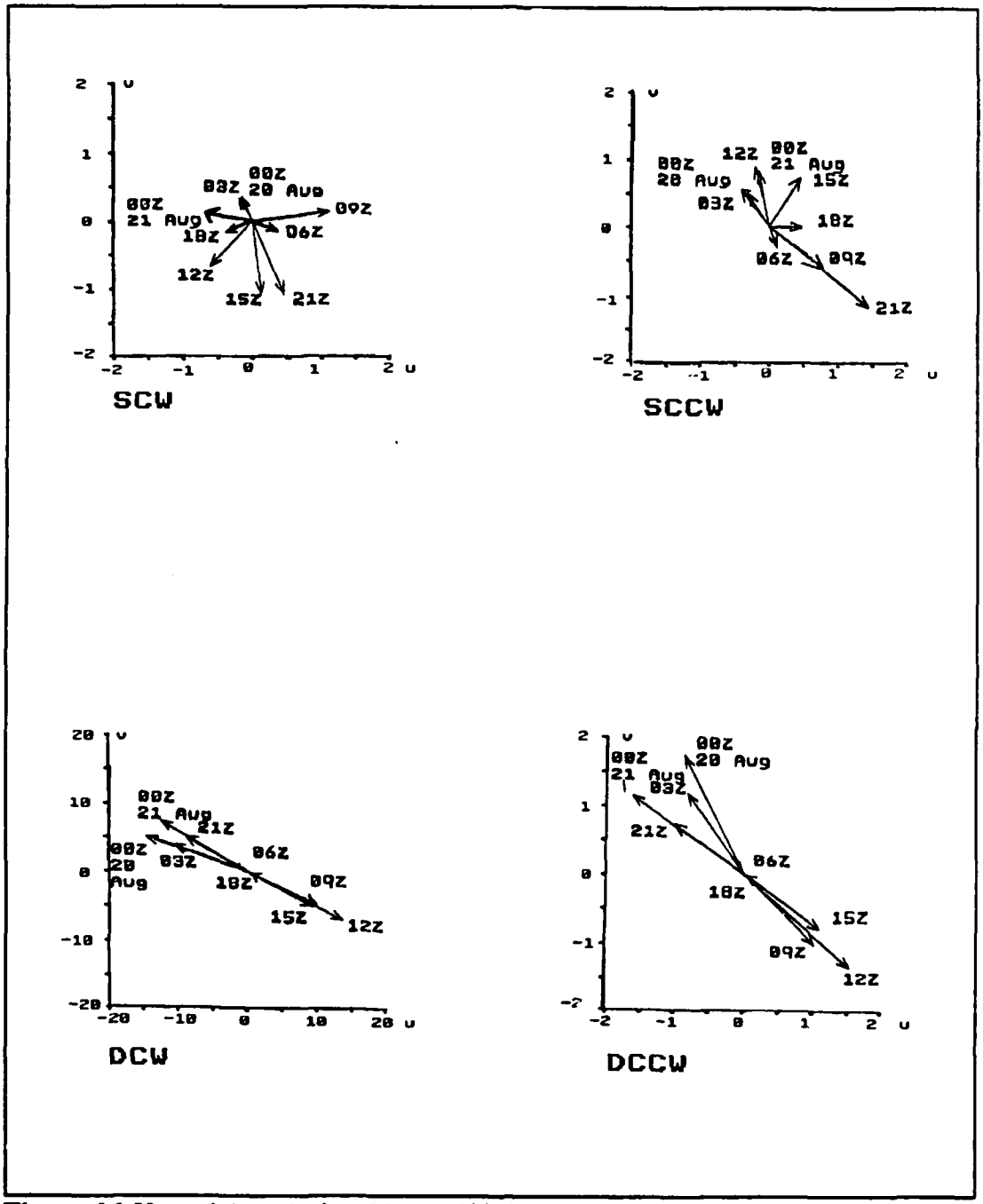

Figure 26 Vectorial analysis of buoy 4991's diurnal loop of 20 August. Note the order of magnitude scale difference for the diurnal clockwise component of motion.

was approximately 7.5 km in diameter for both buoys. Over the next two days the loops increased to diameters of roughly 12 km for days 231 and 232. The most likely explanation for this increase in diurnal clockwise motion is the fortnightly (spring-neap) beat of surface height inequality caused by the superposition of the two principal, M_2 and S_2,semidiurnal tidal components.

McPhee (1987) observed mixed diurnal-inertial/semidiurnal motions over the southwestern flank of the plateau, during an early phase of MIZEX 84. These motions (Figure 28) can be described as open loops, and occurred while the Polar Queen drifted between the 1,000 m and 3,000 m contour. The shape of these loops is most probably the result of a strong mean flow. The ARCTEMIZ 86 closed loops are comparable in size to the MIZEX 84 open loops. Both are diurnal in period and have clockwise rotation. McPhee (1987), using the demodulation technique discussed in the previous section, showed that diurnal currents dominated the inertial/semidiurnal currents during this period (Figure 29). The *u* and *v* diurnal current velocities of the MIZEX 84 open loops are of the same order, approximately 20 and 10 cm/s respectively, as the diurnal clockwise current velocities of the closed loops. Figure 29 also shows that

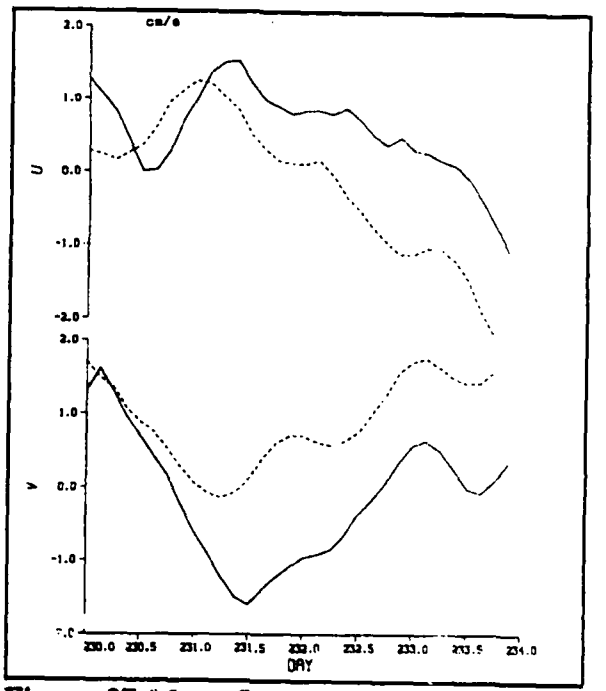

Figure 27 Mean flow, *u* and *v* components, for buoys 4985 (solid) and 4991 (dashed), during the 18-21 August (day 230-233) time period.

the current regime began to show an increase in inertial period motions beginning with day 175 in response to increased wind speeds. This diurnal/inertial motion mix was evidenced by the complex trajectory during the remainder of the observed period and in particular during the last four days (180-184). McPhee acknowledged the presence of inertial currents as an expected result of the prominent role Coriolis forces play in the equation of motion. Following the conclusions of Hunkins (1986) he reasoned that the diurnal motions were a result of some force outside of the wind/ice/boundary layer system.

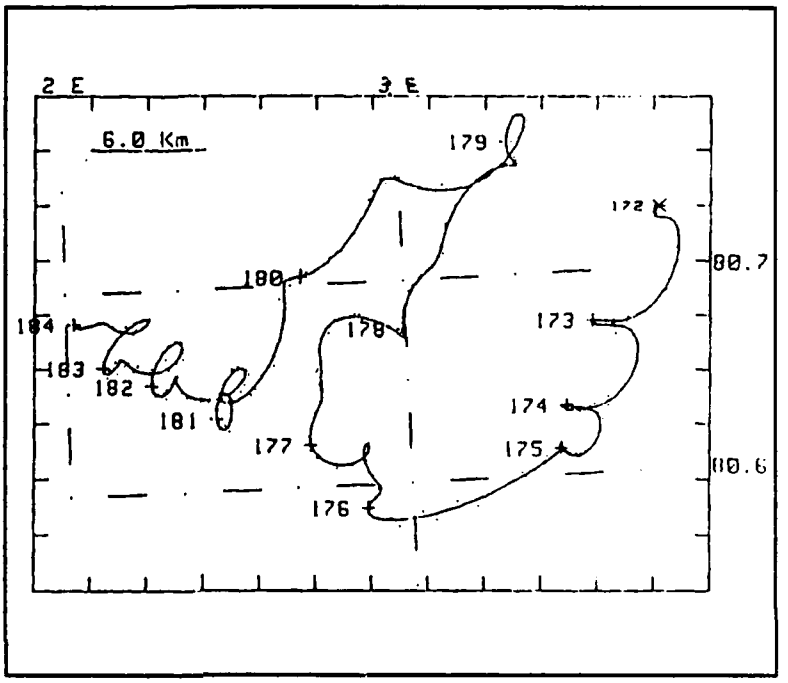

Figure 28 Drift of the R/V Polar Queen during late June and early July 1984 (from McPhee, 1987).

F. TOPOGRAPHIC EFFECT

The periods of strong diurnal currents observed in the data from FRAM III and IV, MIZEX 84 and ARCTEMIZ 86 occurred while the drifting ice was over, respectfully, the northwestern, northern and western slopes, respectively, of the Yermak Plateau between the 800 m and 3,500 m contours.

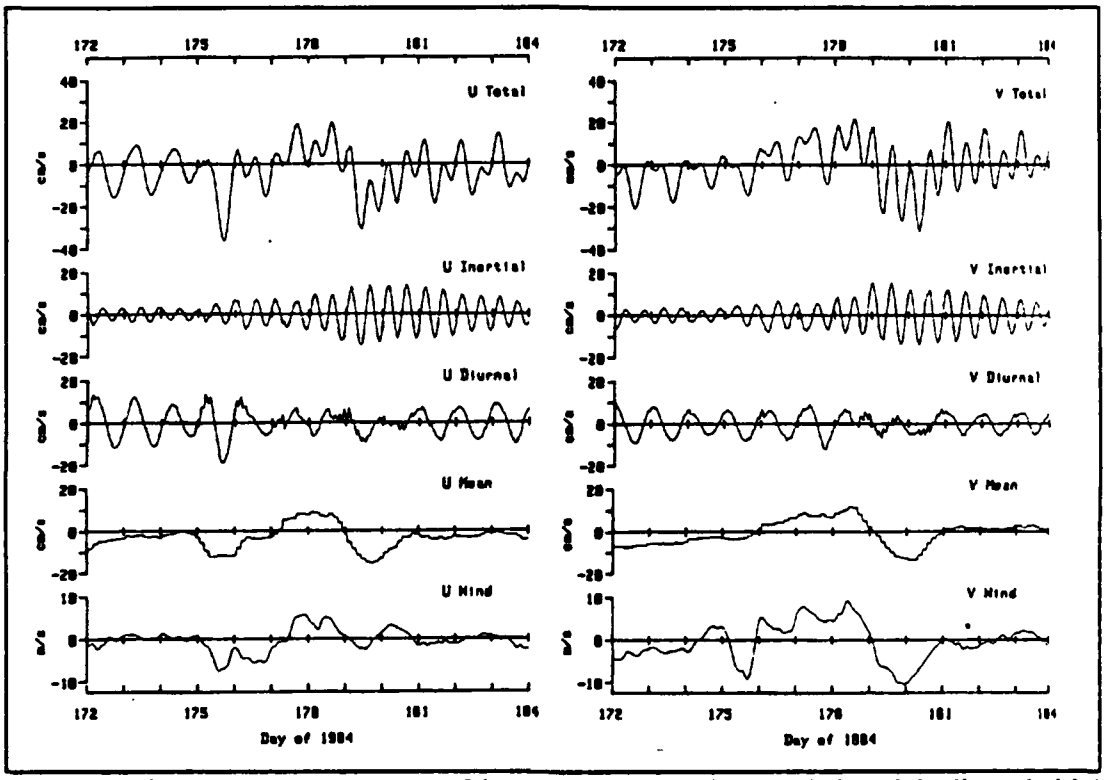

Figure 29 Separated components of ice velocity showing total, inertial, diurnal tidal and mean decompositions, along with observed 10-m wind (east and north positive) (from McPhee, 1987).

During ARCTEMIZ 86 the spatial correlation of enhanced diurnal currents and topography can be seen for buoys 4985 and 4991 in Figure 30. Significant amplification of the diurnal clockwise current appear first for buoy 4991 and then for buoy 4985 as they crossed over the 3,000 m contour and moved into shallower water. Eight large pulses in the enhanced diurnal clockwise currents for these two buoys occurred over a period of 110 day (days 170-280), corresponding to an approximate periodicity of 14 day. The largest of these pulses, number 5 (Figures 23 and 30), which took place between days 220 and 240, corresponded to the period of diurnal looping observed in the previous section while the buoys were over the 2,200 m and 1,400 m contours respectfully.

The slope of the plateau appears to play a key role in determining the amount of diurnal current enhancement. ARCTEMIZ 86 buoys which encountered the plateau over its relatively steep northern and northwestern flanks (buoys 4982, 4985, 4989, 4990, 4991) showed significant enhancements of their diurnal clockwise current signal (Figure 21). These buoys encountered the plateau's steeply sloping northern flank north of 81°30'N and between 5°E-15°E. Buoy 5097 had a significant enhancement of diurnal currents while exiting the plateau over its western slope in the vicinity of 81°30'N and 3°E. This is the same general area where enhanced diurnal currents were reported by McPhee (1987) and Morison (1987) from the MIZEX 84 data.

Buoys 4986, 4987 and 4988 approached the plateau from the enclosed eastern basin and showed (Figure 21) only minor, if any, diurnal current enhancement. As previously noted, Hunkins' (1986) model allows for topographic vorticity waves at the diurnal frequency over the northern, northwestern, and western slopes of the plateau, but not on the

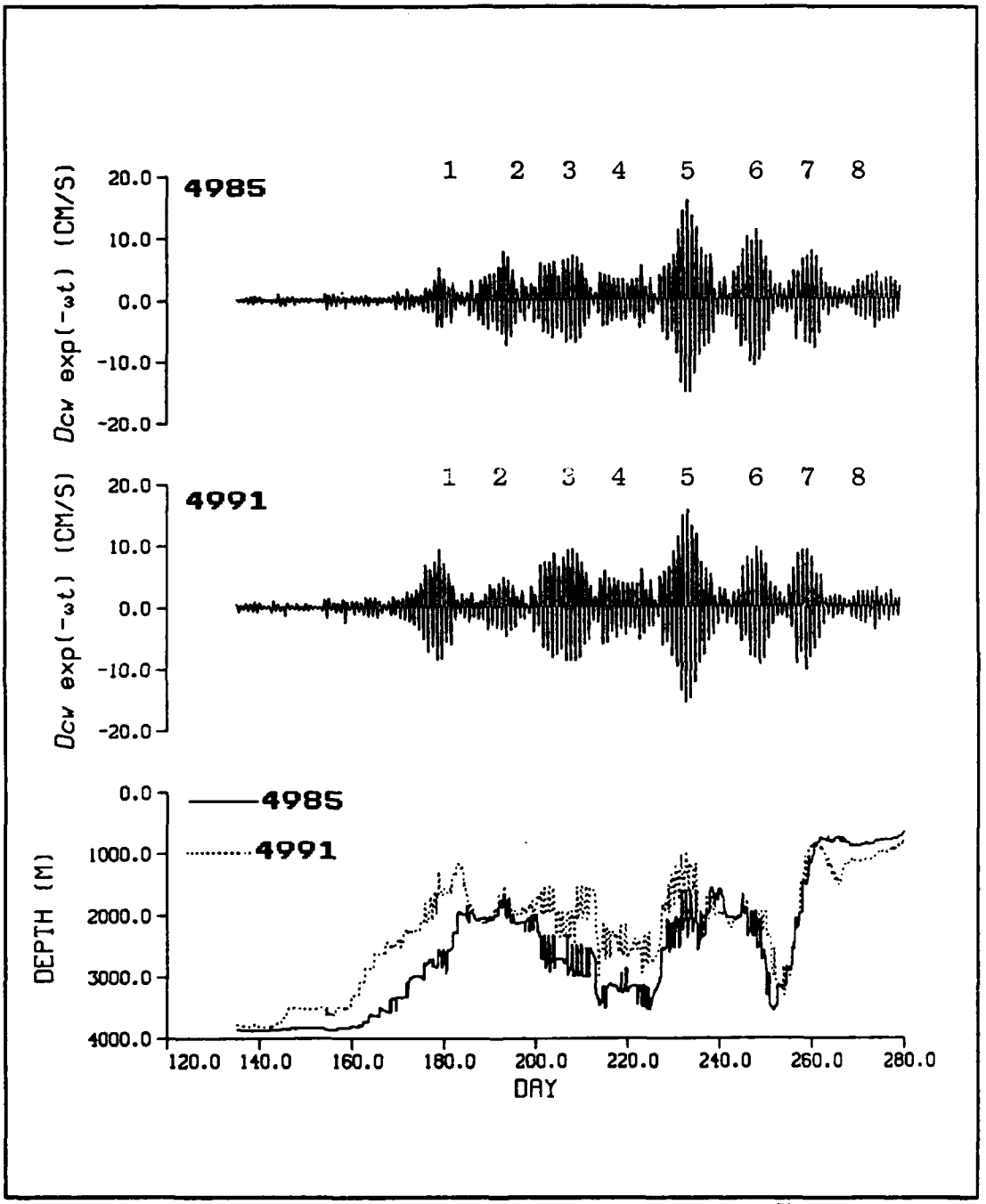

Figure 30 Amplification of the diurnal clockwise tidal current, $D_{cw}e^{-\omega t}$, and bathymetry beneath buoys 4985 and 4991 during days 135-280.

eastern slope. Hence, no source was available to force the diurnal component of these three eastern buoys.

III. DISCUSSION

Relatively strong diurnal surface currents were observed during ARCTEMIZ 86 by drifting ice buoys near the Yermak Plateau confirming the observations of Hunkins (1986), Morison (1987) and McPhee (1987) based upon current meter observations. These diurnal currents exist in a region where the tidal surface displacement is dominated by the semidiurnal (M_2) tidal component. Through time series analysis and complex demodulation a strong correlation has been shown between these enhanced diurnal currents and the bathymetry in the region.

Following the theory of Cartwright (1969), Hunkins (1986) developed a mathematical model of the Yermak Plateau which showed that topographically trapped vorticity waves of diurnal periodicity can exist along the plateau's western, northwestern and northern slopes. Resonant forcing of these topographic vorticity waves by the K_1 diurnal tide generates abnormally strong surface currents of diurnal periodicity in agreement with the drifting buoy observations.

Strong diurnal tidal currents in regions dominated by semidiurnal surface displacements have been reported in five other locations: near St. Kilda, Scotland (Cartwright, 1969); the southern end of Rockall Bank west of Britain (Huthnance, 1974); Vancouver Island, Canada (Crawford and Thomson, 1982); the southern Weddell Sea (Middleton et al., 1987) and the Campbell Plateau near New Zealand (Heath, 1983). In each of these steeply sloping regions the phenomenon was attributed to the selective enhancement of topographic vorticity waves. Hunkins noted that resonant forcing of these

topographic vorticity waves by weak diurnal tides is the mechanism favored most by investigators to explain the enhanced diurnal currents. Other explanations have been suggested which include Huthnance (1974) who suggested that direct gravitational forces drive the strong diurnal tides at the southern end of Rockall Bank and Cartwright et al. (1980) who felt the diurnal wave near St. Kilda was a superposition of a Kelvin and vorticity wave in anti-phase.

Diurnal looping was observed in the data from both MIZEX 84 and ARCTEMIZ 86. The loops were similar in size, had comparable demodulated u and v diurnal current velocities and were clockwise in rotation.

Concurrent surface (ice) and subsurface (current meter) measurements taken during the FRAM III and IV and MIZEX 84 programs showed current velocities to be greater at depth compared to the ice drift rate. This implies the presence of subsurface diurnal tidal currents even stronger than those observed from the ARCTEMIZ 86 ice drift data. Periods of low ice concentrations in this region would allow more free ice drift and result in greater surface tidal current velocities as observed by drifting buoys. Ice concentration, as depicted by the ice analysis charts produced by the Naval Polar Oceanographic Center, was predominantly eight to ten tenths during the entire period of interaction between the ARCTEMIZ 86 buoys and the Yermak Plateau.

Severe winter weather hinders accurate scientific observations in this region. Hence the majority of observations to date have focused on the other three seasons. For example, the ARCTEMIZ 86 buoys interacted with the plateau during the period June to November 1986. The current meter data examined by Hunkins from the FRAM III and IV drift

stations were centered on the April and May time frame during 1981 and 1982. The MIZEX 84 R/V Polar Queen drift and current meter data chronicled the circulation in June and July 1984. Similar observations during the winter season are needed prior to claiming that the enhancement of the diurnal tidal currents in the vicinity of the Yermak Plateau is a year-round phenomena. Winter pack ice conditions would hinder free ice drift. Winter storms with their associated high wind speeds would add significant forcing to the inertial periodicity. These two conditions would lessen the surface diurnal tidal currents observed by ice drift buoys. In contrast, subsurface current measurements would not be as affected. The author feels subsurface current meters suspended below ARGOS tracked ice drift buoys would be the instrument package of choice for current observations in this region during the winter season.

Following ARCTEMIZ 86 the intent of the scientists aboard the R/V Polarstern during the summer of 1987 was to bring the ship to the North Pole along the 30°E meridian in order to seed both the Polar and Siberian branches of the Transpolar Drift with buoys. Their goal was to obtain data which would add validity to the theory of a two tongued Transpolar Drift first forwarded by Gascard et al. (1988) from observations made during MIZEX 83 and 84. Just north of 86°N ice conditions prevented the Polarstern from transitting any farther north. Observations were made of the drift dynamics, composition and morphology of the ice in the Siberian Branch which was found to differ greatly from those made previously in the Polar branch (Pfirman et al., 1989).

The drift dynamics of ARCTEMIZ 86 buoys deployed in the western and eastern entrances to Fram Strait were clearly different in respect to their tidal current energies at the

diurnal period. The added tidal current energy shown by the eastern buoys will contribute to differences in morphology when ice from the two branches is observed in the southern reaches of Fram Strait. Ice from the Polar branch of the Transpolar Drift is typically clear with large undeformed floes suggestive of its oceanic origin and unperturbed drift. Conversely, Siberian branch ice is dirty and thinner with smaller but deformed floes indicative of its formation in proximity to the northern coast of the Soviet Union (Personal communication with J.-C. Gascard). The divergent grinding motion caused by the enhanced diurnal clockwise currents in the vicinity of the Yermak Plateau will add to the already distorted morphology of Siberian branch ice.

IV. CONCLUSIONS AND RECOMMENDATIONS FOR FUTURE STUDIES

Enhanced diurnal tidal currents are present over the northwestern and northern slopes of the Yermak Plateau as observed by ARCTEMIZ 86 ice drift buoys. First observed by Hunkins (1986) in the current meter records of the FRAM III and FRAM IV ice stations, they have also been observed by Morison (1987) and McPhee (1987) in MIZEX 84 current meter and ship drift records. The diurnal tidal currents are the result of resonant forcing of topographic vorticity waves by the K_1 diurnal tide over the steeply sloping flanks of the plateau.

Future studies of the dynamics of sea ice drift in the vicinity of the Yermak Plateau might concentrate on the role that the enhanced diurnal tidal currents play in the break-up/freezing of ice in this region. Recent observation during CEAREX 89 showed a significant increase in turbulent vertical shear flux (200 W/m^2) associated with diurnal currents and diurnal oscillations of the depth of the isotherm in this region which typically has turbulent heat flow values of approximately 30 W/m^2 (Padman and Dillon, 1990). The added energy from the enhanced diurnal clockwise currents can be expected to add a grinding divergent motion to sea ice drifting through this region. The effect of the enhancement appears to be localized to the western, northwestern and northern flanks of the plateau where the bathymetry supports topographic vorticity waves. Remotely sensed sea ice morphology from SAR and AVHRR (during cloud free periods) should show a distinctly different ice morphology above this portion of the eastern entrance to Fram Strait.

APPENDIX A

Trajectories of all the ARCTEMIZ 86 buoys. The tracks are marked beginning with the deployment date and at thirty day intervals until the end of the record. Expanded views of the trajectories for buoys which passed through the eastern margin of Fram Strait and in the vicinity of the Yermak Plateau are presented in Appendix B.

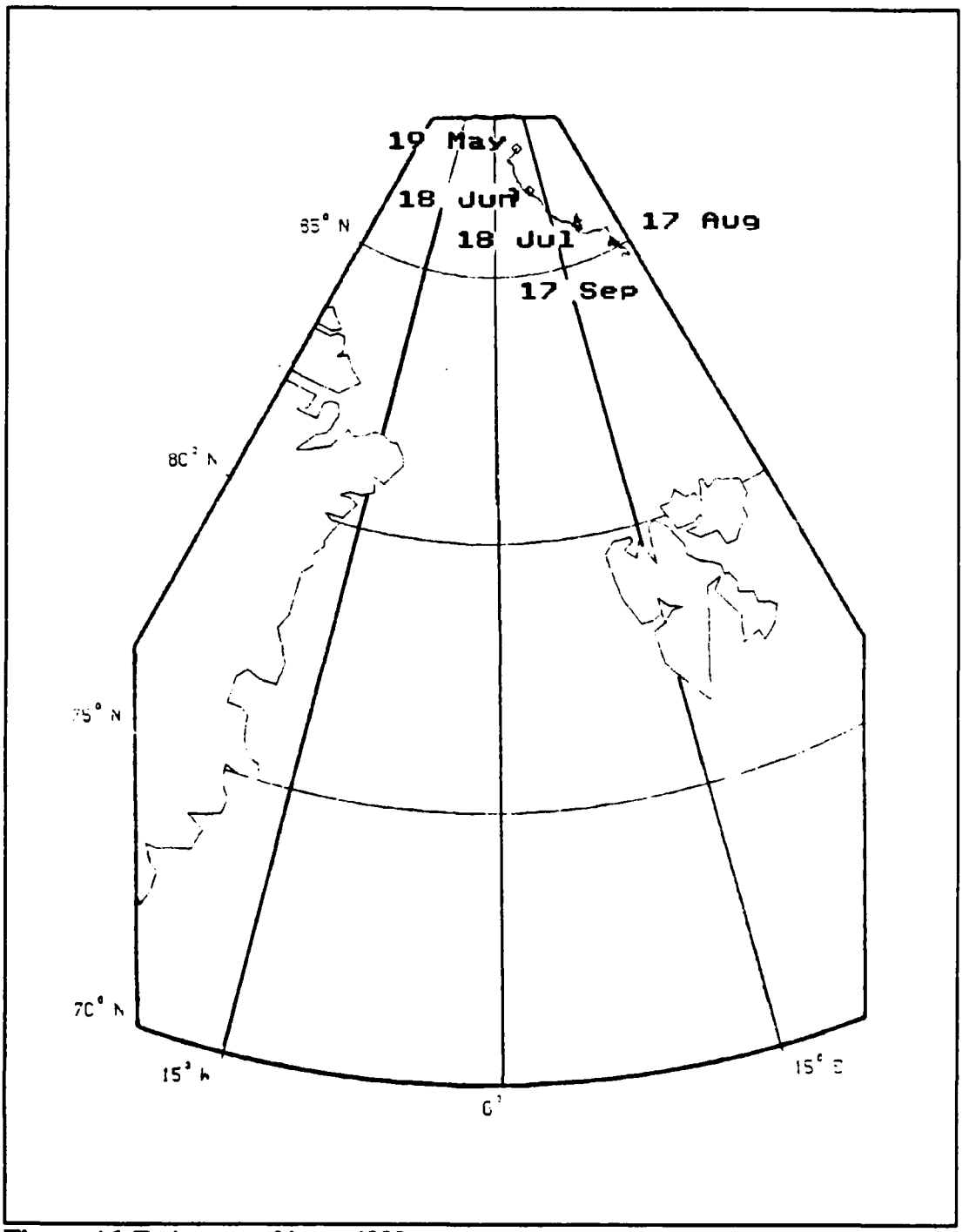

Figure A1 Trajectory of buoy 4980.

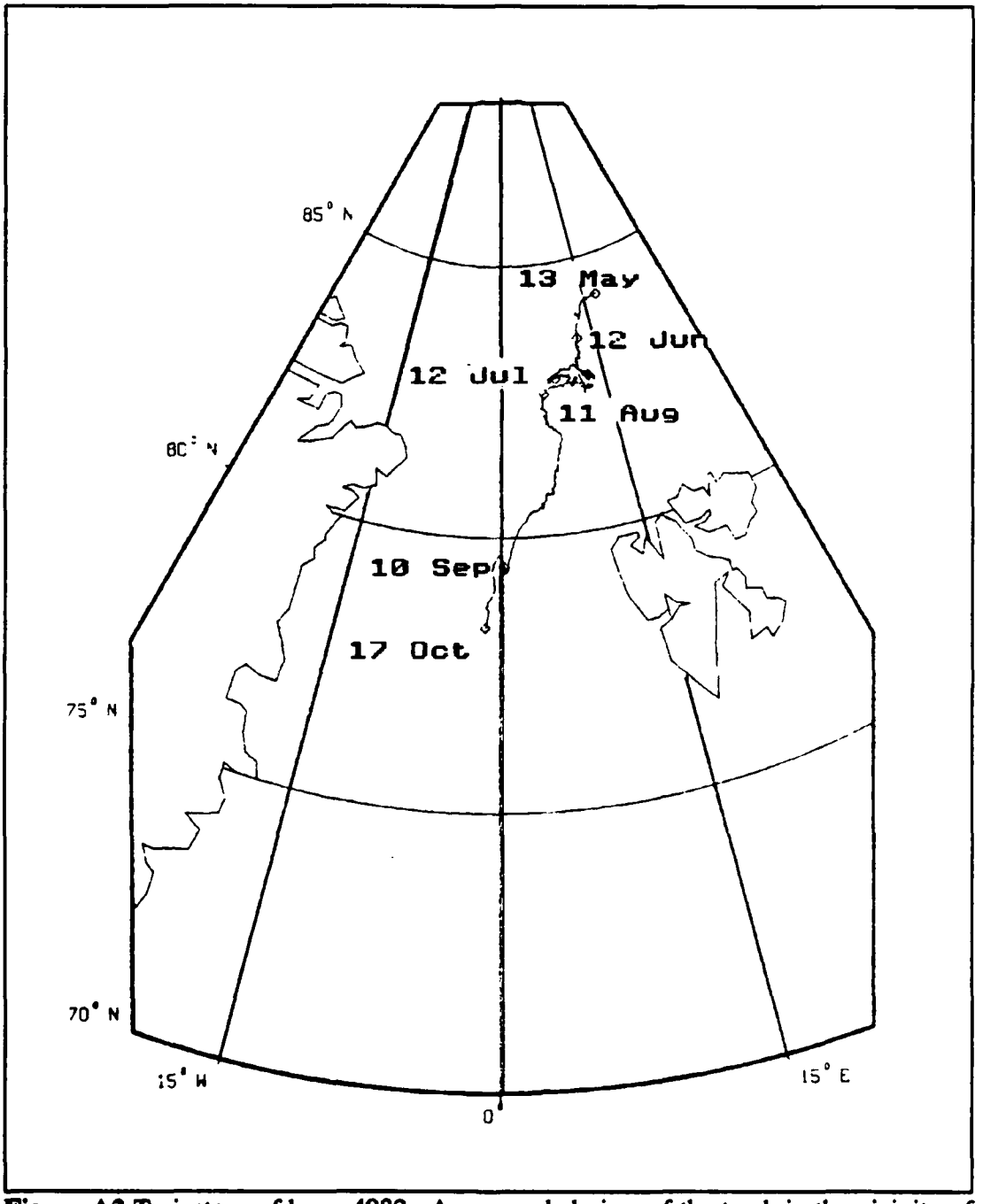

Figure A2 Trajectory of buoy 4982. An expanded view of the track in the vicinity of the Yermak Plateau is shown in Figure B1.

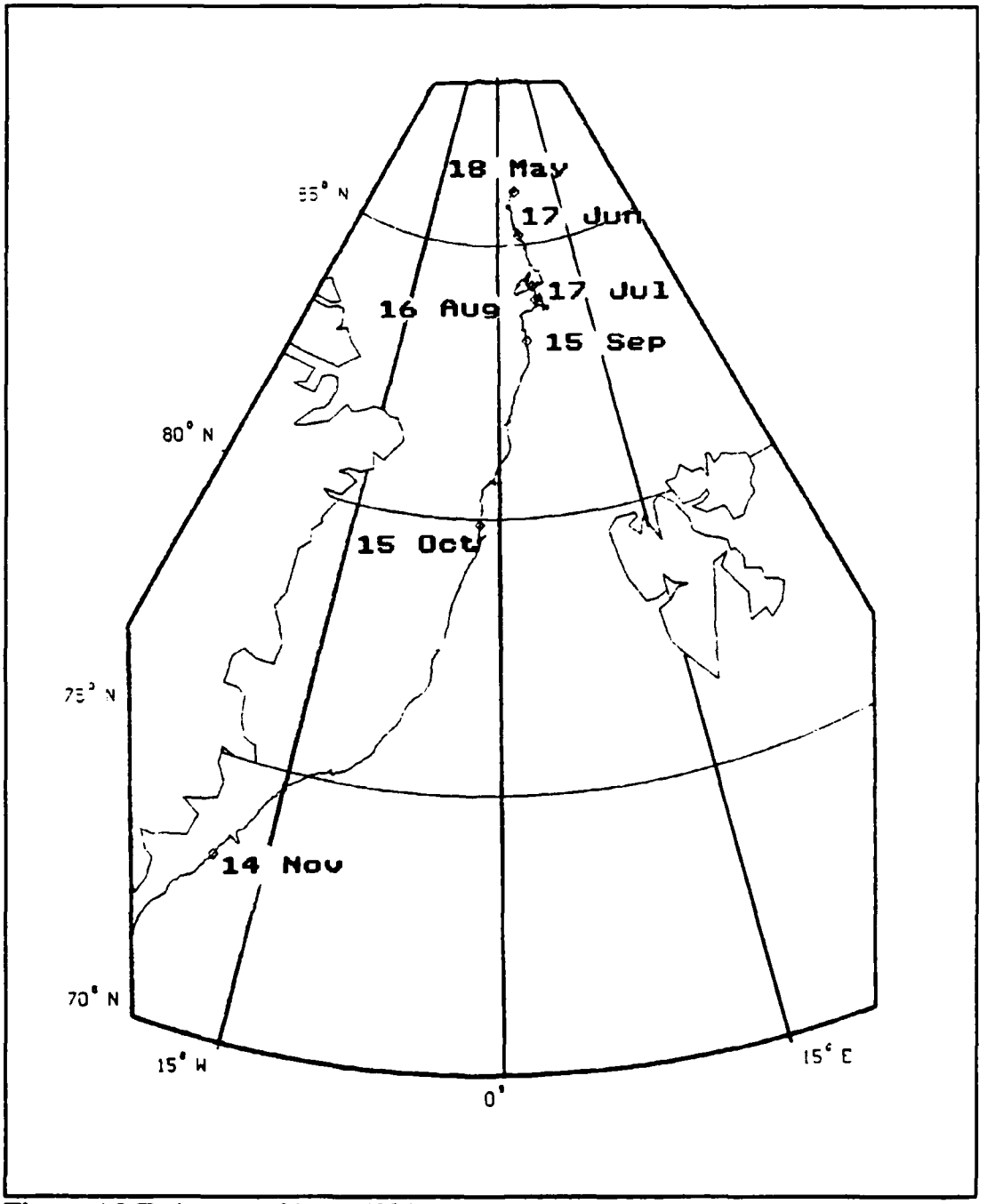

Figure A3 Trajectory of buoy 4984.

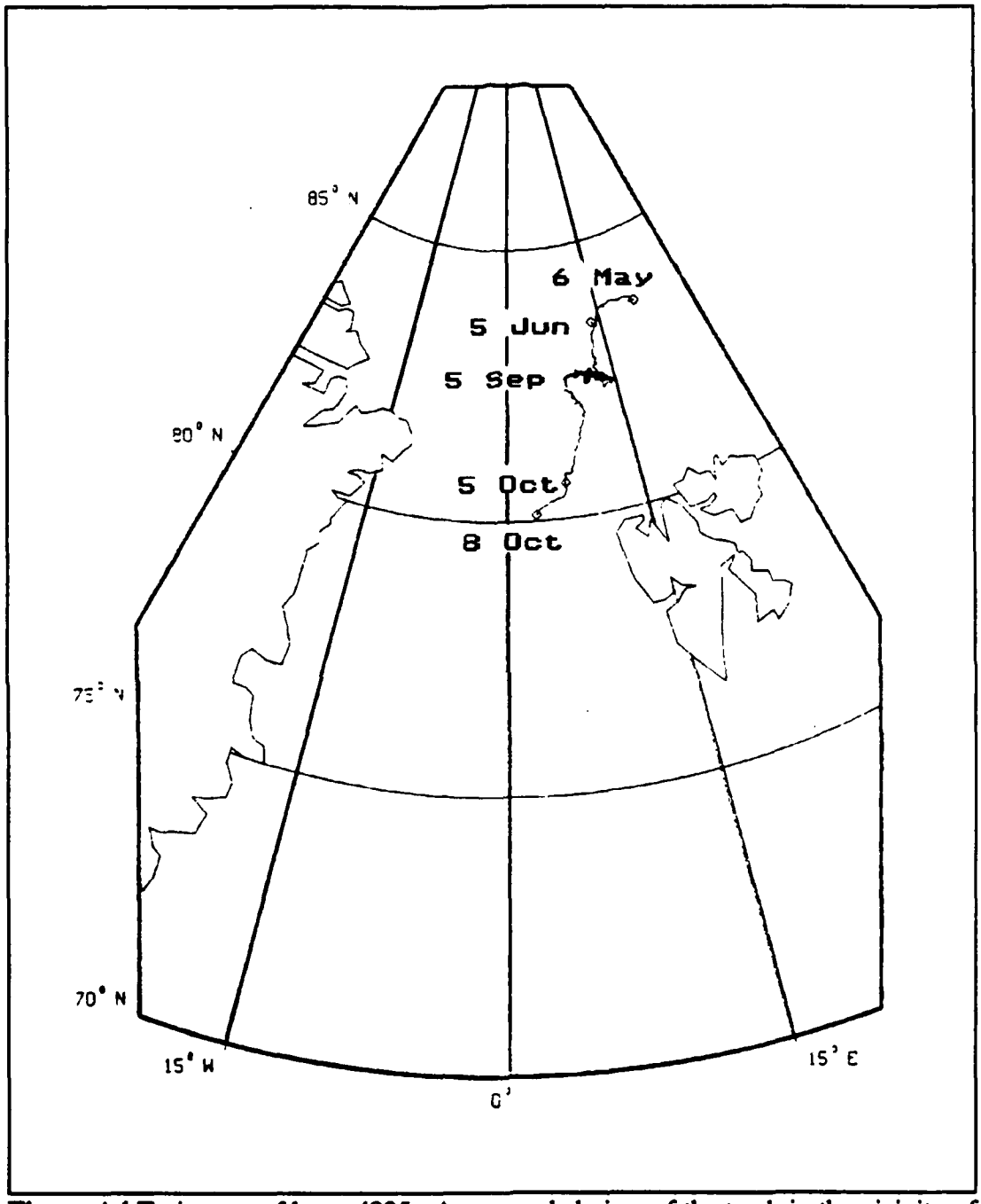

Figure A4 Trajectory of buoy 4985. An expanded view of the track in the vicinity of the Yermak Plateau in shown in Figure B2.

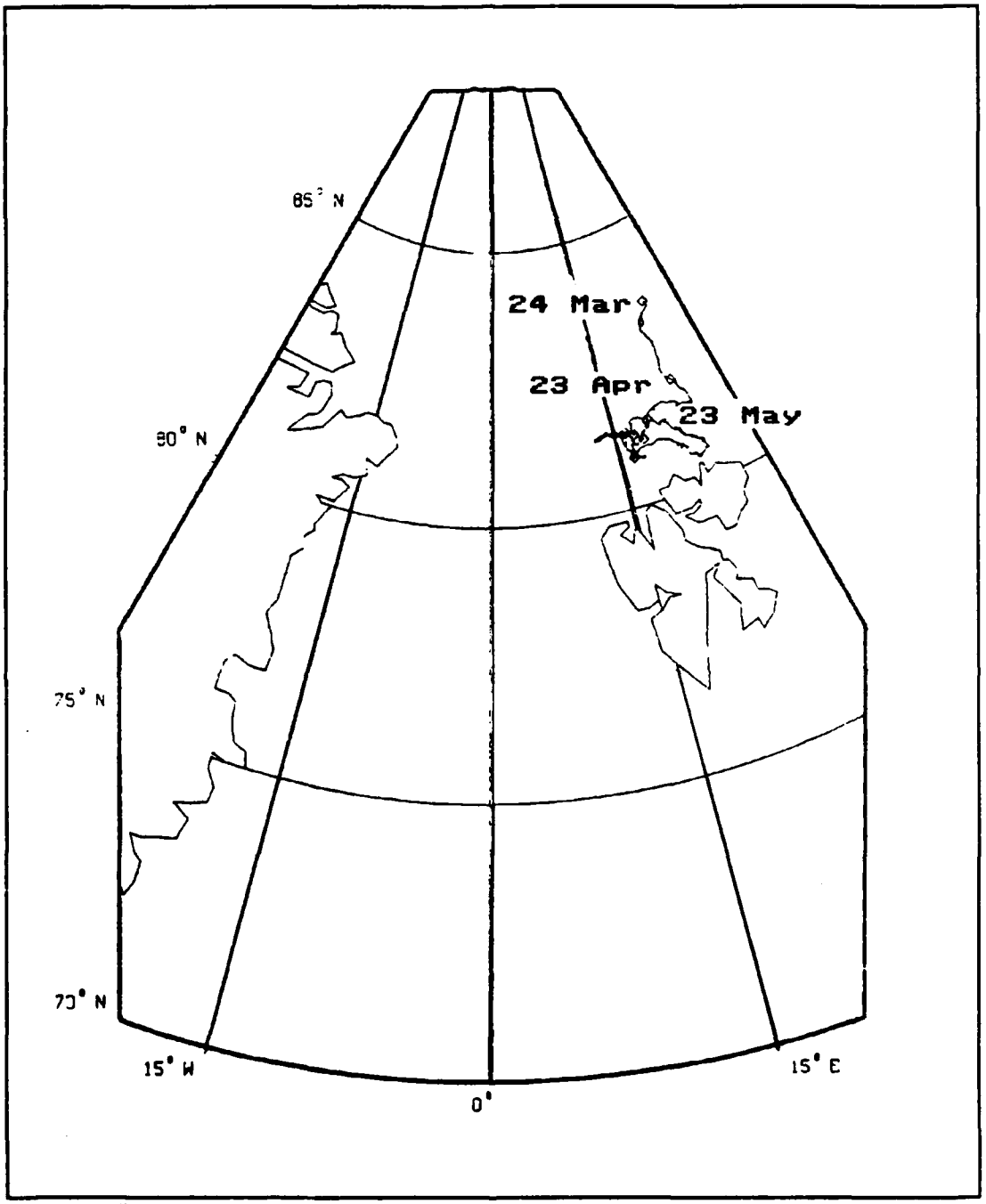

Figure A5 Trajectory of buoy 4986. An expanded view of the track in the vicinity of the Yermak Plateau in shown in Figure B3.

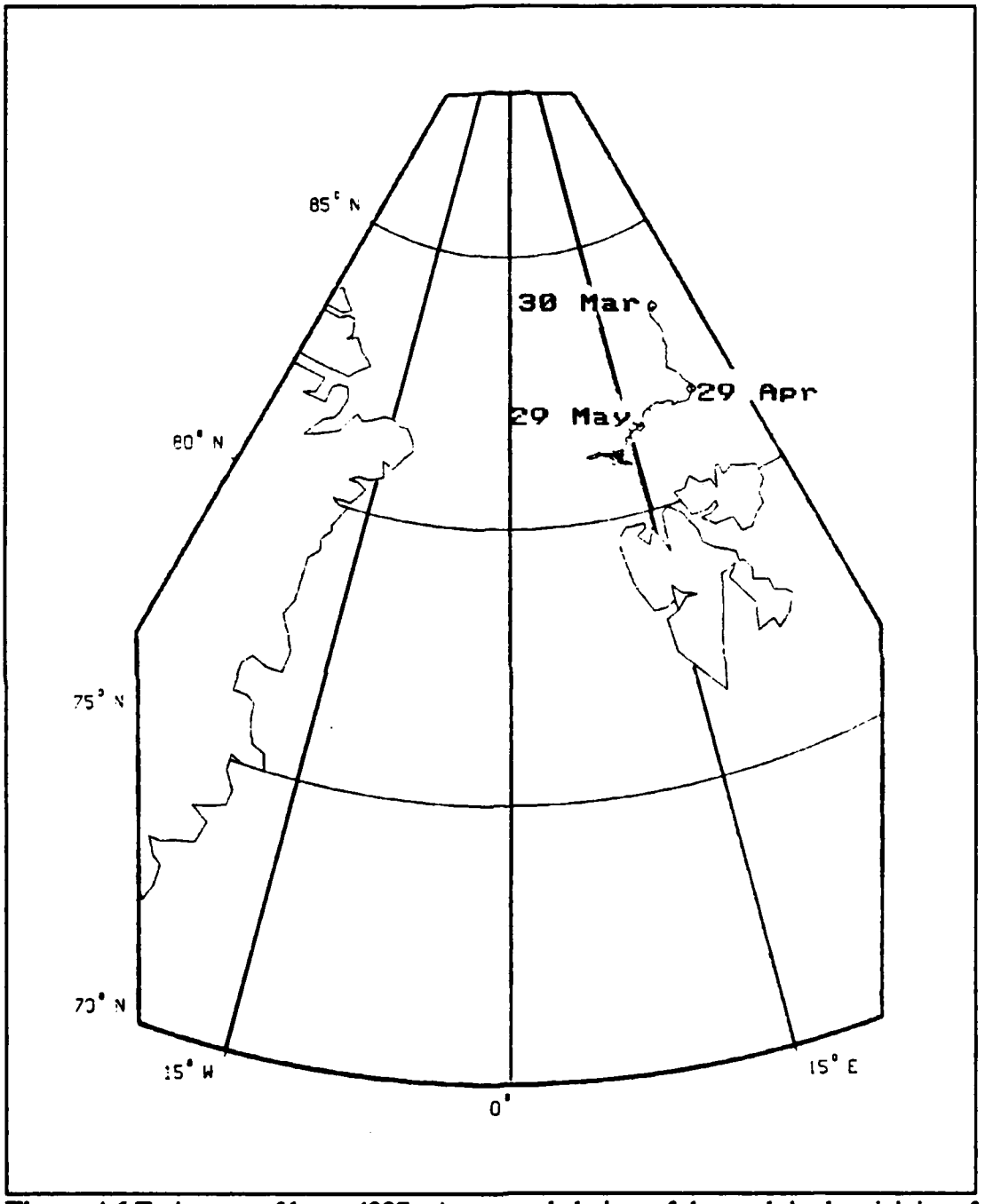

Figure A6 Trajectory of buoy 4987. An expanded view of the track in the vicinity of the Yermak Plateau in shown in Figure B4.

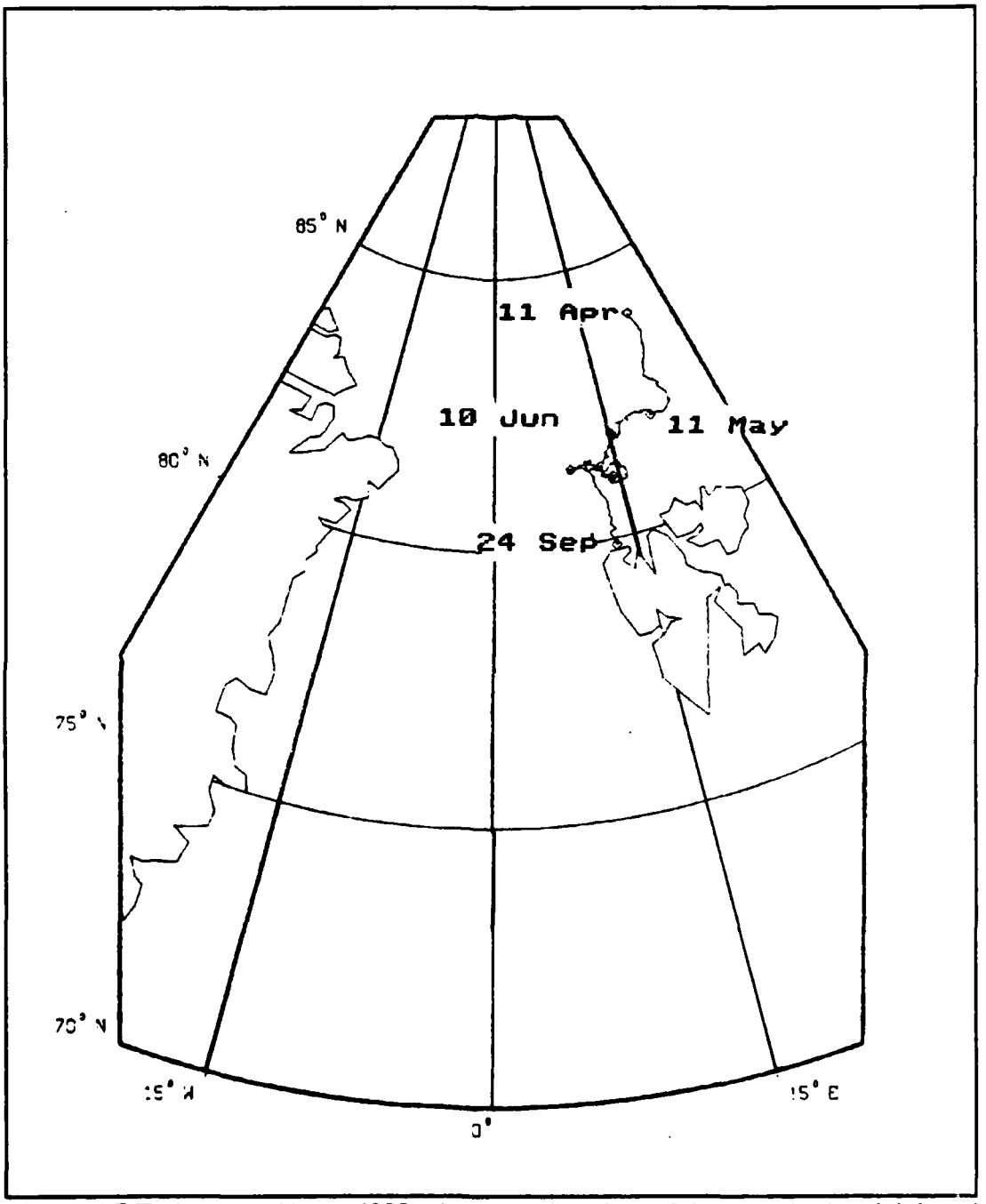

Figure A7 Trajectory of buoy 4988. An expanded view of the track in the vicinity of the Yermak Plateau in shown in Figure B5.

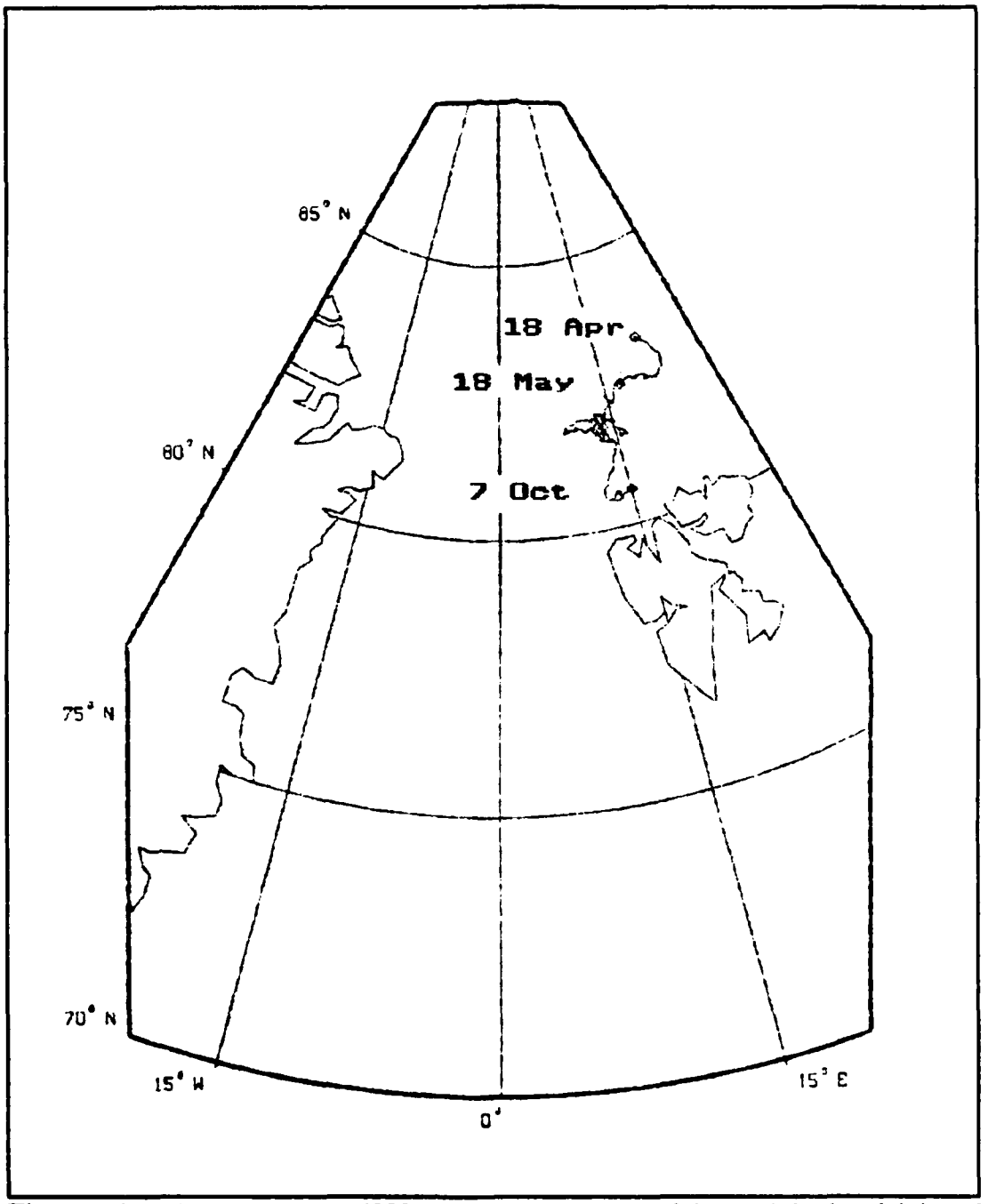

Figure A8 Trajectory of buoy 4989. An expanded view of the track in the vicinity of the Yermak Plateau in shown in Figure B6.

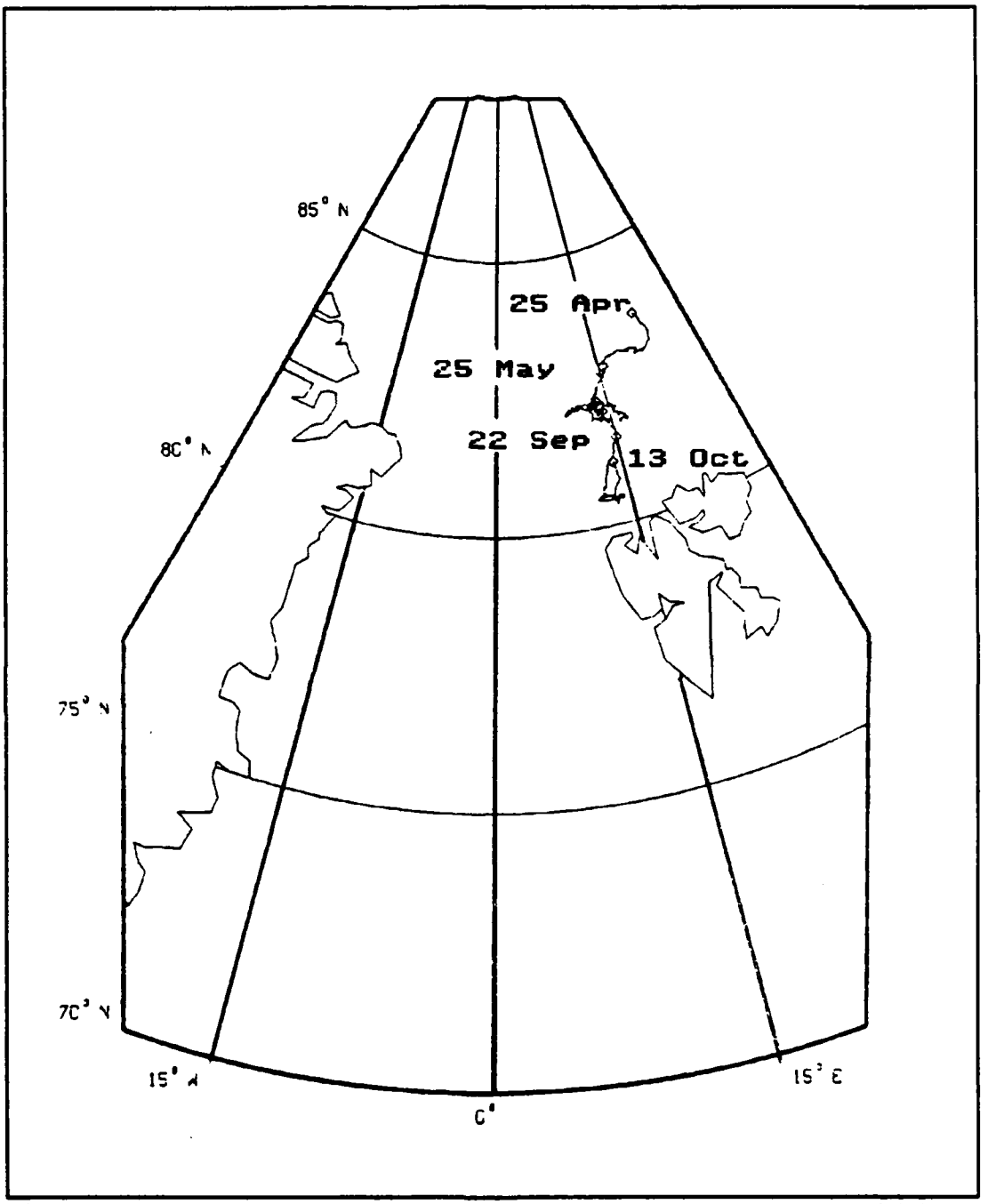

Figure A9 Trajectory of buoy 4990. An expanded view of the track in the vicinity of the Yermak Plateau in shown in Figure B7.

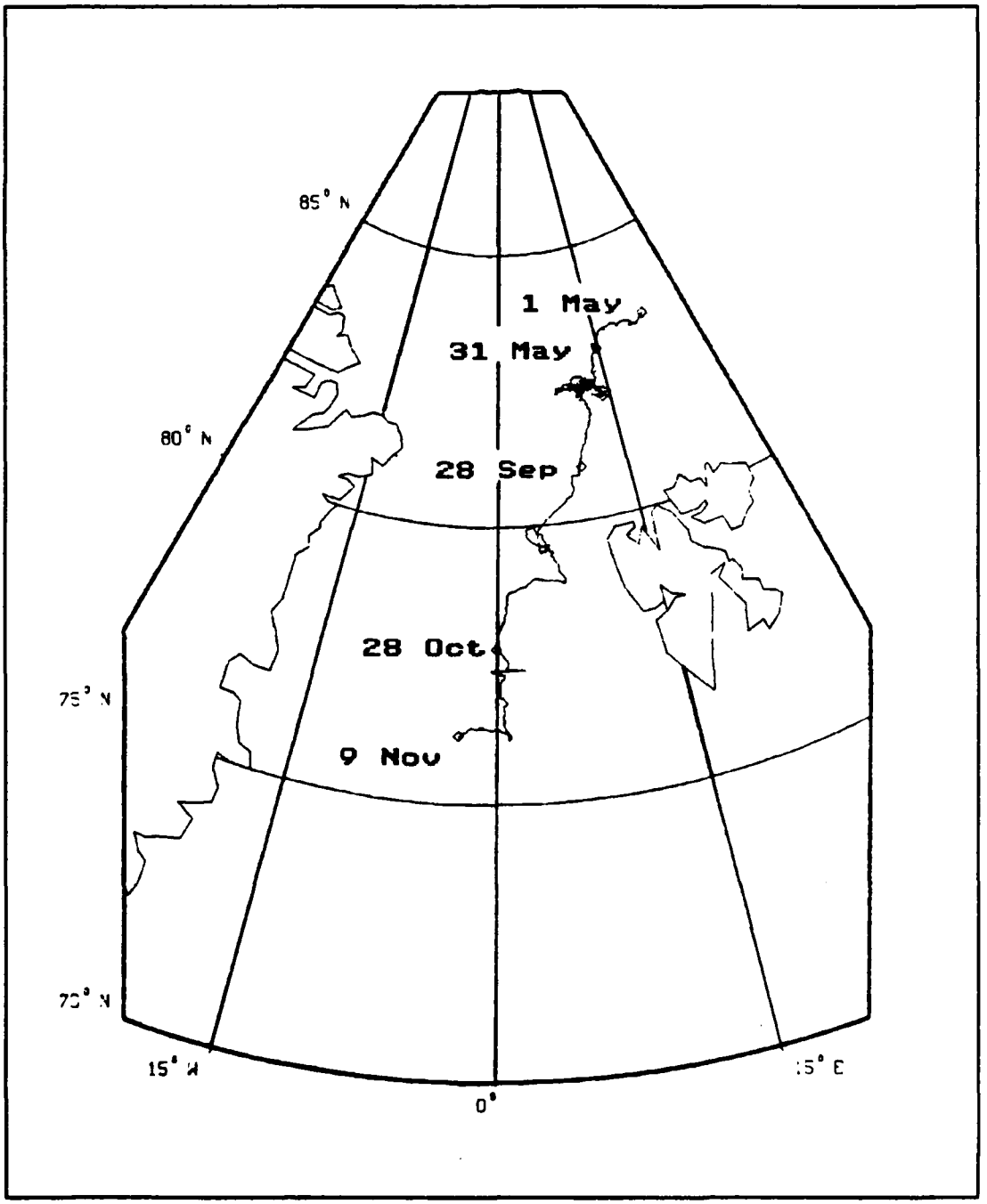

Figure A10 Trajectory of buoy 4991. An expanded view of the track in the vicinity of the Yermak Plateau in shown in Figure B8.

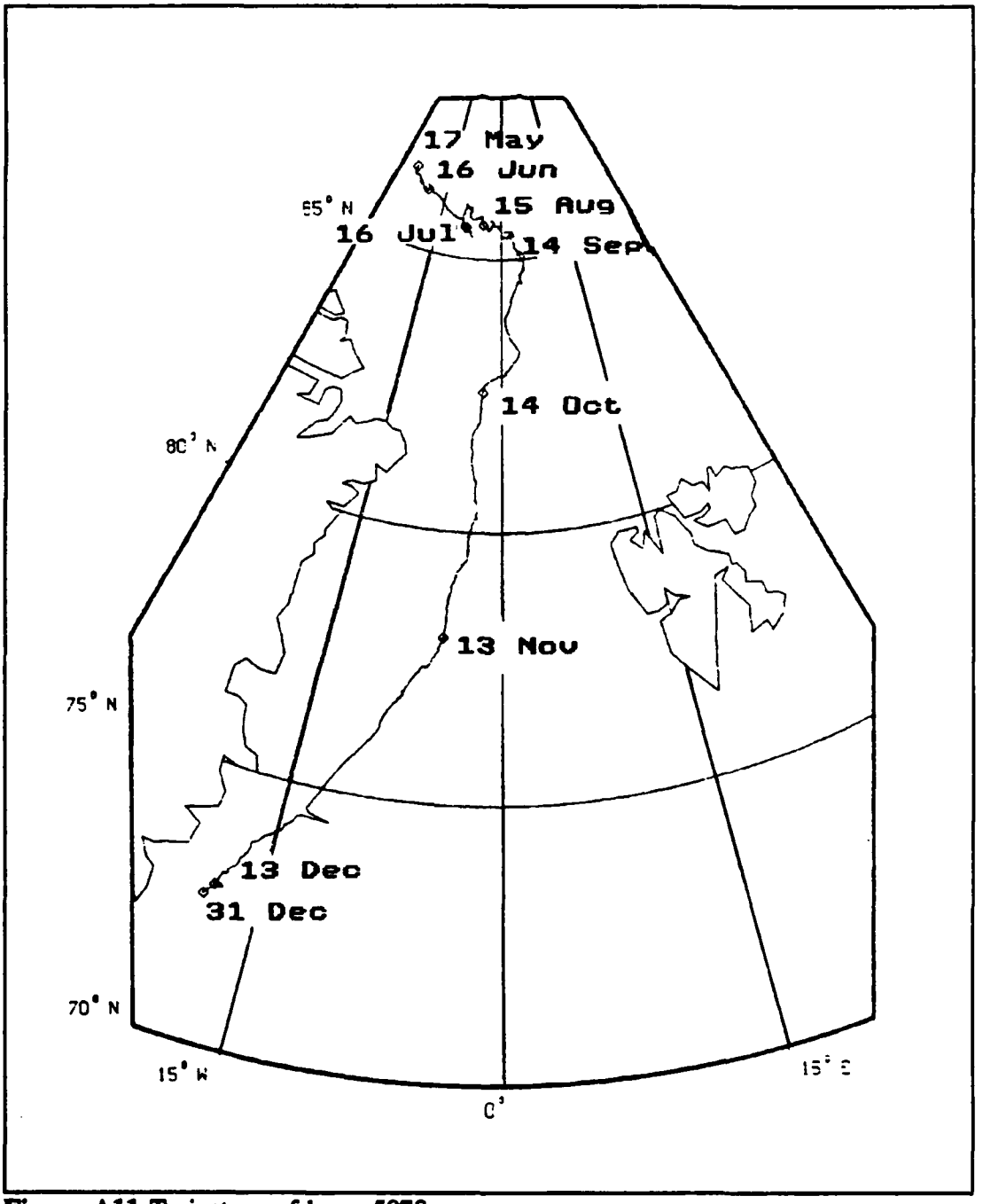

Figure A11 Trajectory of buoy 5078.

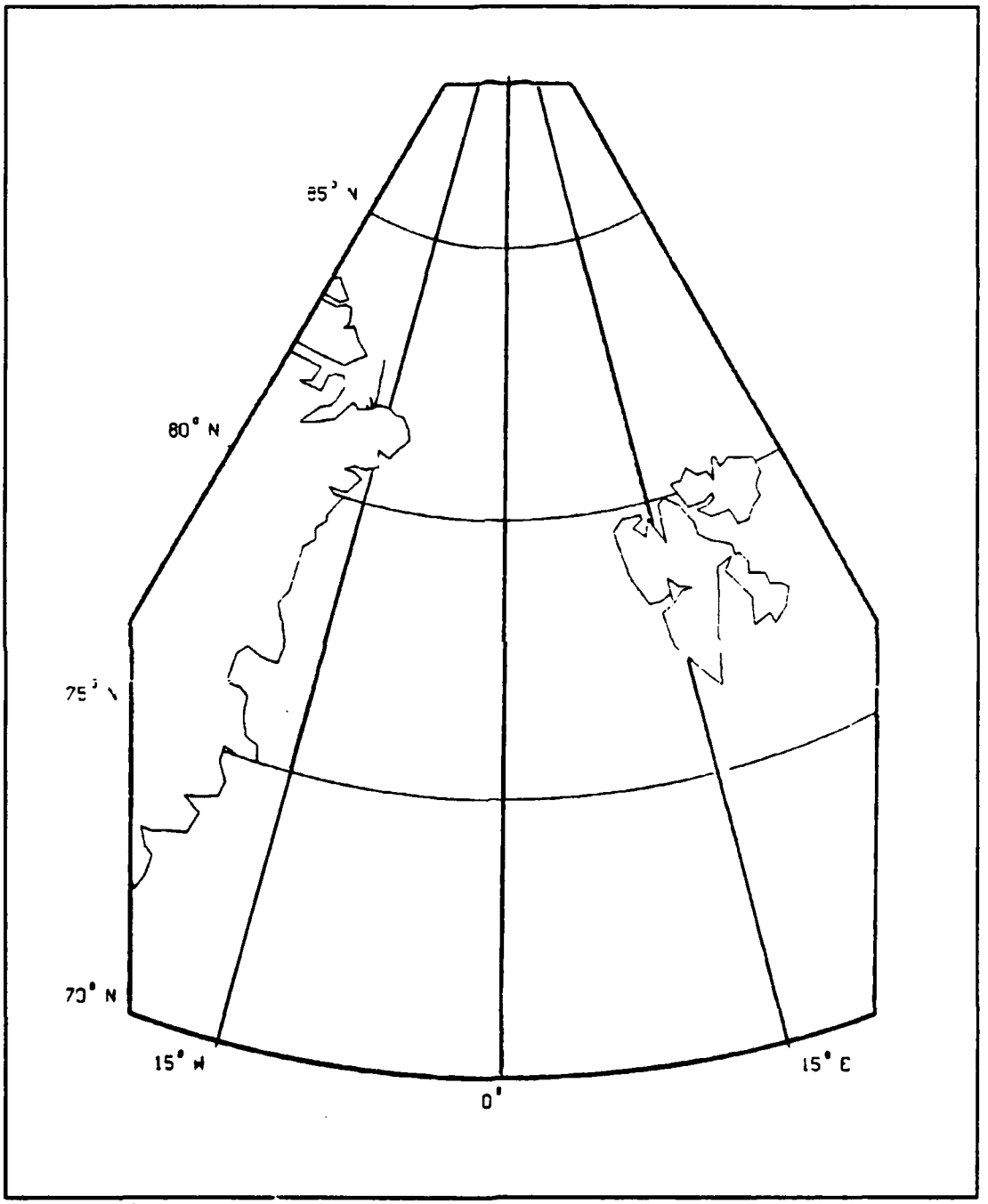

Figure A12 Trajectory of buoy 5079.

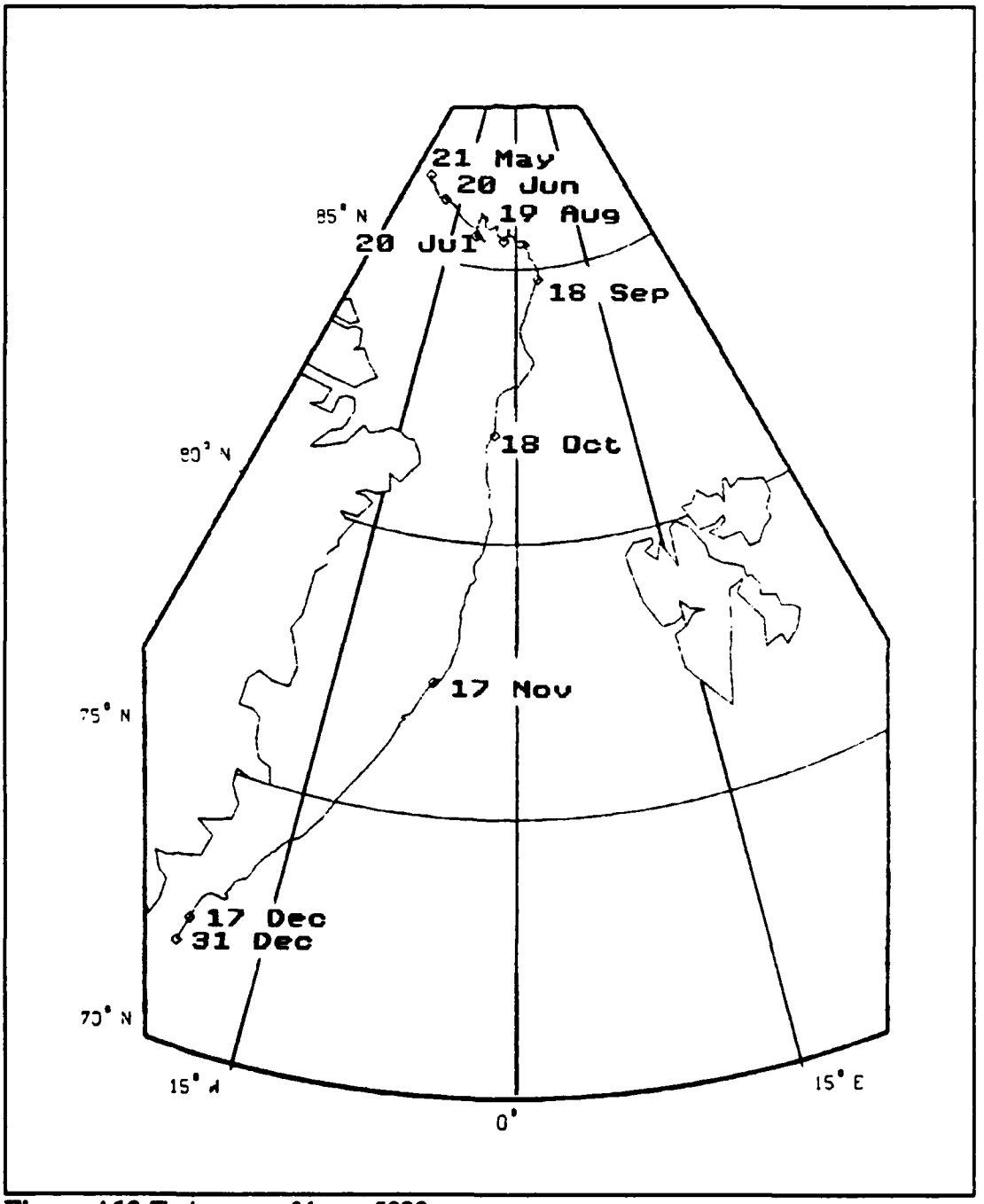

Figure A13 Trajectory of buoy 5088.

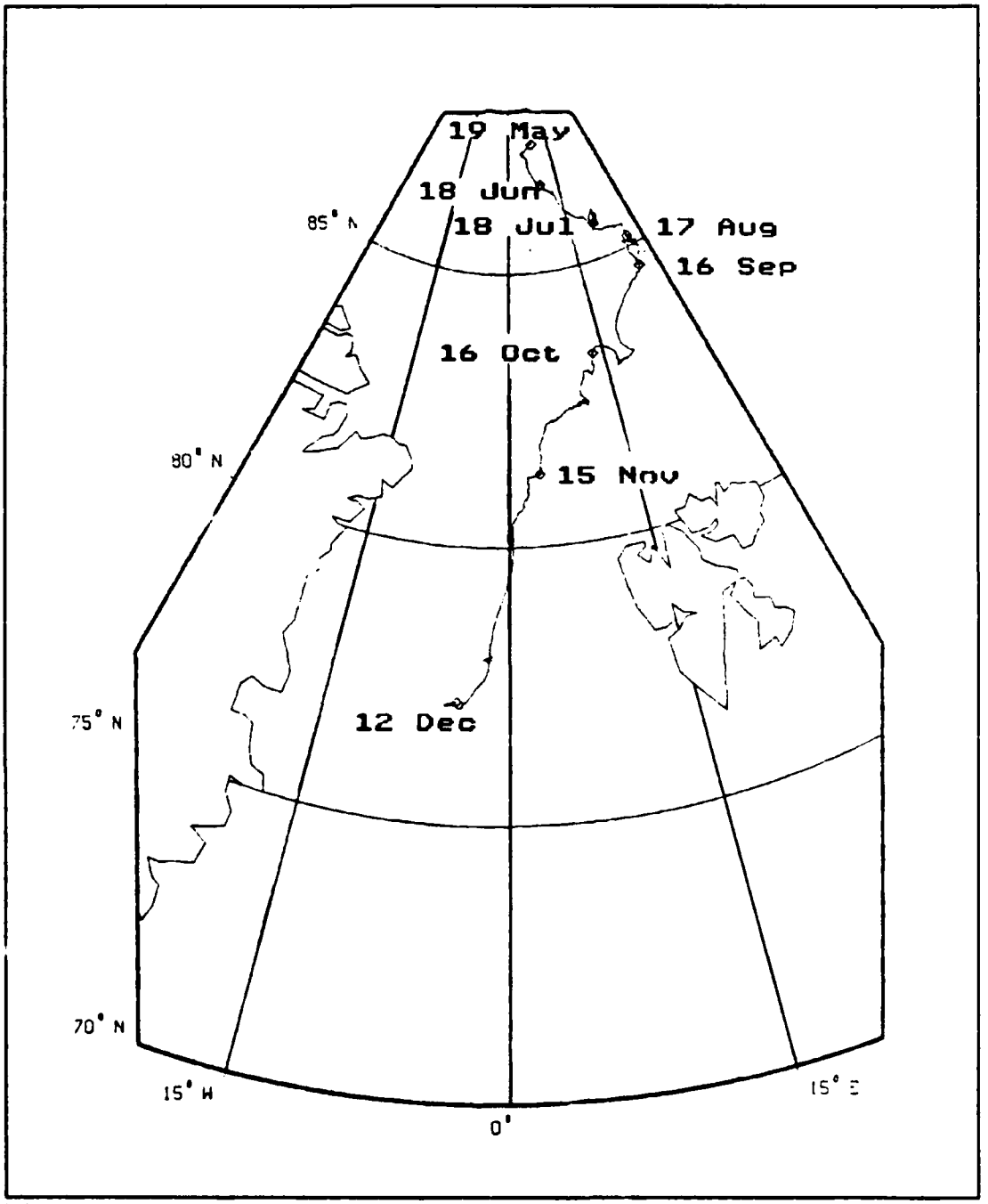

Figure A14 Trajectory of buoy 5097. An expanded view of the track in the vicinity of the Yermak Plateau in shown in Figure B9.

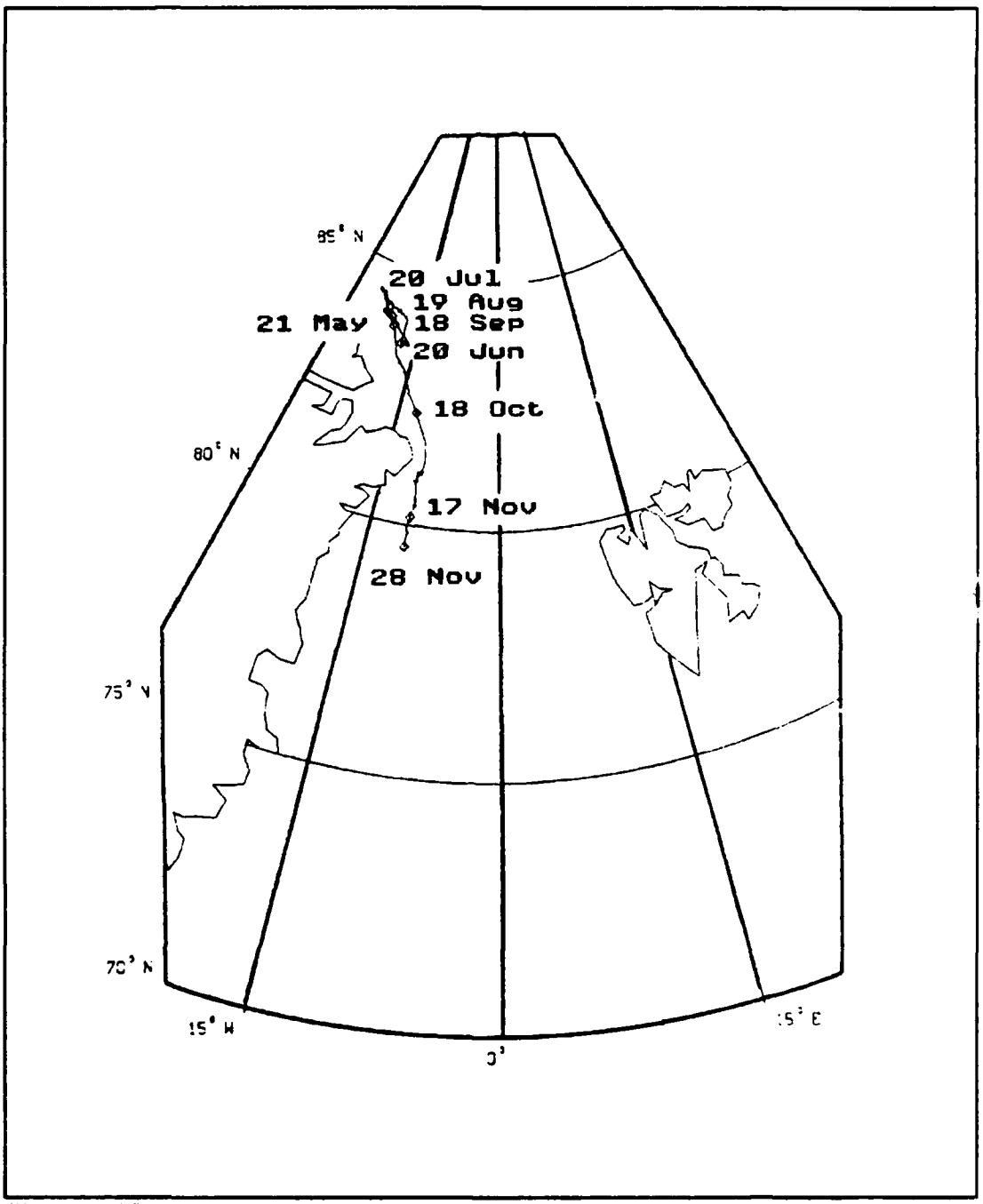

Figure A15 Trajectory of buoy 5098.

APPENDIX B

Trajectories of buoys in the vicinity of the Yermak Plateau. The tracks are marked beginning with the deployment date and then every thirty days until the end of the record.

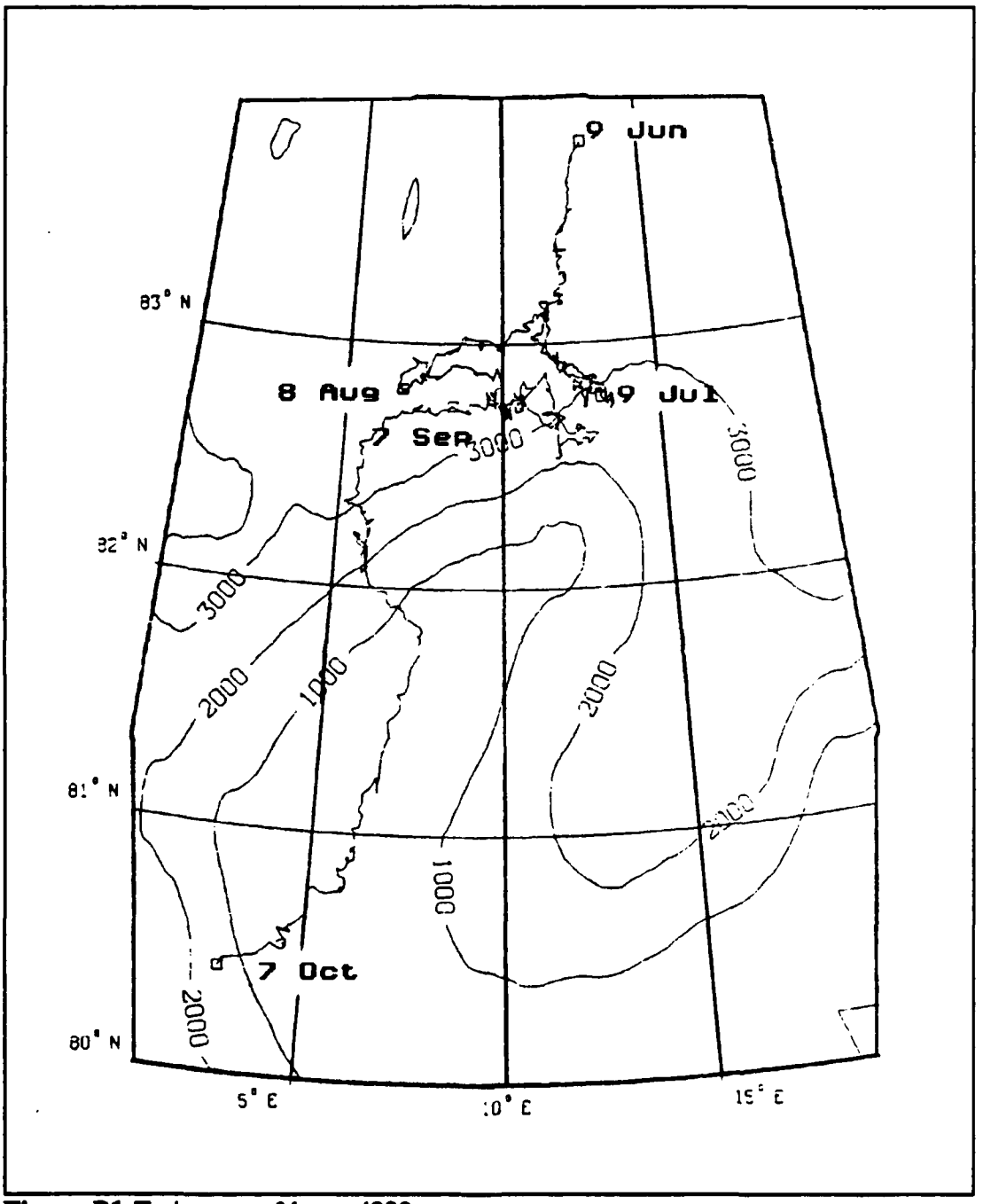

Figure B1 Trajectory of buoy 4982.

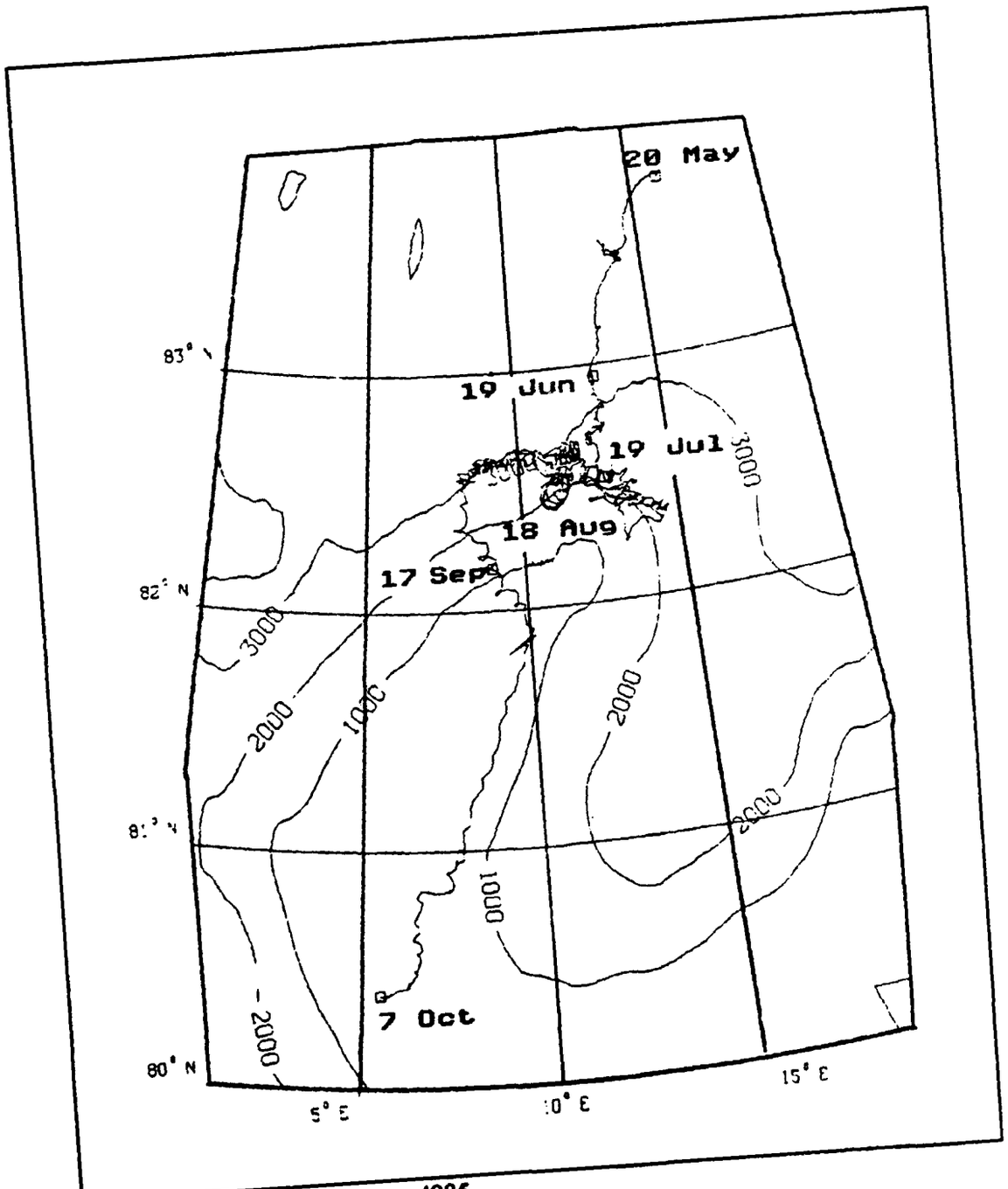

Figure B2 Trajectory of buoy 4985.

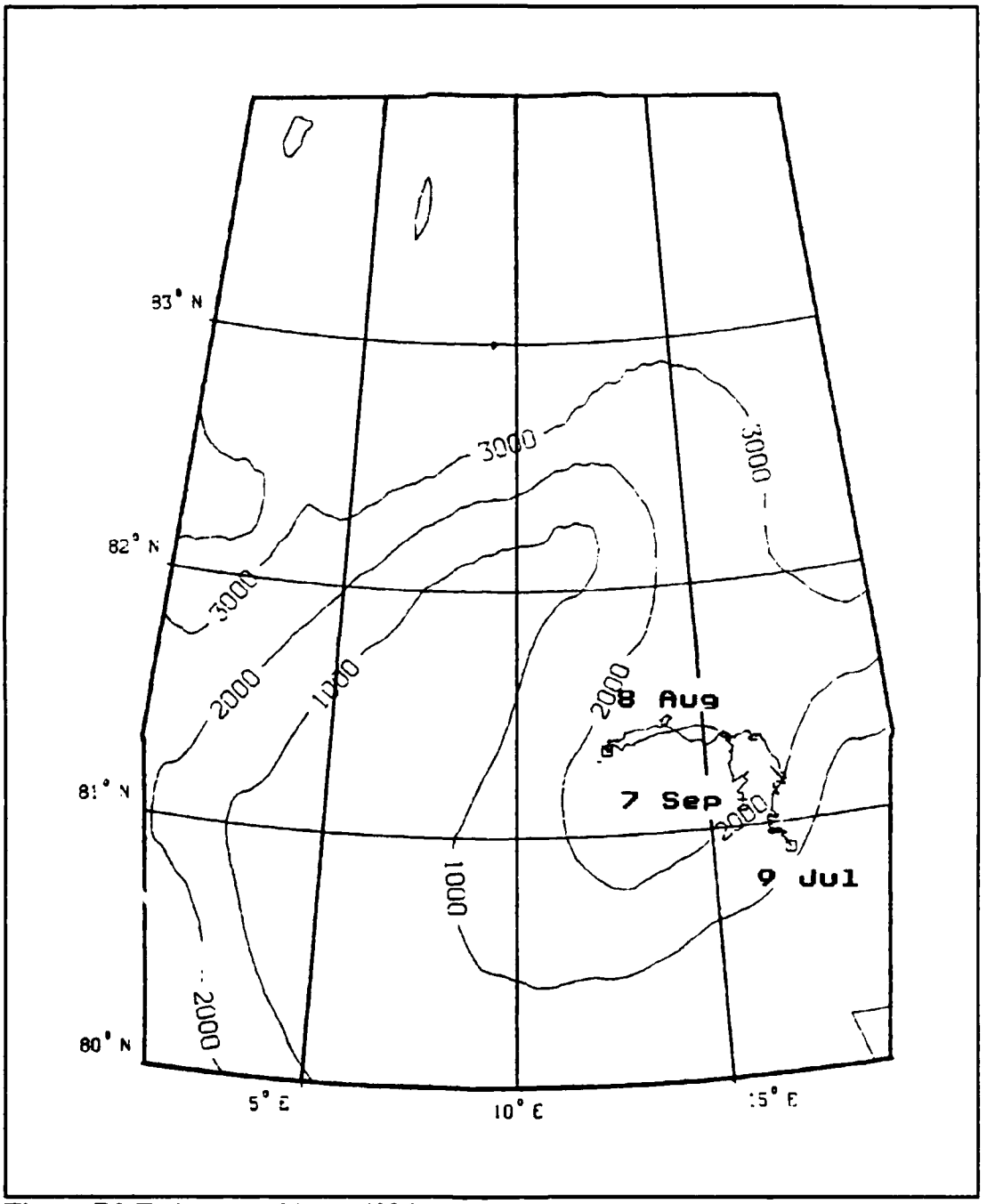

Figure B3 Trajectory of buoy 4986.

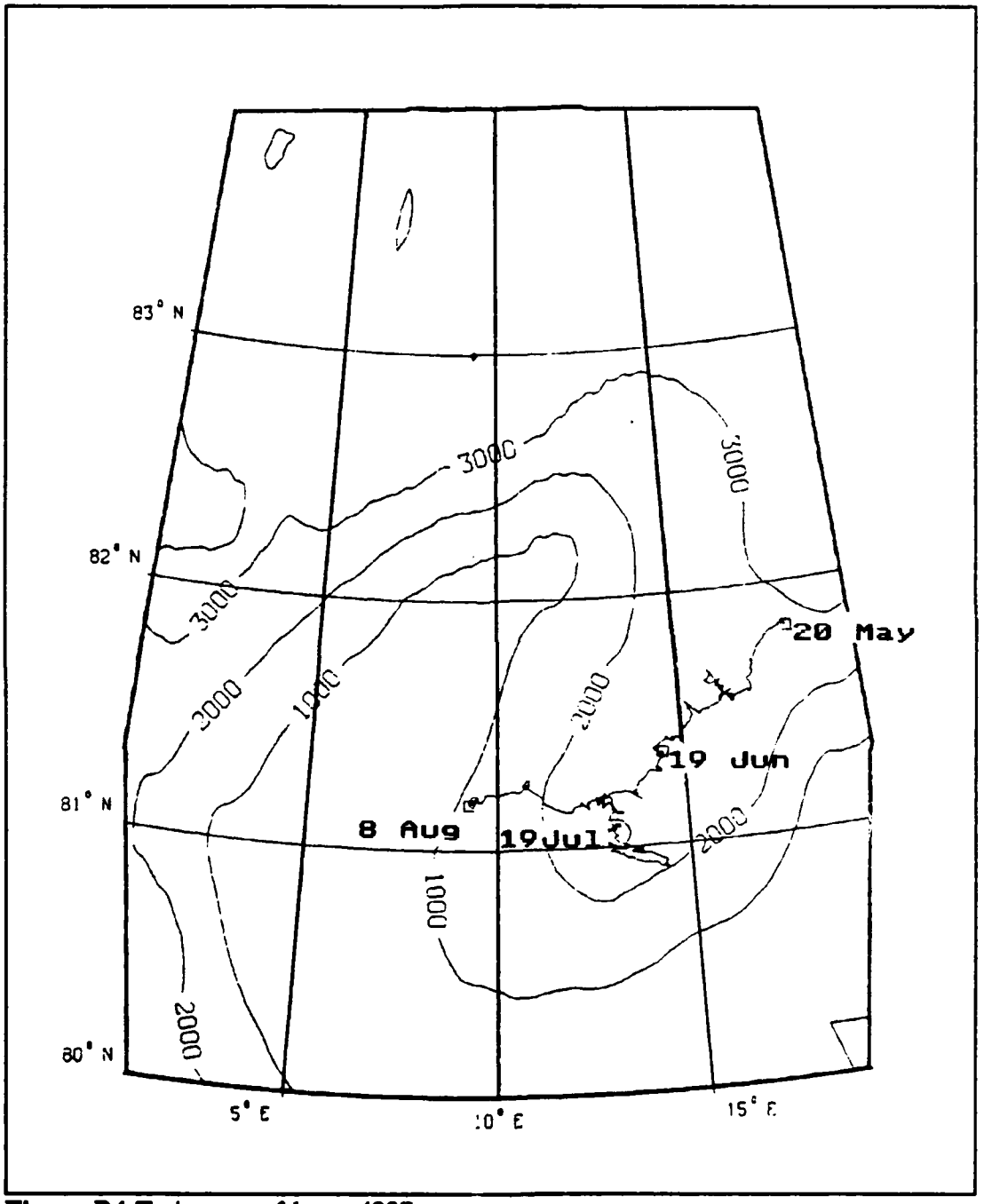

Figure B4 Trajectory of buoy 4987.

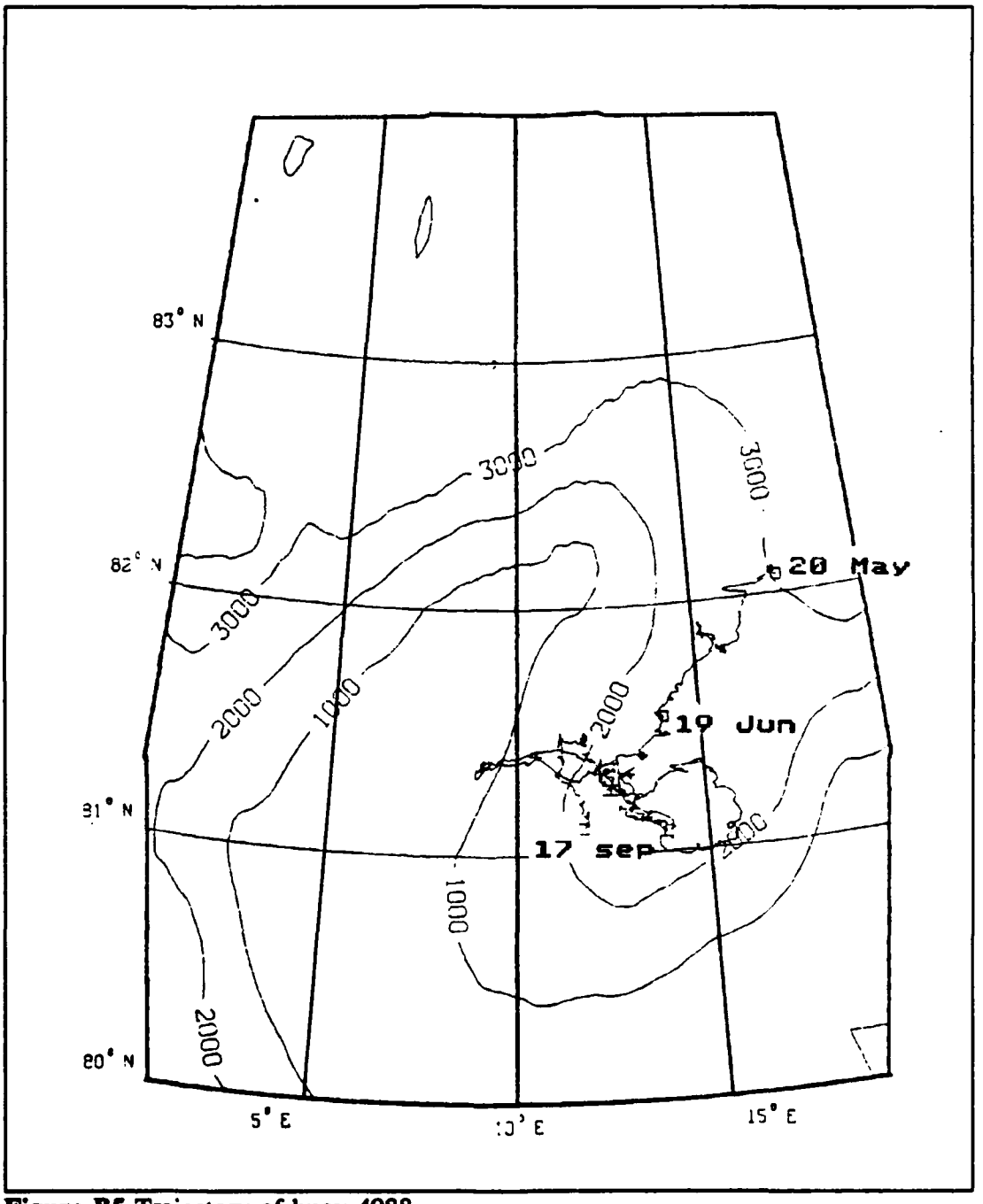

Figure B5 Trajectory of buoy 4988.

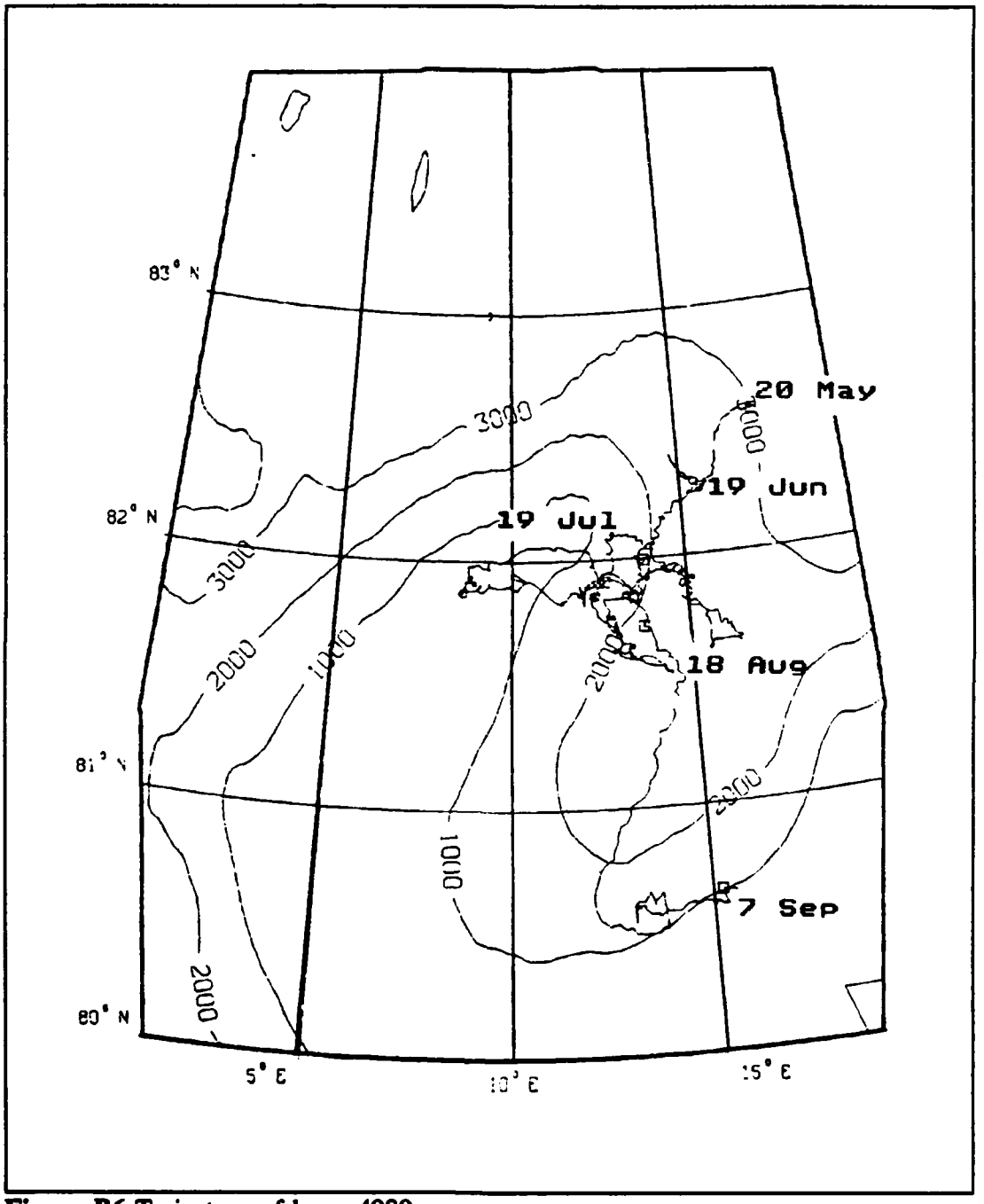

Figure B6 Trajectory of buoy 4989.

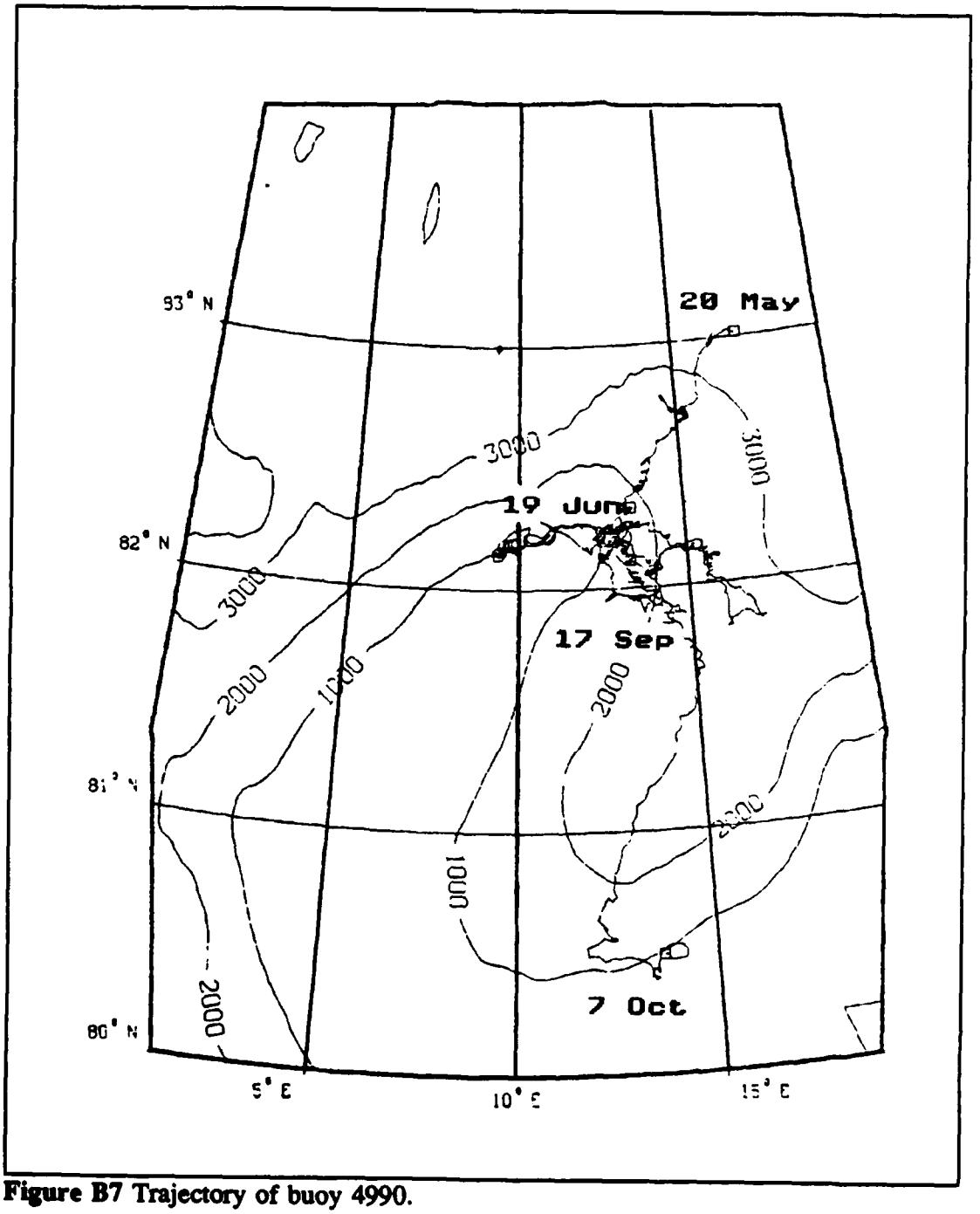

Figure B7 Trajectory of buoy 4990.

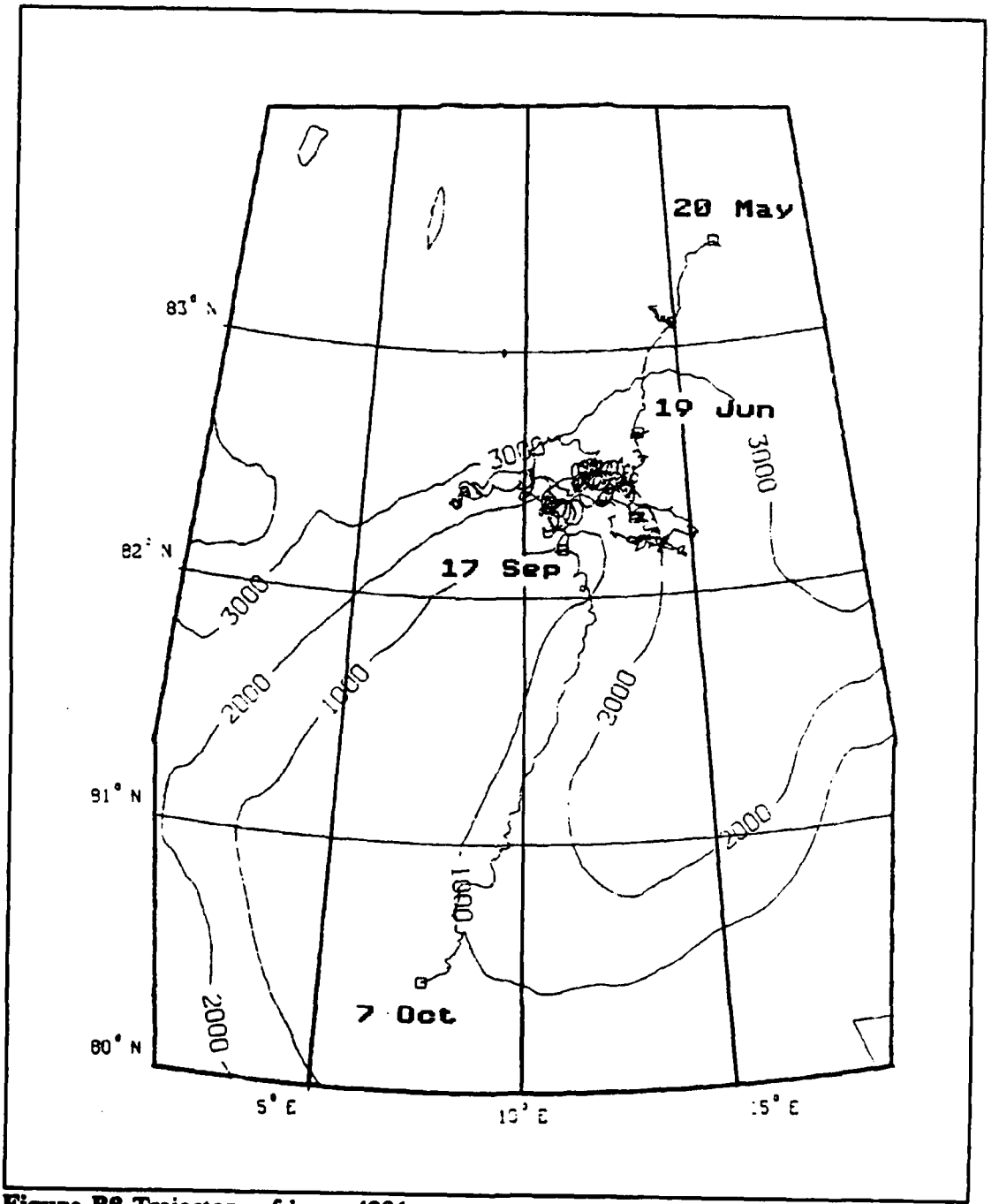

Figure B8 Trajectory of buoy 4991.

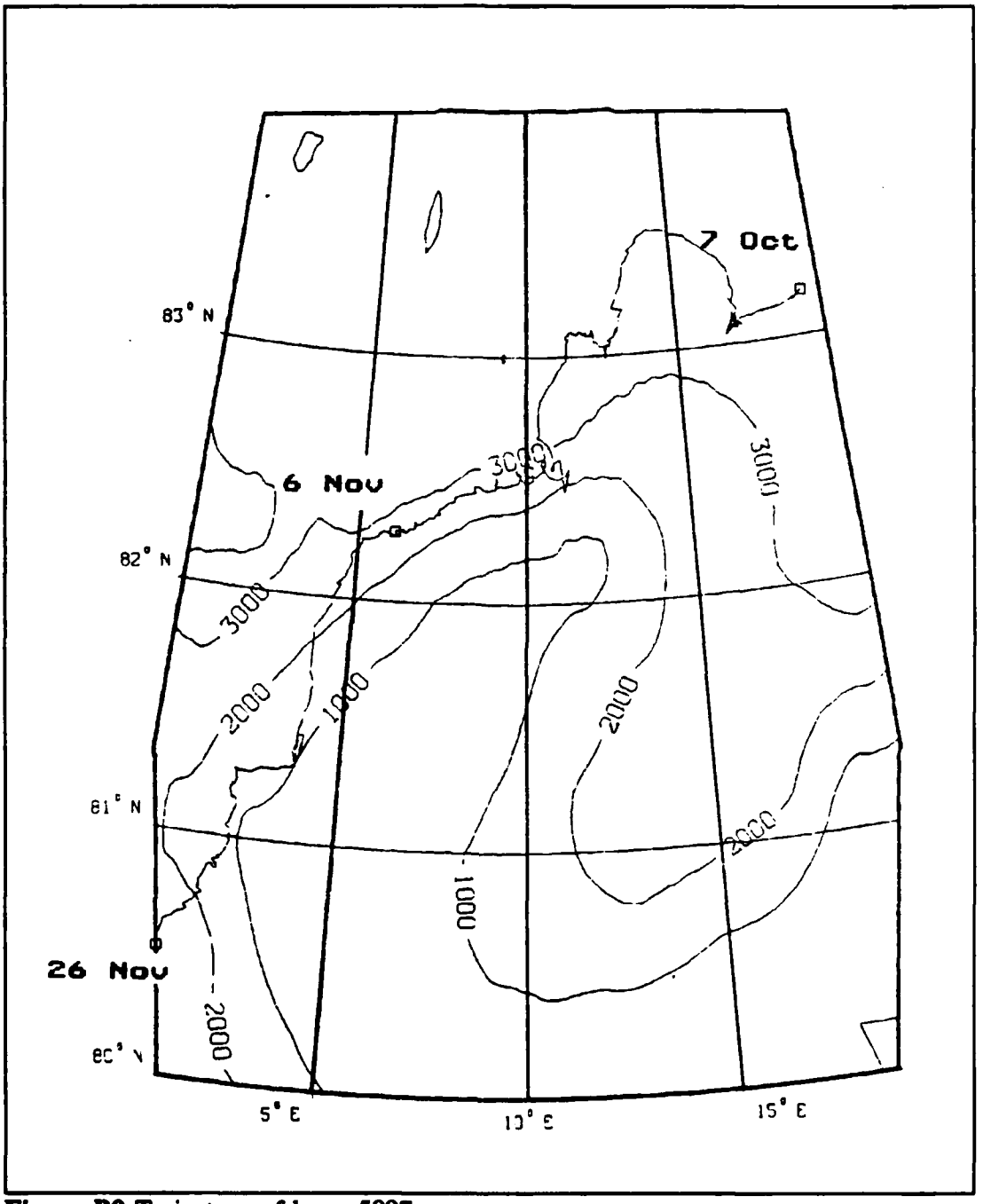

Figure B9 Trajectory of buoy 5097.

APPENDIX C

Demodulated tidal current u and v velocities for ARCTEMIZ 86 buoys. Demodulation was performed using the technique of McPhee (1986). Details of the technique can be found in Chapter 2 Section D.

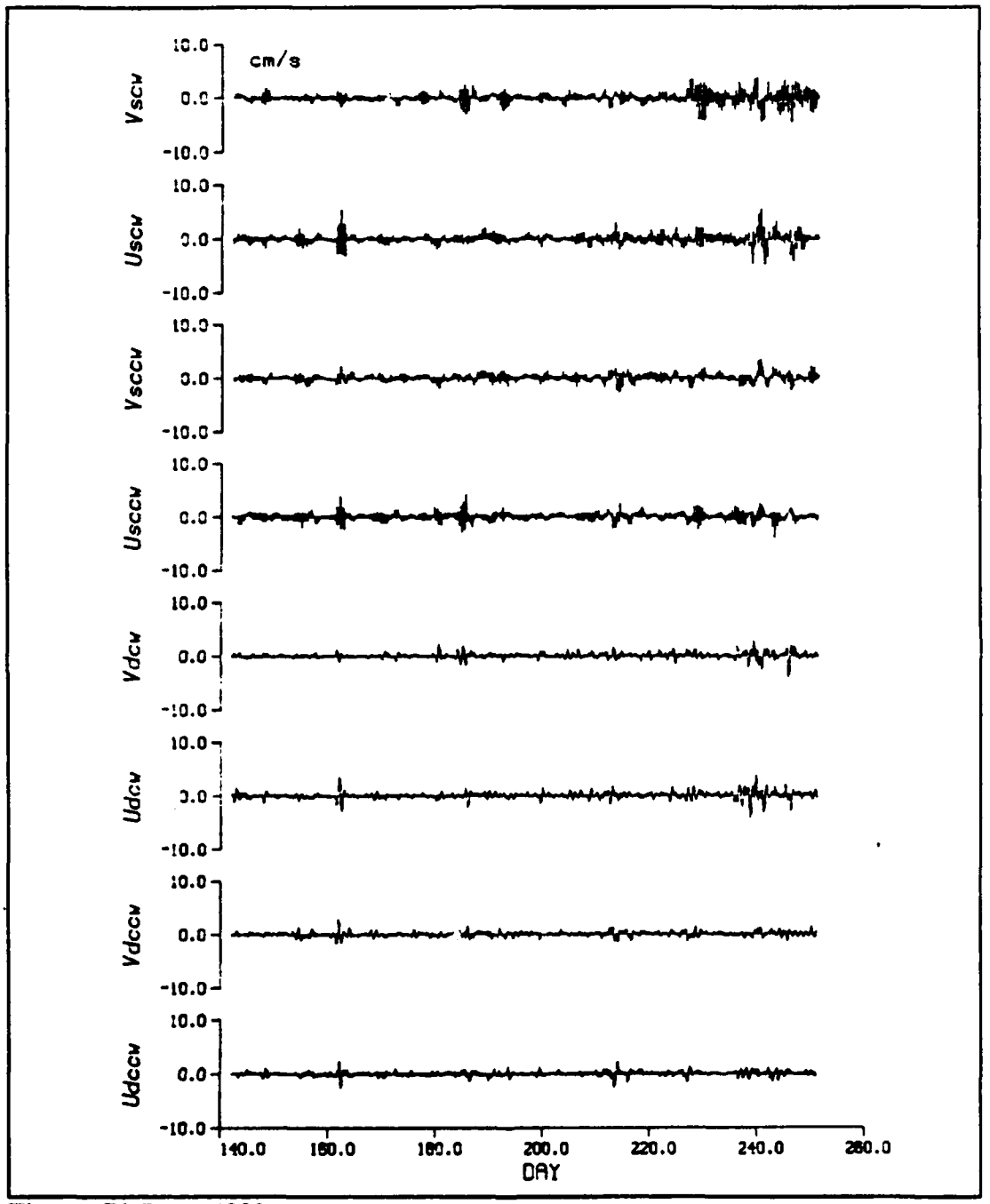

Figure C1 Buoy 4980.

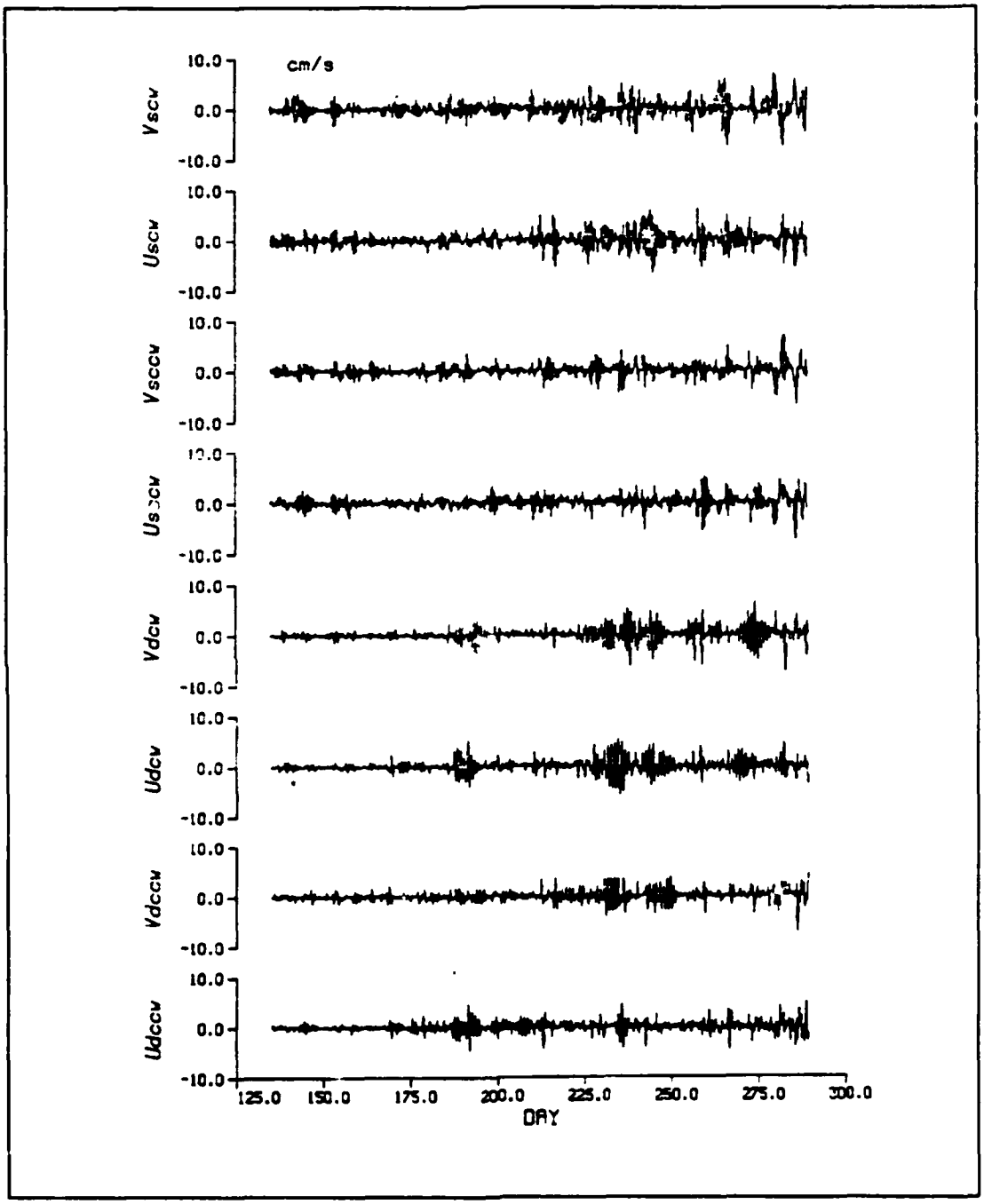

Figure C2 Buoy 4982.

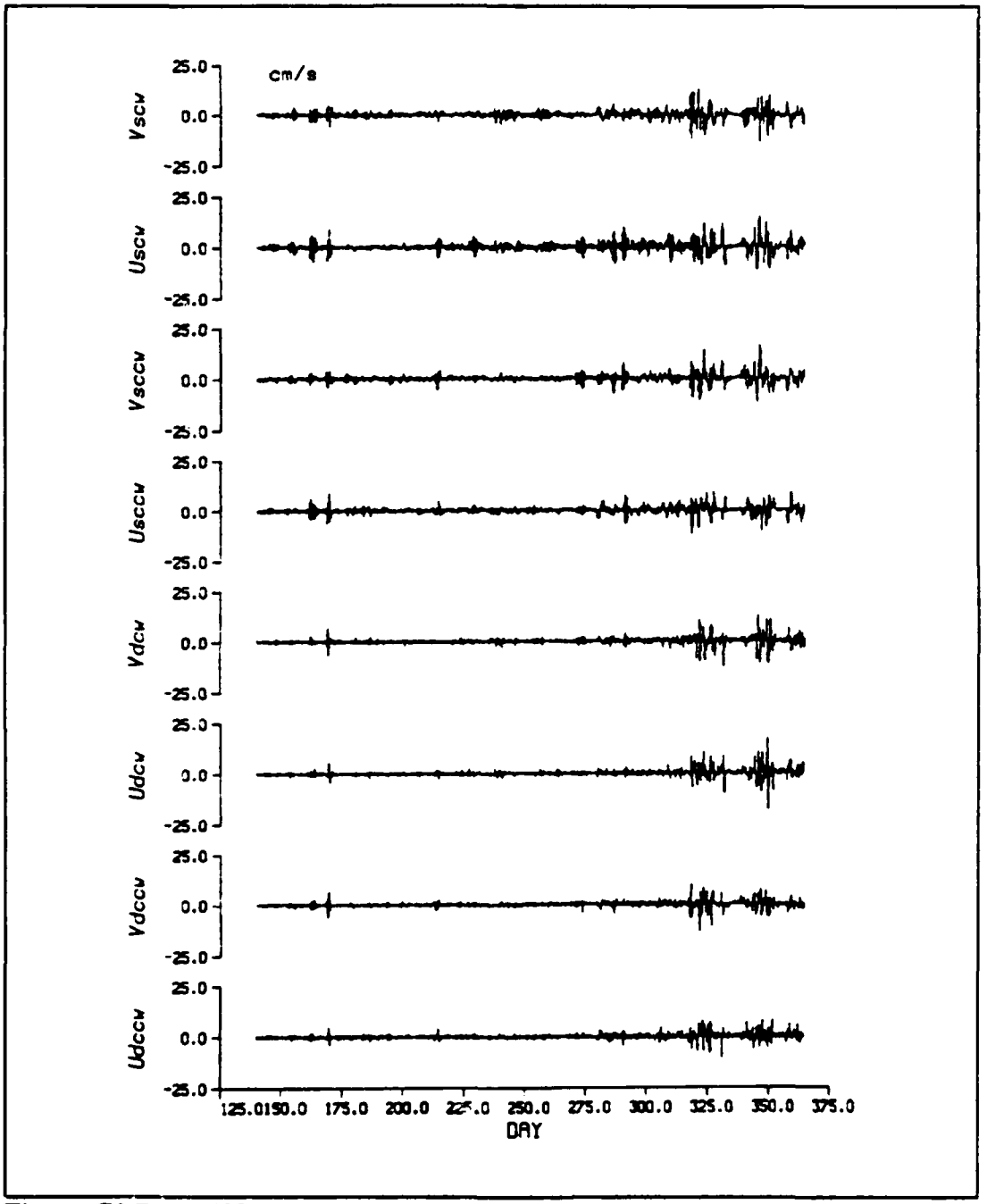

Figure C3 Buoy 4984.

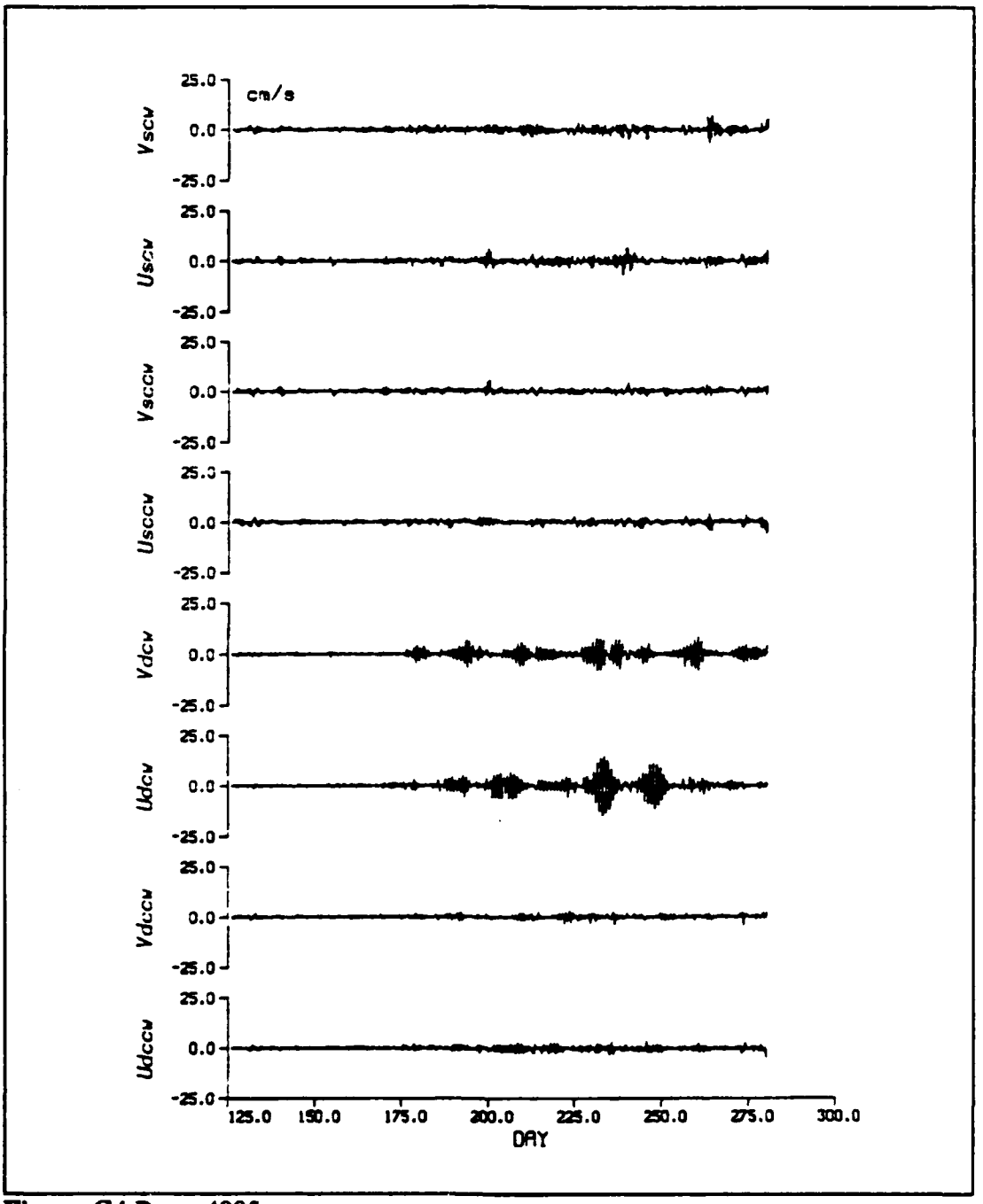

Figure C4 Buoy 4985.

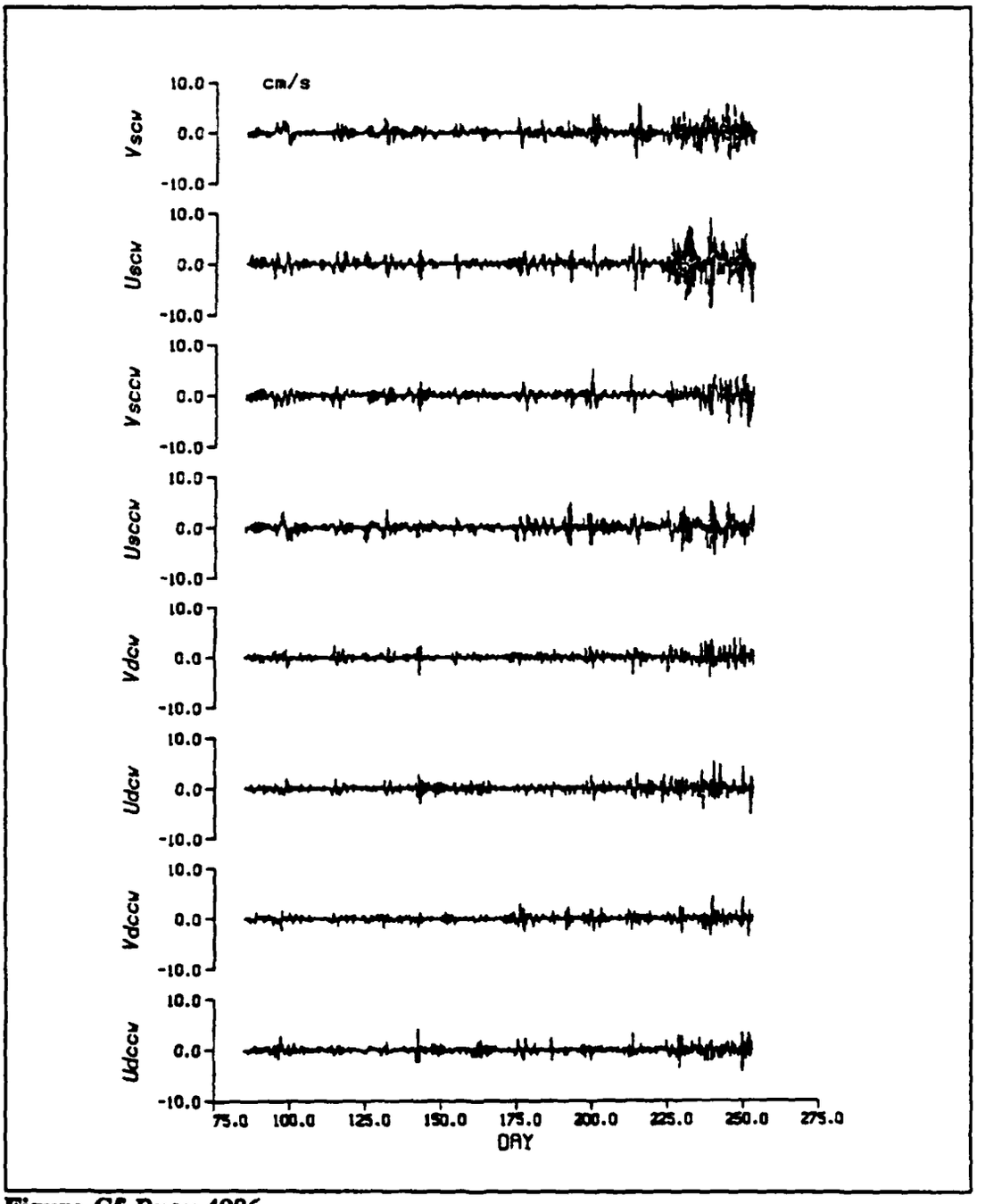

Figure C5 Buoy 4986.

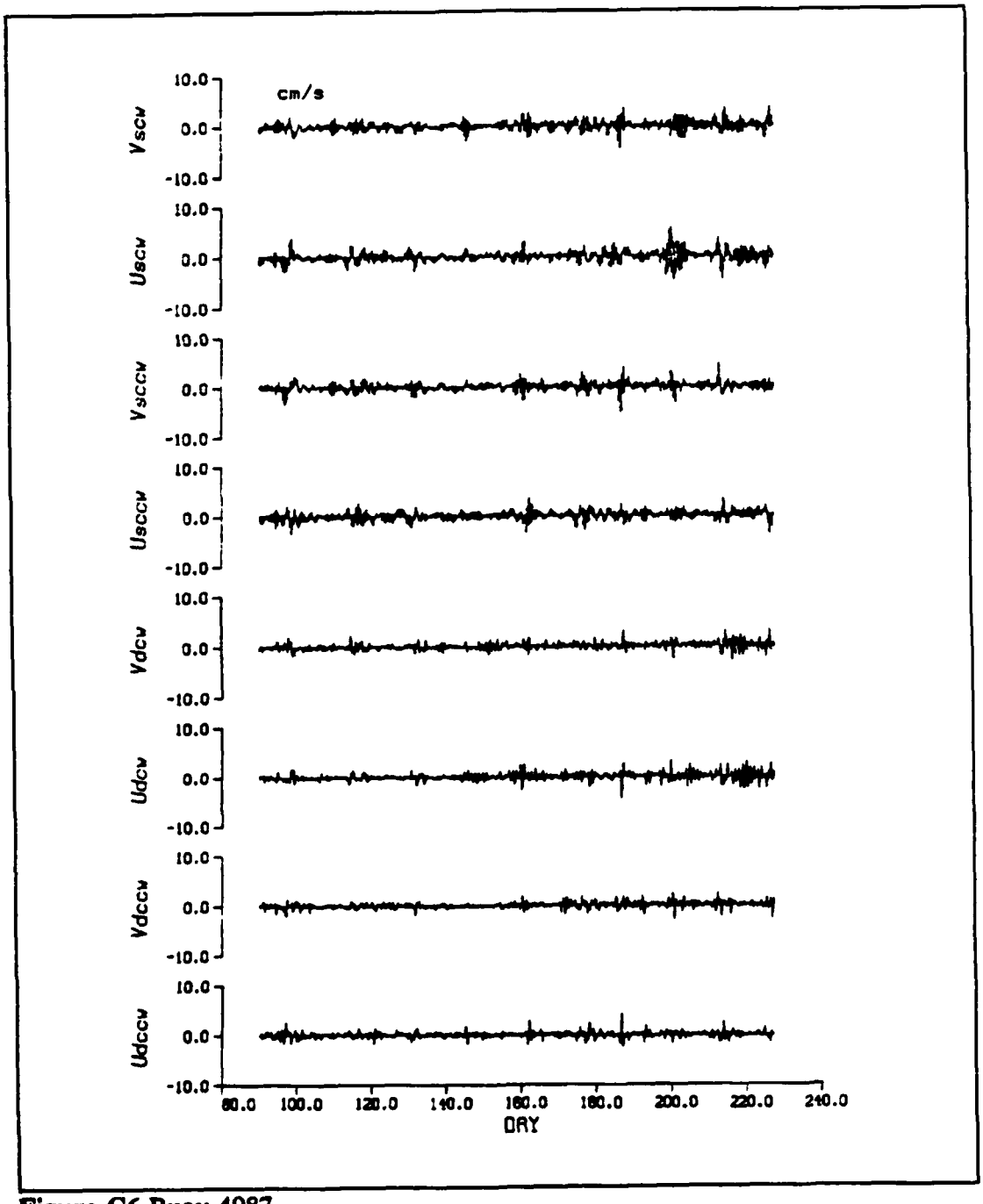

Figure C6 Buoy 4987.

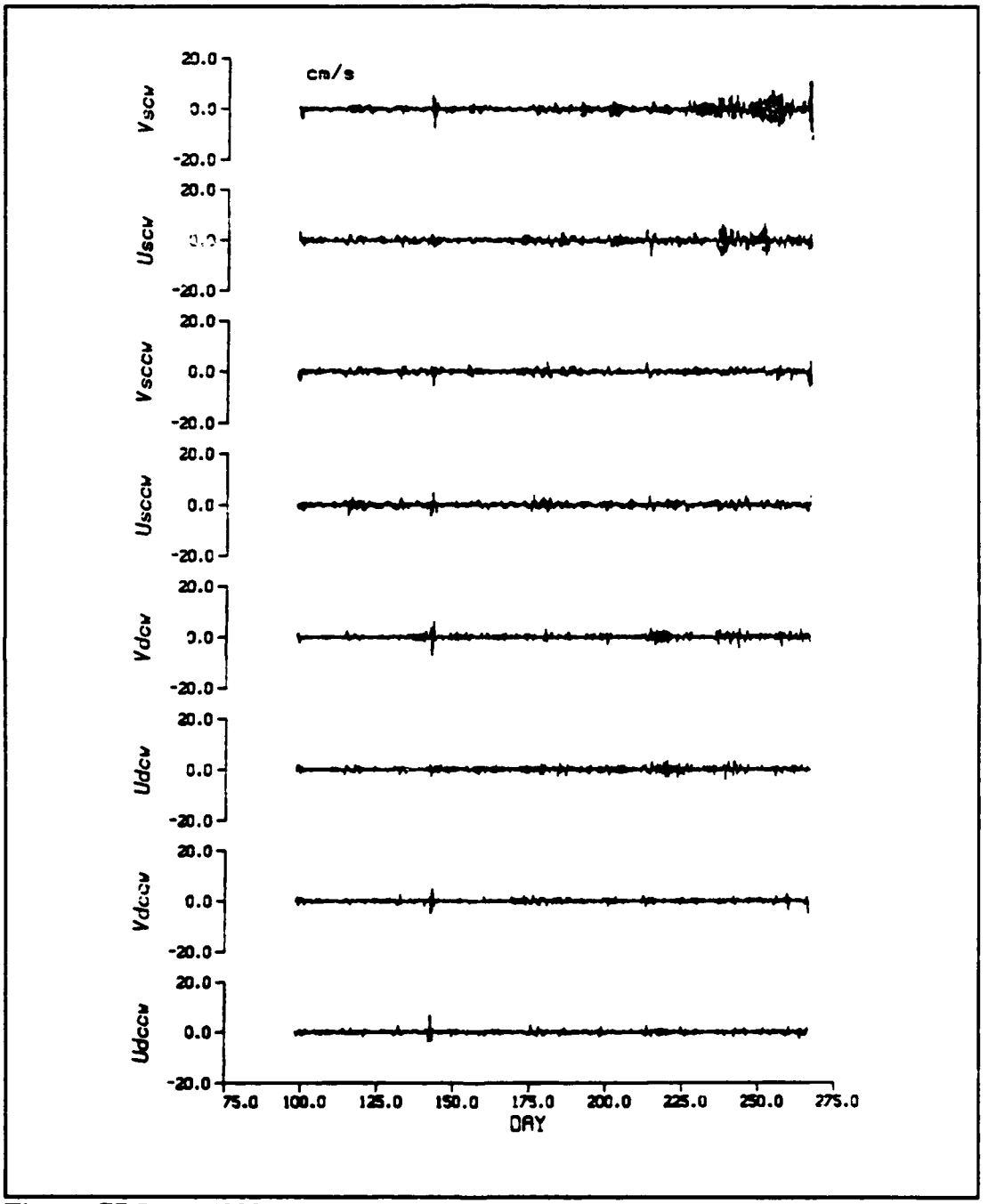

Figure C7 Buoy 4988.

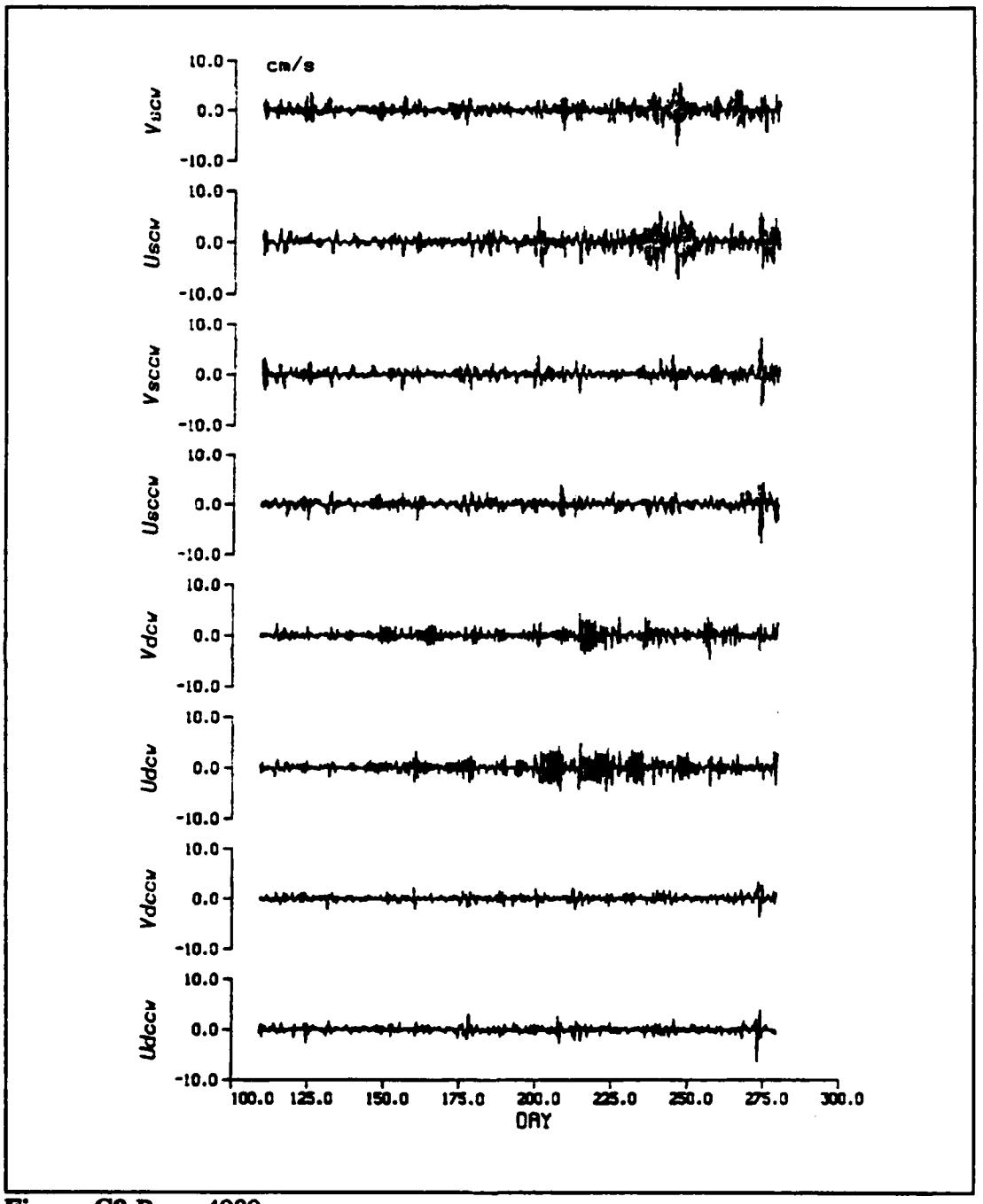

Figure C8 Buoy 4989.

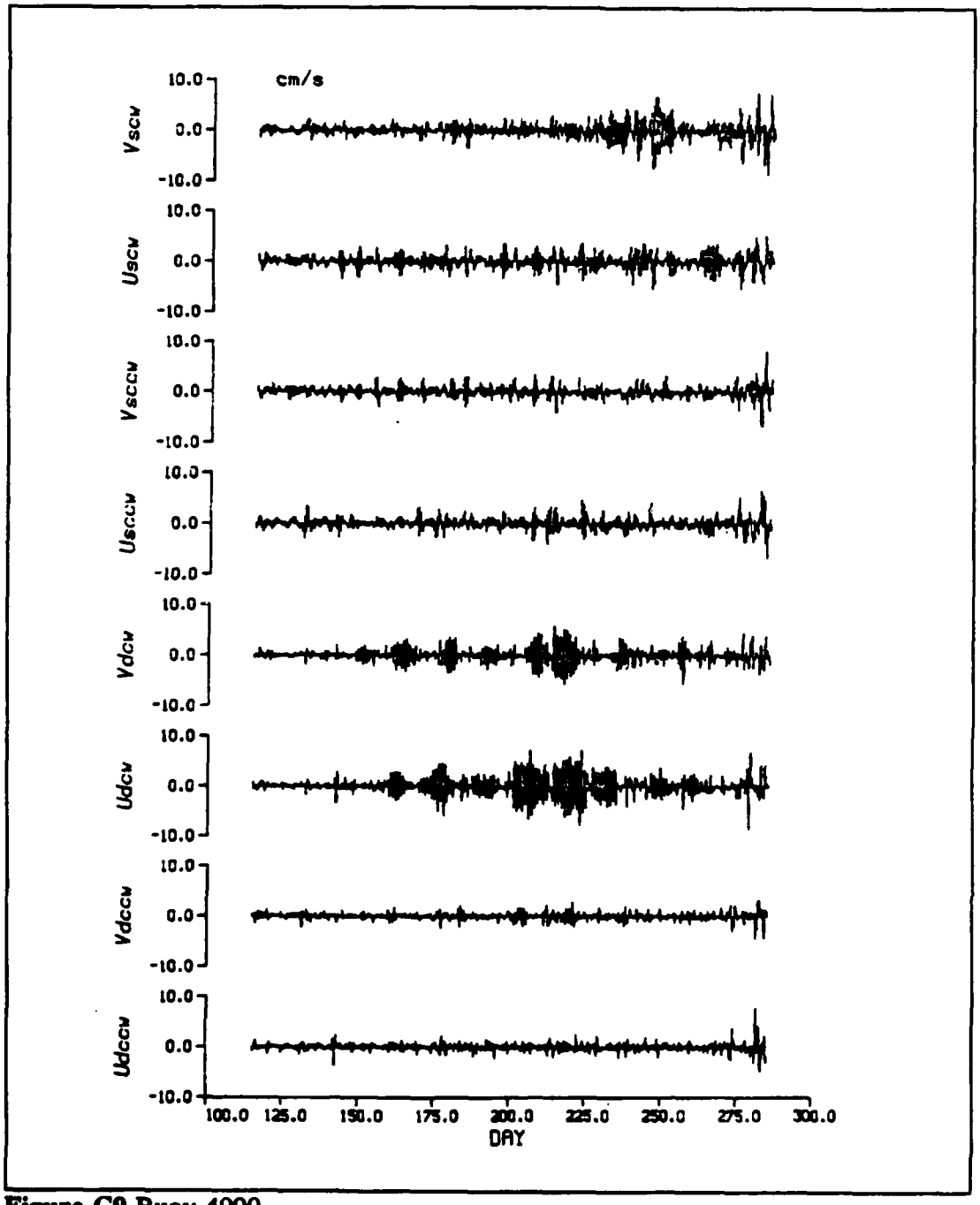

Figure C9 Buoy 4990.

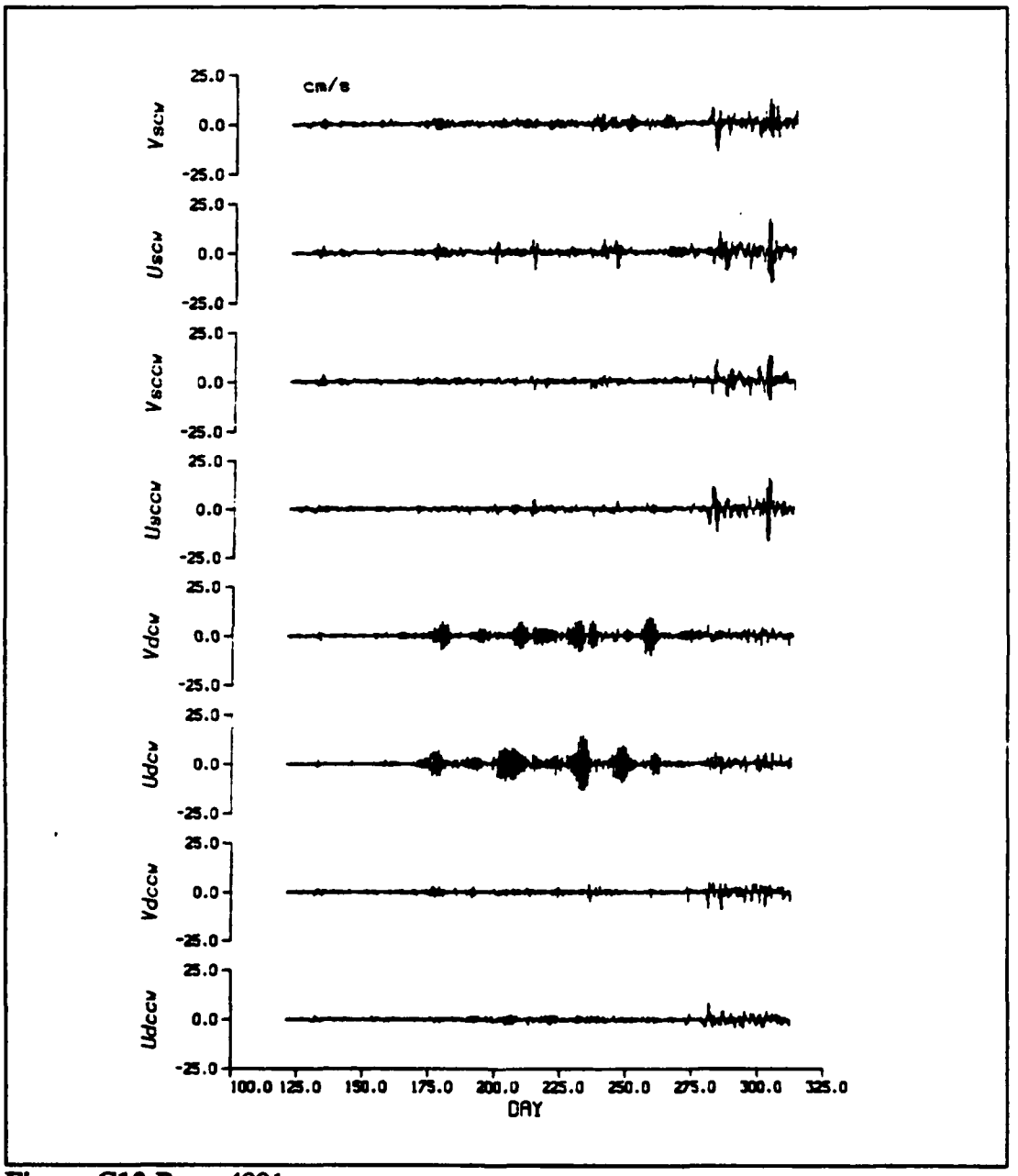

Figure C10 Buoy 4991.

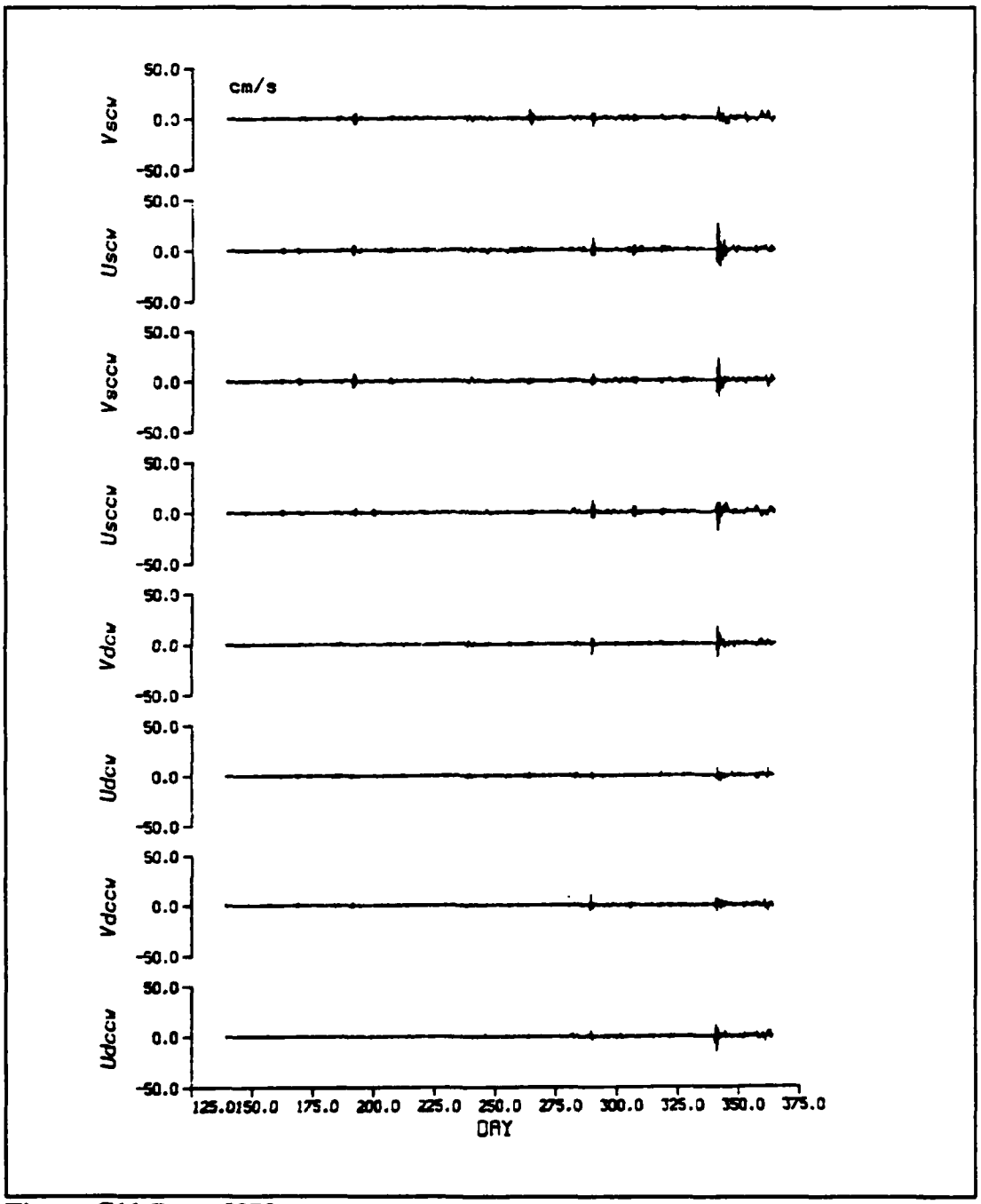

Figure C11 Buoy 5078.

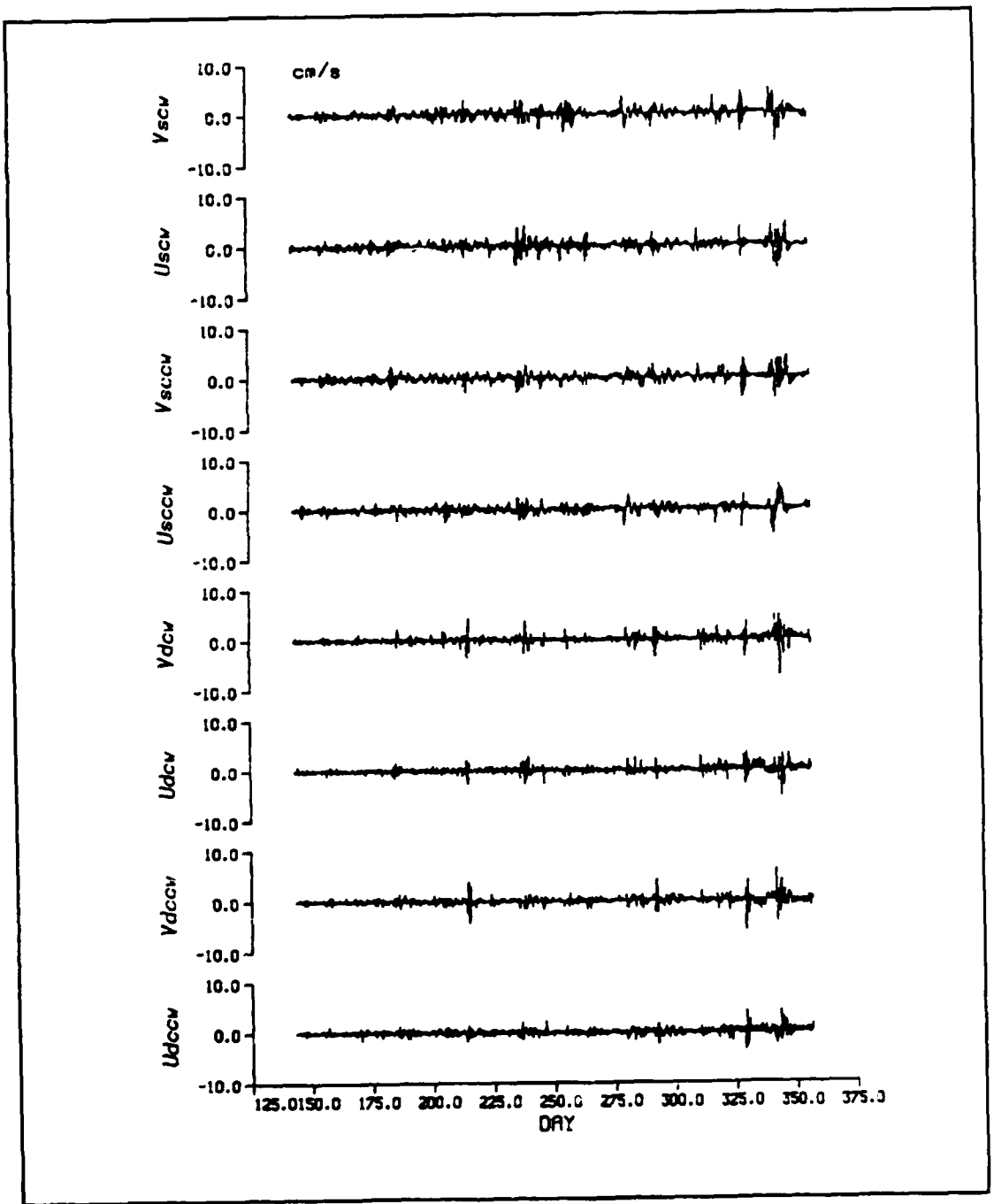

Figure C12 Buoy 5088.

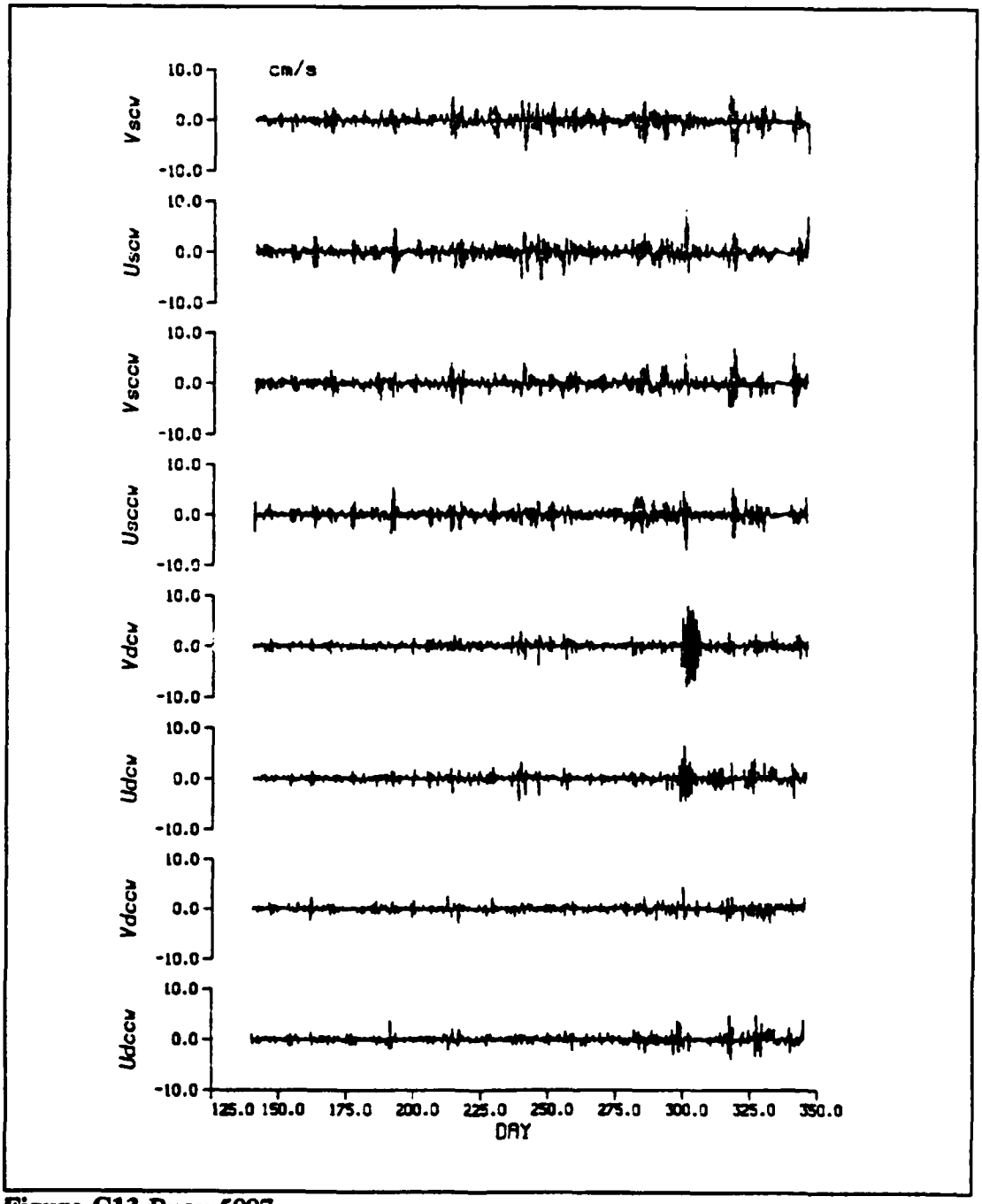

Figure C13 Buoy 5097.

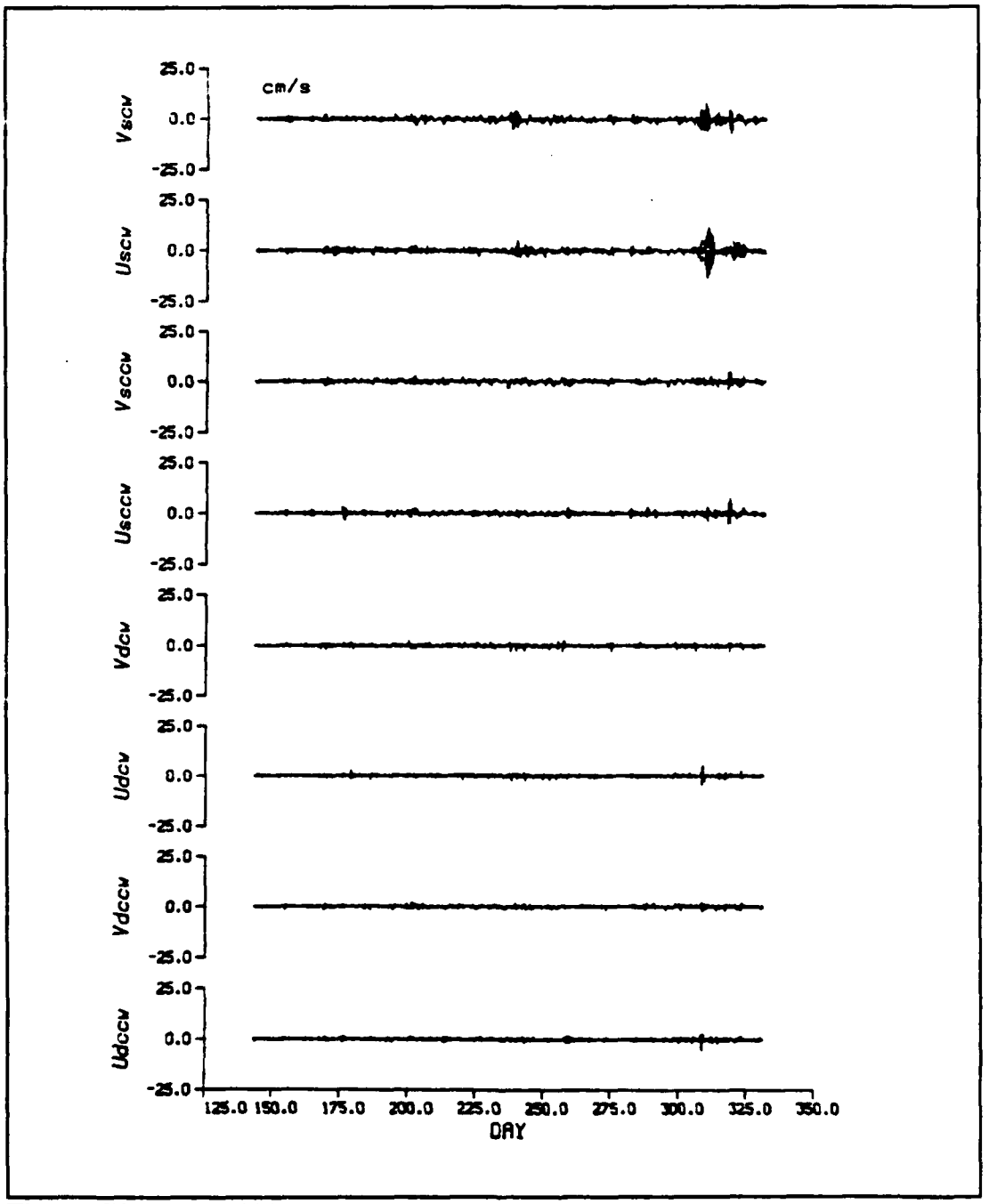

Figure C14 Buoy 5098.

LIST OF REFERENCES

Aagaard, K., and P. J. Greisman, Towards new mass and heat budgets for the Arctic Ocean, *J. Geophys. Res., 80*, 3821-3827, 1975.

Cartwright, D. E., Extraordinary tidal currents near St. Kilda, *Nature, 223*, 928-932, 1969.

Cartwright, D. E., J.M. Huthnance, R. Spencer and J.M. Vassie, On St. Kilda shelf tidal regime, *Deep-Sea Res., 27A*, 61-79, 1980.

Colony, R., and A. S. Thorndike, An estimate of the mean field of Arctic sea ice motion, *J. Geophys. Res., 89*, 10,623-10,629, 1984.

Crawford, W. R. and R. E. Thomson, Continental shelf waves of diurnal period along Vancouver Island, *J. Geophys. Res., 87*, 9516-9522, 1982.

Englebretson, R. E., and J. E. Walsh, Fram Strait ice flux calculations and associated Arctic ice conditions, *GeoJournal, 18.1*, 61-67, 1989.

Gascard, J.-C., ARCTEMIZ 86 Mission Report, Lab. d'Oceanographie Dynamique et de Climatologie, Universite Paris, Internal Report, July 1987.

Gascard, J.-C., C. Kergomard, P.-F. Jeannin and M. Fily, Diagnostic study of the Fram Strait marginal ice zone during summer from 1983 and 1984 marginal ice zone experiment lagrangian observations, *J. Geophys. Res., 93*, 3613-3641, 1988.

Gill, A.E., *Atmosphere-Ocean Dynamics*, p 411, Academic Press, Inc., Orlando, 1982.

Gordienko, P.A., and A.F. Laktionov, Circulation and physics of the Arctic Basin waters, in *Annals of the International Geophysical Year, XLVI Oceanography*, 94-112, Pergamon Press, 1969.

Heath, R. A., Tidal currents in the southwestern Pacific Basin and Campbell Plateau, southeast of New Zealand, *Deep-Sea Res., 30*, 393-409, 1983.

Hunkins, K., Anomalous diurnal tidal currents on the Yermak Plateau, *J. Mar. Res., 44*, 51-69, 1986.

Huthnance, J. M., On the diurnal tidal currents over Rockall Bank, *Deep-Sea Res., 21*, 23-35, 1974.

Kowalik, Z., A note on the co-oscillating M_2 tide in the Arctic Ocean, *Dt. Hydogr. Z., 32*, 100-112, 1979.

Longuet-Higgins, M.S., Steady currents induced by oscillations round islands, *J. Fluid Mech., 42*, 701-720, 1970.

McPhee, M. G., Analysis and prediction of short-term ice drift, *Proc of 5th Int. Conf. on offshore mechanics and Arctic Engr.*, Am. Soc. of Mech. Eng., Apr. 1986.

McPhee, M. G., A time-dependent model for turbulent transfer in a stratified oceanic boundary layer, *J. Geophys. Res., 92*, 6977-6986, 1987.

Middleton, J. H., T. D. Foster, and A. Foldvik, Diurnal shelf waves in the southern Weddell Sea, *J. Phys. Oceanogr., 17*, 784-791, 1987.

Morison, J. H., M. G. McPhee, and G. A. Maykut, Boundary layer, upper ocean, and ice observations in the Greenland Sea marginal ice zone, *J. Geophys. Res., 92*, 6987-7011, 1987.

Moritz, R. E., and R. Colony, Statistics of sea ice motion, Fram Strait to North Pole, *Proc of 7th Int. Conf. on offshore mechanics and Arctic Engr.*, Am. Soc. of Mech. Eng., Feb 1988.

Padman, L. and Dillon, T.M., Turbulent Mixing near the Yermak Plateau during CEAREX, Presented at CEAREX 89 Workshop, Long Beach, Miss., 8-9 Feb. 1990.

Parkinson, C.L., J.C. Comiso, H.J. Zwally, D. J. Cavalieri, P. Gloersen, and W.J. Campbell, Arctic ice, 1973-1976: Satellite passive-microwave observations, *NASA SP-489*, National Aeronautics and Space Administration, Washington, D.C. pp. 296, 1987.

Perry, R. K., Bathymetry, in *The Nordic Seas*, edited by B. Hurdle, pp. 219, Springer-Verlag, New York, Berlin, Heidelberg, Tokyo, 1986.

Pfirman, S., J.-C. Gascard , I. Wollenburg, P. Mudie and A. Abelmann, Particle-laden Eurasian Arctic sea ice: observations from July and August 1987. *Polar Res., 7*, 59-66, 1989.

Schwiderski, E. W., Tides, in *The Nordic Seas*, edited by B. Hurdle, pp. 219, Springer-Verlag, New York, 1986.

Tucker, W. B., A. J. Gow, and W. F. Weeks, Properties of summer sea ice in the Fram Strait. *J. Geophys. Res., 92*, 6787-6803, 1987.

Wadhams, P., Sea ice thickness distribution in Fram Strait, *Nature, 205*, 108-111, 1983.

INITIAL DISTRIBUTION LIST

1.	Defense Technical Information Center Camerson Station Alexandria, VA 22304-6145	2
2.	Library, Code 0142 Naval Postgraduate School Monterey, CA 93943-5002	2
3.	Chairman (Code OC/CO) Department of Oceanography Naval Postgraduate School Monterey, CA 93943	1
4.	Chairman (Code MR/RD) Department of Meteorology Naval Postgraduate School Monterey, CA 93943	1
5.	Jean-Claude Gascard Department of Oceanography Naval Postgraduate School Monterey, CA 93943	1
6.	Robert H. Bourke Department of Oceanography Naval Postgraduate School Monterey, CA 93943	1
7.	James H. Morrison Department of Oceanography Naval Postgraduate School Monterey, CA 93943	1
8.	Director Naval Oceanography Division Naval Observatory 34th and Massachusetts Avenue NW Washington, DC 20390	1

9. Commander — 1
Naval Oceanography Command
NSTL Station
Bay St. Louis, MS 39522

10. Commanding Officer — 1
Naval Oceanographic Office
NSTL Station
Bay St. Louis, MS 39522

11. Commanding Officer — 1
Fleet Numerical Oceanography Center
Monterey, CA 93940

12. Commanding Officer — 1
Naval Ocean Research and Atmospherics
Laboratory
NSTL Station
Bay St. Louis, MS 39522

13. Commanding Officer — 1
Naval Ocean Research and Atmospherics
Laboratory, West
Monterey, CA 93940

14. Chairman, Oceanography Department — 1
U. S. Naval Academy
Annapolis, MD 21402

15. Chief of Naval Research — 1
800 N. Quincy Street
Arlington, VA 22217

16. Office of Naval Research (Code 420) — 1
Naval Ocean Research and Development
Activity
800 N. Quincy Street
Arlington, VA 22217

17. Commander — 1
Oceanographic Systems Pacific
Box 1390
Pearl Harbor, HI 96860

18. Commanding Officer 1
Naval Polar Oceanography Center, Suitland
Washington, DC 20373